



POLITECNICO MILANO 1863

Scuola di ingegneria Industriale e dell'Informazione
Corso di Laurea Magistrale in Ingegneria Meccanica

X-RAY COMPUTED TOMOGRAPHY: DESIGN AND APPLICATION OF A PROCEDURE FOR THE ESTIMATION OF THE INFLUENCE OF UNPROCESSED POWDER

Supervisor: Prof. Quirico Semeraro

Co-supervisor: Eng. Stefania Cacace

Ahmed Taballa

Matr. 882505

Academic Year 2018 / 2019

Contents

Introduction and Problem Statement	1
1 State of the Art	6
2 Hardware Concept and Design	12
1 Giacomazzi's Model	12
1.1 Pores' Features	14
2 The Case Design	17
2.1 Giacomazzi's Case Design	17
2.2 Drawbacks of Giacomazzi's Case design	19
2.3 Proposed Solution	20
2.3 Case Production	23
3 The powder	27
3 The Work Flow	28
1 Influencing Factors	30
2 Measured Dimensions	32
3 Reference Values	33
4 Response Variables	33
5 Software and Matlab Code	34
5.1 Matlab	34
5.2 CloudCompare	36
5.3 Minitab	36

CONTENTS

4	Single Disk Experiment and Analysis	37
1	Single Disk Experiment	37
1.1	Without Powder	38
1.2	With Powder	40
2	ANOVA Analysis	43
2.1	Difference in mean diameter [ΔD_m]	44
2.2	Difference in height [Δh]	45
2.3	Difference in area [ΔA]	47
2.4	Difference in volume [ΔV]	48
5	Full Case Experiment and Analysis	50
1	Full Case Experiment	50
2	Preliminary Tests	51
3	ANOVA Analysis	53
3.1	Difference in mean diameter [ΔD_m]	53
3.2	Difference in height [Δh]	55
3.3	Difference in area [ΔA]	57
3.4	Difference in volume [ΔV]	59
6	Powder's Influence on Pore's Reconstruction	61
1	Pore's Reconstruction	61
1.1	Pore Isolation – Manual Cutting Tool	63
1.2	Pore Isolation – Matlab Code	65
7	Conclusions and Future Development	70

CONTENTS

Conclusions	71
Future Development	75
 APPENDIX	 77
A. RESPONSES' TABLES	77
A.1 Responses' Table of the Single Disk Experiment	77
A.2 Responses' Table of the Full Case Experiment	81
 B. ANOVA MODEL VERIFICATION	 91
B.1 Single Disk Experiment	92
1.1 Difference in mean diameter [ΔD_m]	92
1.1 Difference in height [Δh]	93
1.1 Difference in area [ΔA]	94
1.1 Difference in volume [ΔV]	95
 B.1 Full Case Experiment	 96
1.1 Difference in mean diameter [ΔD_m]	96
1.1 Difference in height [Δh]	97
1.1 Difference in area [ΔA]	98
1.1 Difference in volume [ΔV]	99

List of Figures

I.	Schematic representation of an XCT system [1]	1
II.	Example of fusing defects containing unmelted powder [3]	2
III.	Crack growth rate curve	3
IV.	North Star Imaging, model X25.....	4
1.1	Hermanek and Carmignato's reference object for accuracy evaluation of XCT porosity measurements; a) 3D image of the object, b) magnified image of a pin, c) general dimensions of the object. [7].....	7
1.2	A simulation of a number of disks piled on top of each other simulating a cylindrical bar with internal porosities. Top disk showing an example of the artificial open pores [8].....	8
1.3	Alicona Infinite Focus Instrument.....	9
1.4	Beam Hardening; on the left, the outer zones appear more dense than the internal ones; on the right, a filter has been applied.....	10
2.1	Example of a single disk used in the experiment with the artificial pores drilled on the top face	13
2.2	A 3D simulation of a number of disks piled on top of each other simulating a cylindrical bar with internal porosities	13
2.3	Polar plot of the pore's configuration, and the number associated to each pore.....	15
2.4	Section view of a simulation of Giacomazzi's Design of the lower case that will be housing the disks.....	17
2.5	Final design of the case containing the aluminum pile, the spacers (in orange), and the upper case positioned on top	19
2.6	3D model of the case design with the first modification	20
2.7	A 3D model of the case design with the second modification of the threaded holes and screws.....	21

LIST OF FIGURES

2.8	<i>A section view of the complete model after placing the pile and the screws.....</i>	<i>22</i>
2.9	<i>A section view of the model showing the upper and lower limits of the XCT's field of vision.....</i>	<i>23</i>
2.10	<i>Example of pan head self-drilling screws as the ones used for the case model.....</i>	<i>24</i>
2.11	<i>A section view of the case while its being designed using SolidWorks with dimensions assigned it.....</i>	<i>25</i>
2.12	<i>The Final model of the case after production including the three screws...26</i>	
2.13	<i>The Final model of the case after Assembly</i>	<i>27</i>
3.1	<i>Schematic representation of the procedure activities and the work flow of the experiment campaign.....</i>	<i>29</i>
3.2	<i>Schematic representation indicating where the cavities will be positioned regarding the vertical axis.....</i>	<i>30</i>
3.3	<i>Representation of the variables chosen to study the porosities.....</i>	<i>33</i>
3.4	<i>Reconstruction of the 3D model by the Matlab Code with the artificial pores indicated in red.....</i>	<i>35</i>
4.1	<i>Examples of grayscale images that are obtained as an output of the XCT machine</i>	<i>38</i>
4.2	<i>Reconstruction of the 3D model by the Matlab Code with the artificial pores indicated in red.</i>	<i>39</i>
4.3	<i>Examples of grayscale images with powder added.....</i>	<i>40</i>
4.4	<i>Reconstruction of the 3D model by the Matlab Code with the artificial pores indicated in red.</i>	<i>41</i>
4.5	<i>A side by side comparison of the two cases after alignment using CloudCompare.....</i>	<i>42</i>
4.6	<i>A scatter plot and main effect plot of ΔD_m</i>	<i>44</i>
4.7	<i>A scatter plot and main effect plot of Δh</i>	<i>45</i>
4.8	<i>A scatter plot and main effect plot of Δh</i>	<i>47</i>

LIST OF FIGURES

4.9	<i>A scatterplot and main effect plot of ΔV.....</i>	<i>48</i>
5.1	<i>Schematic representation indicating where the cavities will be positioned regarding the vertical axis.....</i>	<i>50</i>
5.2	<i>Comparison of the grayscale images obtained as single disk (Left) and with the 38mm diameter plastic case (Right).....</i>	<i>52</i>
5.3	<i>Grayscale image obtained with the 26mm diameter plastic case.....</i>	<i>52</i>
5.4	<i>A scatter plot and main effect plot of ΔD_m.....</i>	<i>54</i>
5.5	<i>A scatter plot and main effect plot of Δh.....</i>	<i>55</i>
5.6	<i>A scatter plot and main effect plot of ΔA.....</i>	<i>57</i>
5.7	<i>A scatter plot and main effect plot of ΔV.....</i>	<i>59</i>
6.1	<i>Reconstruction of a 3D model of the disk with and without powder using CloudCompare after being scanned by XCT.....</i>	<i>61</i>
6.2	<i>Reconstruction of a 3D model of the disk with powder using CloudCompare after being scanned by XCT.....</i>	<i>62</i>
6.3	<i>Close-up shot of the 3d Model constructed by CloudCompare.....</i>	<i>62</i>
6.4	<i>Different side views of a single pore isolated in CloudCompare – Pore without powder (Right) – Pore with powder (Left).....</i>	<i>64</i>
6.5	<i>Example of the pores after they have been isolated using Matlab and viewed by CloudCompare.....</i>	<i>65</i>
6.6	<i>Comparison of the pores after they have been isolated using Matlab and viewed by CloudCompare.....</i>	<i>66</i>
6.7	<i>Plan view comparison of the corresponding pores without powder (up) and with powder (down).....</i>	<i>67</i>
6.8	<i>Side view comparison of the corresponding pores without powder (up) and with powder (down).....</i>	<i>67</i>
6.9	<i>Plan view comparison of the corresponding pores without powder (left) and with powder (right).....</i>	<i>68</i>
7.1	<i>Examples of grayscale image with powder added.....</i>	<i>70</i>

LIST OF FIGURES

7.2	<i>The beam hardening artifact influence on the construction of pores from the full case experiment.....</i>	<i>72</i>
7.3	<i>Cone Beam Artifact.....</i>	<i>73</i>
7.4	<i>Example of the pores being isolated from the rest of the aluminum disk using the Matlab code.....</i>	<i>74</i>
7.5	<i>Different scenarios of adding powder into the pores, and constructed by the Matlab code.....</i>	<i>75</i>
B.1	<i>Normality plot, Scatterplot and Test for equal variance of std. residuals of ΔD_m.....</i>	<i>92</i>
B.2	<i>Normality plot, Scatterplot and Test for equal variance of std. residuals of Δh.....</i>	<i>93</i>
B.3	<i>Normality plot, Scatterplot and Test for equal variance of std. residuals of ΔA.....</i>	<i>94</i>
B.4	<i>Normality plot, Scatterplot and Test for equal variance of std. residuals of ΔV.....</i>	<i>95</i>
B.5	<i>Normality plot, Scatterplot and Test for equal variance of std. residuals of ΔD_m.....</i>	<i>96</i>
B.6	<i>Normality plot, Scatterplot and Test for equal variance of std. residuals of Δh.....</i>	<i>97</i>
B.7	<i>Normality plot, Scatterplot and Test for equal variance of std. residuals of ΔA.....</i>	<i>98</i>
B.8	<i>Normality plot, Scatterplot and Test for equal variance of std. residuals of ΔV.....</i>	<i>99</i>

List of Tables

2.1	<i>Table representing the configuration chosen to study the radial and angular factor ρ and θ, and the number associated to each pore.....</i>	16
4.1	<i>ANOVA Table of the response $[\Delta D_m]$.....</i>	44
4.2	<i>ANOVA Table of the response $[\Delta h]$.....</i>	46
4.3	<i>ANOVA Table of the response $[\Delta A]$.....</i>	47
4.4	<i>ANOVA Table of the response $[\Delta V]$.....</i>	49
5.1	<i>ANOVA Table of the response $[\Delta D_m]$</i>	54
5.2	<i>ANOVA Table of the response $[\Delta h]$</i>	56
5.3	<i>ANOVA Table of the response $[\Delta A]$.....</i>	58
5.4	<i>ANOVA Table of the response $[\Delta V]$.....</i>	60
6.1	<i>Geometrical dimensional changes due to unprocessed powder</i>	69
A.1	<i>Responses' Table of the single disk experiment</i>	77
A.2	<i>Responses' Table of the full case experiment.....</i>	81

Abstract

La produzione additiva è cresciuta rapidamente nell'ultimo decennio e molte industrie hanno iniziato a muoversi verso queste tecnologie grazie alla sua capacità di creare forme complesse con diversi tipi di materiali. Se da un lato si hanno caratteristiche vantaggiose, dall'altro vi sono degli inconvenienti legati a delle caratteristiche interne indesiderate come difetti, porosità e polvere non trasformata, che potrebbero avere un'influenza negativa sulle proprietà meccaniche. Per questi motivi, X-Ray Computed Tomography (XCT) ha avuto un grande successo nel caratterizzare le funzionalità interne. In effetti, questa tecnologia offre vantaggi unici, come la capacità di misurare sia le geometrie interne che quelle esterne e di essere una tecnologia non distruttiva.

In questa tesi è stata sviluppata una procedura per valutare la capacità dello strumento di misure XCT nel rilevare le porosità in cui è presente della polvere non processata. La presenza di polvere non processata è un difetto tipico di alcune tecnologie additive.

Abstract

Additive Manufacturing has been growing rapidly over the last decade, and many industries started moving towards these technologies due to its ability to create complex shapes with different kinds of materials. With these features comes the drawbacks of undesired internal features such as defects, porosities, and unprocessed powder, which could have a significant influence on the mechanical properties. For these reasons, X-Ray Computed Tomography (XCT) had great success in detecting internal features. Indeed, this technology offers unique advantages such as the capacity of measuring both internal and external geometries and for being a non-destructive technology.

In this thesis, a procedure has been developed to evaluate the capability of the XCT instrument to detect porosities filled with unprocessed powder, which is a typical defect of some additive technologies.

Introduction and Problem Statement

Born in the late '60 from an intuition of the British Engineer Godfrey Hounsfield, the Computed Tomography (CT) initially had applications only in the medical field; then, just a decade later, it had spread also in the industrial field. It is now mostly used in material analysis and Non-Destructive Tests (NDT), due to the possibility of measuring internal and external geometries avoiding the physical destruction of the component. Years later, it had been introduced also in the metrological field for dimensional measurements, with future precisions similar to the ones of traditional metrological instruments such as Coordinate Measuring Machines (CMM) and optical ones. The principle of this technology is based on the emission of X-Rays, the penetration of this radiation through the component and the detection of the remaining part. This process is possible by means of a tomographic instrument, which is basically composed by a radiation's source, a detector and a rotating table that is able to correctly position the component inside the machine. The X-Ray source produces the radiation that will propagate through the component and that will be attenuated by a quantity proportional to the thickness and the type of the penetrated material. Then, the remaining energy of the radiation will be detected and measured by the detector. A representation of a generic XCT system is shown in Figure I [1].

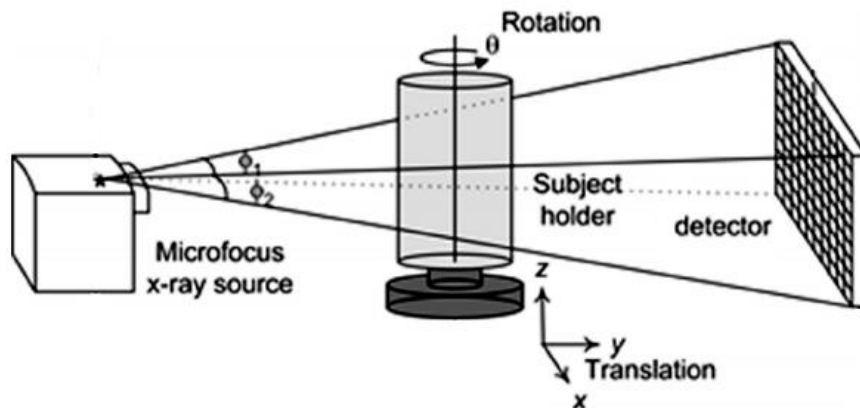


Figure I: Schematic representation of an XCT system [1]

INTRODUCTION AND PROBLEM STATEMENT

XCT is being used in areas such as manufacturing, automotive, aerospace, and geology, where the variety of materials being imaged includes: metals, plastic castings, additive manufacturing, electrical components, mummies and antiquities. The advantages of using XCT for dimensional metrology, are its ability to highlight defects and voids in a non-destructive manner of both traditional and additive manufactured parts along with reverse engineering and material composition analysis [2].

The unprocessed powder is a defect, caused by the incomplete melting of the material powder that is used during additive manufacturing technologies such as Selective Laser Melting (SLM). This usually happen during the construction of the part when parameters such as the energy density or power is insufficient, causing incomplete melting or fusing of the part, creating pores and defects with unmelted powder trapped inside of it as illustrated in figure II.

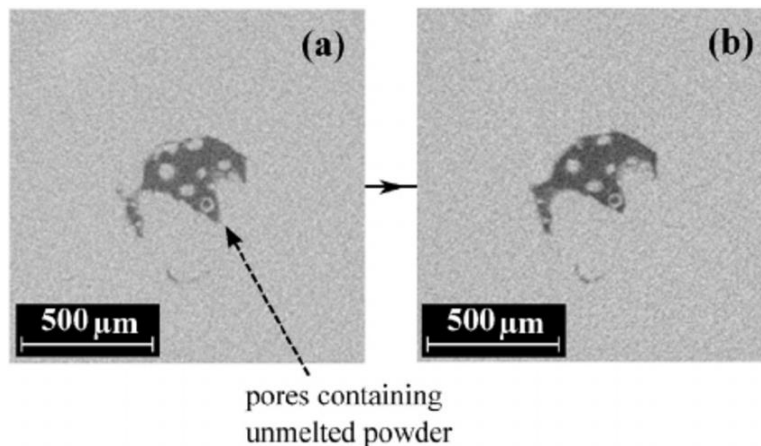


Figure II. Example of fusing defects containing unmelted powder [3]

In most cases, pores and internal defects can not be completely avoided. Instead, having a method to detect these pores and measure them in terms of geometrical dimensions can help to estimate the size of pores which would have a major influence on the mechanical properties of the part, for instance, the fatigue life.

INTRODUCTION AND PROBLEM STATEMENT

Internal defects, pores and cracks could have the tendency to start propagating when the stress intensity factor (ΔK) reaches the threshold value (ΔK_{th}). Once reached, the crack propagates until the stress intensity factor (ΔK) reaches its critical value (K_{Ic}). By understanding this, one can determine the maximum load that can be applied on a part without causing crack propagation. And in case the internal crack is loaded with a higher load and propagation starts, It's possible to determine how long can the part last for before it collapses, also known as the fatigue life [4].

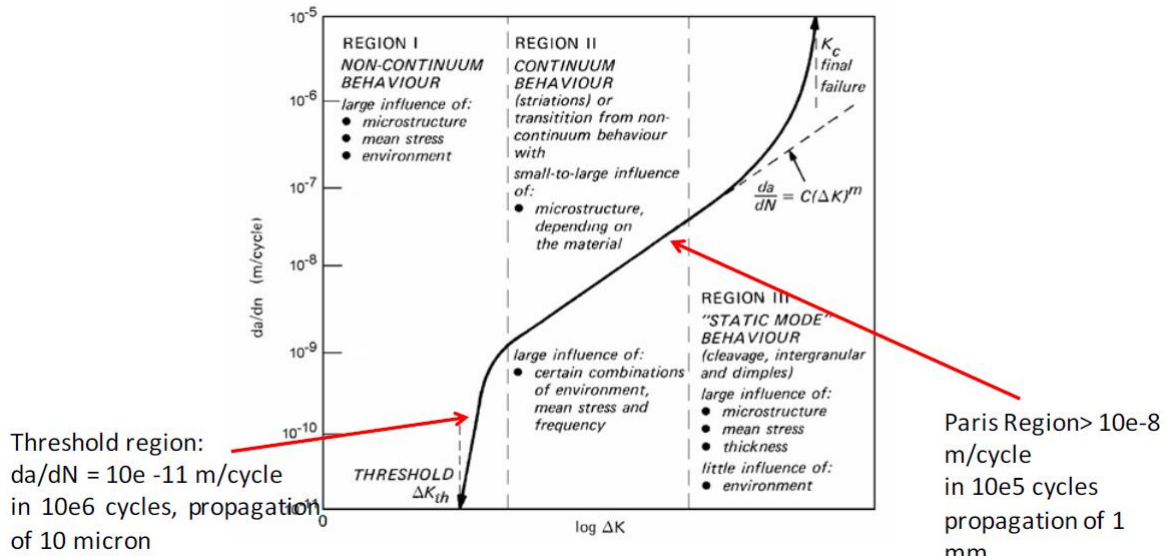


Figure III: Crack growth rate curve

$$[\Delta K = B \cdot \Delta \sigma \cdot \sqrt{\pi a}]$$

ΔK : Stress Intensity Factor

B: Crack Geometry Shape

$\Delta \sigma$: Load Fluctuation

a: Crack Length

ΔK_{th} : Threshold value of ΔK where once reached, crack propagates.

K_{Ic} : Fracture toughness or the critical value of ΔK where once reached, the part collapses.

INTRODUCTION AND PROBLEM STATEMENT

So it can be seen that the maximum load and the fatigue life cycle can be determined if we can determine the crack size and shape. This is where the X-ray computed tomography comes into play with determining the size of these defects. So the problem to be tackled in this thesis work is the capability of the XCT instrument to detect fusing defects and pores filled with unmelted powder. As it is possible that if the unmelted powder can not be correctly detected, then it is very likely that we are underestimating or overestimating the sizes of the defects which can possibly lead into inaccurate estimation of the mechanical properties of the constructed part.

The main objective of the thesis is to evaluate the capability of an XCT instrument to detect incomplete melted powder and to analyze the effect that it could have on the readings obtained by the instrument. This experiment will be performed on the XCT instrument at our disposal, illustrated in Figure IV, the model X25 produced by the company North Star Imaging.



Figure IV: North Star Imaging, model X25

We start by having a look at the state of the art in chapter 1. Followed by the hardware design and the experiment's workflow in chapter 2, and chapter 3 respectively.

The experimental campaign will go through two different experiments, the single disk experiment, using only one single disk with pores opened to the air, simulating external pores, and the full case experiment; piling up four disks on top of each other in a way that the pores will be closed, simulating internal pores. Chapter 4 will be dedicated to the single disk experiment, while chapter 5 will focus on the full case experiment.

In Chapter 6 we will take a close look at the pores and how the size and shape changes due to the presence of unprocessed powder. And finally in chapter 7, we will have a conclusion about the experimental campaign, and the XCT's capability and accuracy.

Chapter 1

State of the Art

In the previous chapter, we have mainly discussed how additive Manufacturing technologies deliver products that can suffer from various defects such as internal defects and porosities, and how it can have an effect on the performance of the product and its mechanical properties. Due to technological and economic limits, porosities cannot be completely avoided by optimizing process parameters. It is therefore essential to have a measurement technique that can detect and evaluate these defects accurately. Recently, some models were developed in order to detect an XCT machine's accuracy. The basic common idea was to build an artifact with known geometries and features that can also be measured using a very precise measuring instrument, and then compare the results with the measurements taken from the XCT instrument.

The first authors to propose a possible solution were Nikishkov et al. [5], aiming their efforts to study and understand the effects of threshold choice and of the pixel size on the diameter evaluation. The main issue with this proposal is that the pores to be studied were external pores open to air, and not internal ones, which is of our interest.

Later, Jansson et al. [6] proposed another innovative solution: a metallic sample produced by means of SLS additive manufacturing process that has an external hemispherical features of various diameters, while in the inside there are complete spherical features with the same dimensions of their corresponding external ones. The objective was to compare the different dimensions found by the XCT machine between the internal and the external ones. The first problem with this proposal is that there is not any possibility to measure the internal pores other than with XCT process, making it impossible to validate the metrological significance of an XCT measure. The second problem that could be faced is that the internal pores are produced by additive manufacturing, a process full of unwanted and influencing parameters, meaning that if the internal shapes of the pores have some imperfections, it will be difficult to allocate the error to the additive manufacturing

process or to the XCT measuring one. This problems makes the accuracy estimation impossible to be conducted.

Then, Hermana and Carmignato, [7] developed an idea to simulate internal porosity consisting of 4 cylindrical aluminum samples of different heights, with micro-drilled holes on the bottom plane surface; they are then inserted in an aluminum case with four cavities of corresponding depths with the presence of bolts providing a pressing force to each one of the samples in order to eliminate unwanted slippage movement of the four cylinders during the rotation of the table in the tomographic process. the concept can be seen in Figure 1.1.

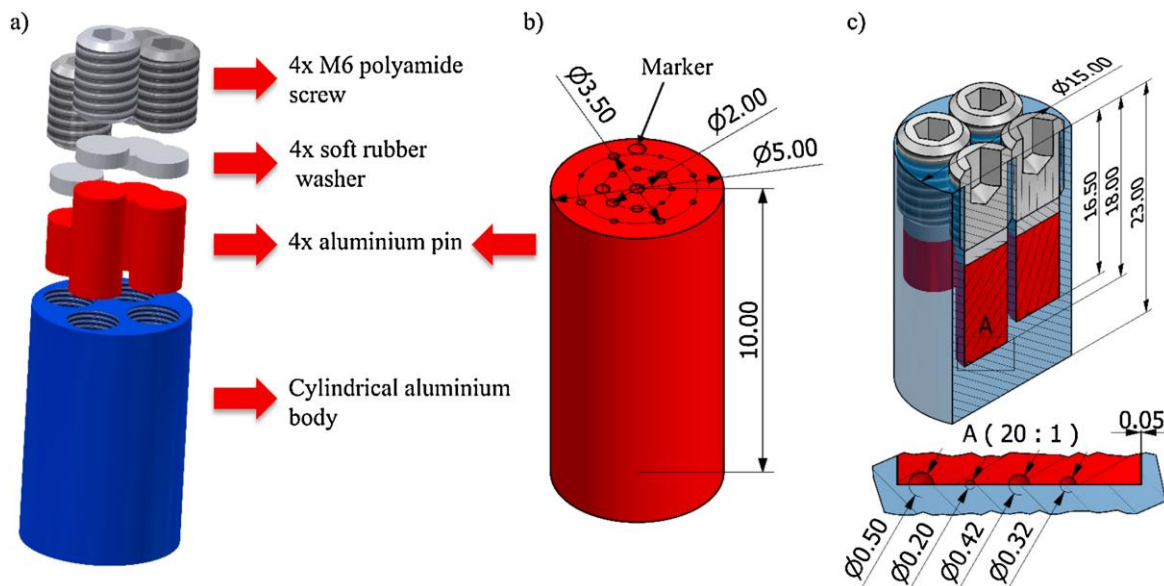


Figure 1.1: Hermanek and Carmignato's reference object for accuracy evaluation of XCT porosity measurements; a) 3D image of the object, b) magnified image of a pin, c) general dimensions of the object. [7]

The micro drilled holes are then measured with a more precise instrument , in order to have a reference dimension of the diameter and the depth for every artificial hole. Then, the four pieces are installed in their corresponding pre-produced cases so that

the cavities are put in contact with the surface, and then the holes are measured using the XCT instrument, then a comparison between the two readings can be performed for accuracy evaluation. Yet, this proposal was not at all free of problems. The first issue was the presence of different materials such as the cylinders, the external body, bolts and washer, this will cause the histogram to have different picks and making it hard to choose the proper threshold value. Also the part to be scanned is too large compared with the pores it self, this means that due to low-resolution machines, we will have larger pixels causing less accurate measurement.

Simone Giacomazzi [8], as his master's thesis, proposed a procedure to estimate the accuracy of the XCT instrument. Giacomazzi's work has proposed to use an aluminum disk with some micro-drilled artificial open pores which can be easily measured using a very high precise instrument such as Alicona Infinite Focus. Then A couple of disks can be placed on top of each other creating a pile with closed internal pores. The pile can be then scanned using the XCT instrument and a comparison of the two readings can be performed to evaluate the accuracy.

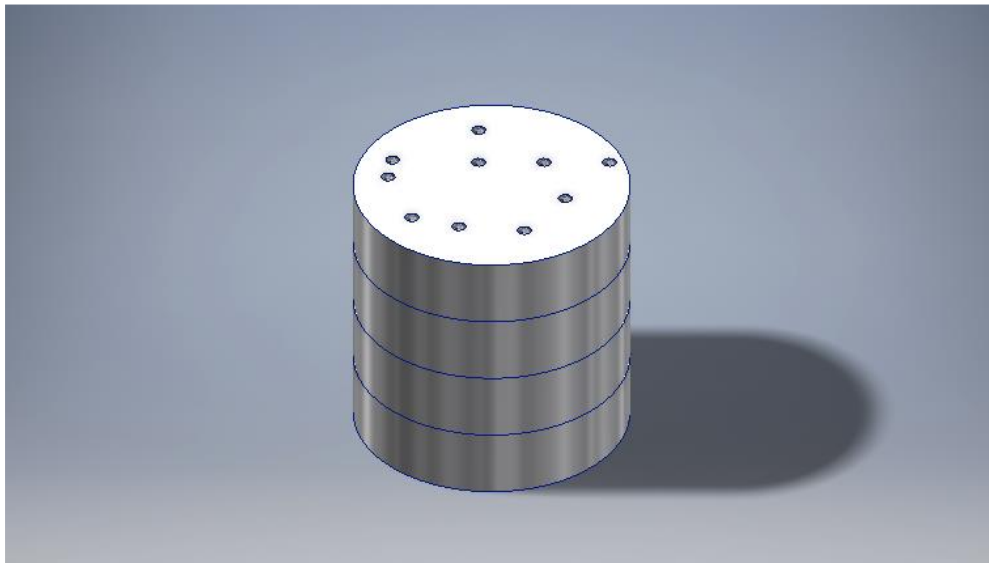


Figure 1.2: A simulation of a number of disks piled on top of each other simulating a cylindrical bar with internal porosities. Top disk showing an example of the artificial open pores [8]

Alicona Infinite Focus is a 3D micro coordinate measurement instrument which uses coaxial illumination and optimized LED ring light to perform the high resolution, high repeatability and high accuracy measurements. The accuracy of the XCT instrument is then evaluated based on the difference between the two readings. The experiment was performed on an XCT instrument of the model X25 produced by the company North Star Imaging that is held by Politecnico di Milano, illustrated in Figure V.



Figure 1.3: Alicona Infinite Focus Instrument

The output of Giacomazzi's thesis is that the XCT instrument is repeatable but not replicable, yet it is reliable as it provides readings that are close to the ones obtained from the Alicona Infinite Focus Instrument. The measurements are independent of the angular position or the orientation of the scanned object. However, the difference between the two readings will slightly increase as we move away from the center of measured object due to the beam hardening effect.

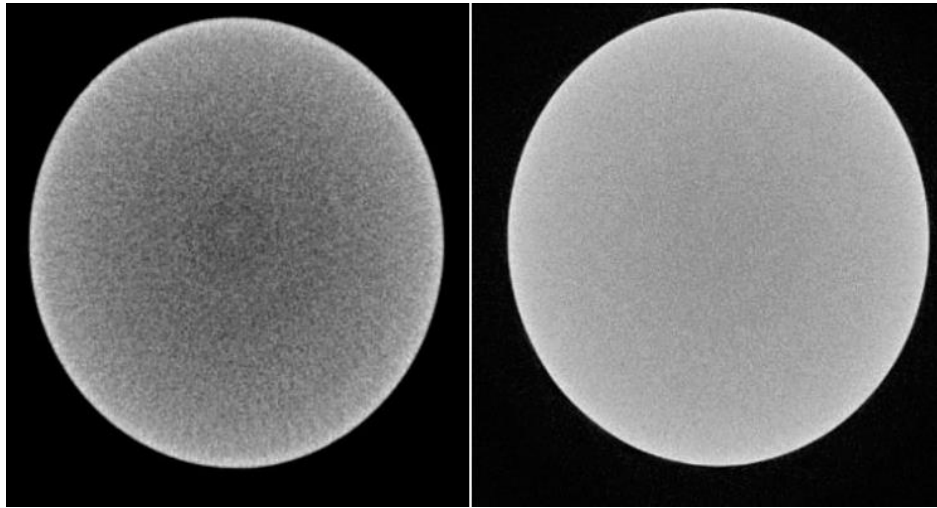


Figure 1.4: Beam Hardening; on the left, the outer zones appear more dense than the internal ones; on the right, a filter has been applied

It can be seen how, as we are moving away from the center, the error in the XCTs' reading could slightly increase due to the effect of the Beam Hardening, where the energy of the X-ray beam gets weaker as we move away from the center, and gets mostly absorbed by the material, making the outer zones appear more dense than they are, as illustrated in Figure 1.4. As a consequence, the outer pores will be underestimated more than the inner ones. This problem can be solved by applying the Beam Hardening filter, reconstructing the same XCT scan with different values of Beam Hardening filter applied or also by using a physical filter.

In conclusion, many authors tried to propose different ways and methods to study and evaluate the accuracy of an XCT instrument. One thing was held in common between all of them, which was empty pores. So a question has been raised whether the accuracy and reliability of the instrument could be affected by the presence of incomplete melted powder that remains in the cavity of the pore while the part is being constructed using an Additive Manufacturing technology. From this question, another question has been intriguing for sometime whether the XCT instrument is able to detect unprocessed powder, and the effect that it could have on the accuracy and the readings obtained by the instrument, and any consequences that it could have in case of false readings.

An article that was published in 2018, “X-ray refraction distinguishes unprocessed powder from empty pores in selective laser melting Ti-6Al-4V” [7] shows that there are mainly two types of cavities or pores that are produced during additive manufacturing by selective laser melting. The first type is the keyhole pores which happens when high heat is used to melt the powder during the SLM process. This will cause rapid solidification during SLM and may cause instabilities during the process, which lead to the formation keyhole pores, which are characterized as small rounded shape empty pores. On the other hand, the second type which goes by the different names such as binding or fusing faults, or unprocessed powder which happens when insufficient heat is used during SLM. These pores are characterized as large complex shape cavities with unprocessed powder inside of it. As the main topic of this thesis is to detect incomplete melted powder and study the influence that it has on the readings obtained by XCT, then in this thesis we will mainly be focusing on the second type of pores that will have the powder inside of it, and from now on, incomplete melted powder will be referred to as unprocessed powder.

The main approach proposed to study this topic is to place some powder inside of the artificial pores. So for our study, we will be using the same aluminum disks that have been built by Giacomazzi, and we will be placing some aluminum powder inside the artificial pores in a way that the powder is representing unprocessed powder. The capability and accuracy of the XCT instrument will then be evaluated by performing a comparison between the readings of the XCT instrument without any powder and the readings with the powder added.

In the next Chapter, the complete model that will be used during the experiment will be described including the disks that has been used during Giacomazzi’s thesis work and the plastic case that will be used to hold the disks together during the full case experiment.

Chapter 2

Hardware Concept & Design

In order to be able to perform the experiments to evaluate the XCT's capability and accuracy, an artifact with simulated internal defects is needed. This model will contain artificial pores that will simulate the internal defects that could be found in a specimen produced by Additive Manufacturing. The artifact that will be used for this experiment has already been developed for *Giacomazzi's* thesis work with exception of an improved design of a case that will be explained later in this chapter. So, we start with a brief description of *Giacomazzi's* model that will be explained next.

1. *Giacomazzi's* Model

The main concept behind the model is to build a circular shaped disks where a specific number of holes that are drilled on the face of the disk are representing the artificial pores. Figure 2.1 shows an example of a single disk used in the experiment with the artificial pores drilled on the top face. In order to simulate internal pores, a number of disks are stacked on top of each other simulating a pile of disks or a cylindrical bar with internal closed pores. A simulation of the pile of disks can be seen in figure 2.2. By using this design, it is possible to have a very large amount of changeable parameters such as disks' diameter and thicknesses, holes' patterns and dimensions, disks' position and orientation in the pile, generating in this way a very high number of possible case scenarios to study.

Next, we speak about the physical characteristics of the pile, such as its material and its geometrical dimensions. Considering both manufacturing's and measuring's points of view, the smarter choice seems to be a commercial aluminum alloy due to its easy machinability and to the fact that it is easily penetrated by the X-Rays. Another reason why aluminum has been chosen is because it is one of the most used material in manufacturing applications.



Figure 2.1: Example of a single disk used in the experiment with the artificial pores drilled on the top face

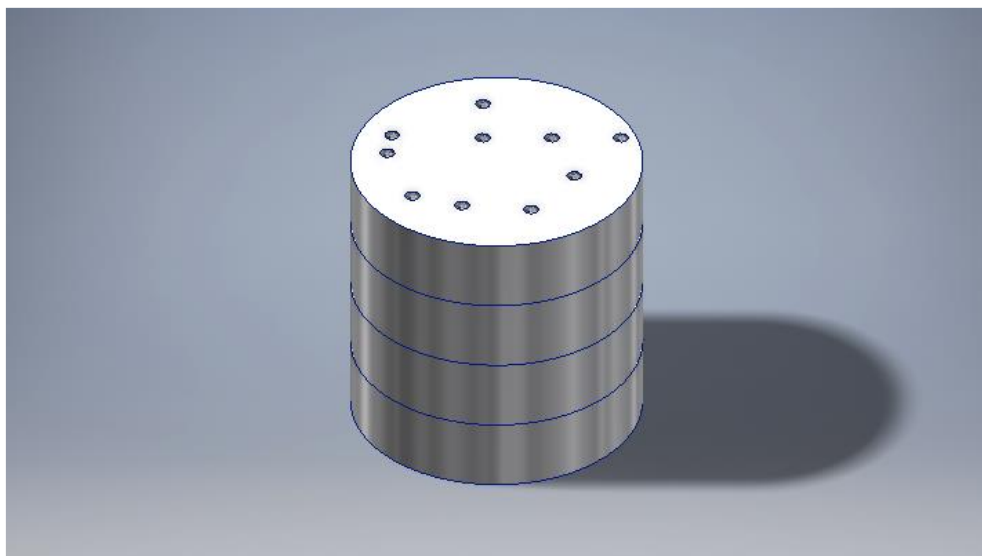


Figure 2.2: A 3D simulation of a number of disks piled on top of each other simulating a cylindrical bar with internal porosities

1.1 Pores' Features

In this section we will have a closer look at the features of the pores that have been drilled into the top surface of the disks using micro-drilling. The first thing to be considered is the number of the pores that can be produced as it will be influenced by the geometrical dimensions of the single pore and by the physical dimension of the aluminum disk. As the diameter of the disks are already known and the available tools at disposal that could be used to produce marks, it is decided to drill $N=36$ pores for each disk surface. Also to keep this experiment as close as possible to a real life scenario, the most obvious pattern of pore's distribution to be is a completely random one.

The next two features to talk about will be $[\rho]$, the radial distance from the center of the disk, and $[\theta]$, the angular position of the pore. Having set these two parameters, all the pores can just be defined as a combination of them. The decision of using ρ and θ instead of the coordinate x and y is due to the fact that the radial coordinates can give us information about the influence or not of the distance from the center, while the x and y cannot. Other important elements to be defined are the boundaries of these parameters in order to avoid incomplete pores close to the external edge of the disk, as also two intersecting cavities; in this way, the variables ρ and θ are set to have their values in two ranges:

$$0.3\mu\text{m} \leq \rho \leq 2.7\mu\text{m}$$

$$0 \leq \theta \leq 2\pi$$

Having a fixed number of pores N and the boundaries for $[\rho]$ and $[\theta]$, an acceptable random configuration of the pores' distribution can be chosen. In particular, between all the ones randomly produced by the automated algorithm, the one with no intersecting and efficiently distributed marks have been chosen; in this way the parameters $[\rho]$ and $[\theta]$ can be correctly studied.

As a result of this simulation and of the choices made, the pores' configuration that will be used to study a tomographic instrument's accuracy can be represented in Figure 2.3, together with the relative coordinates' list.

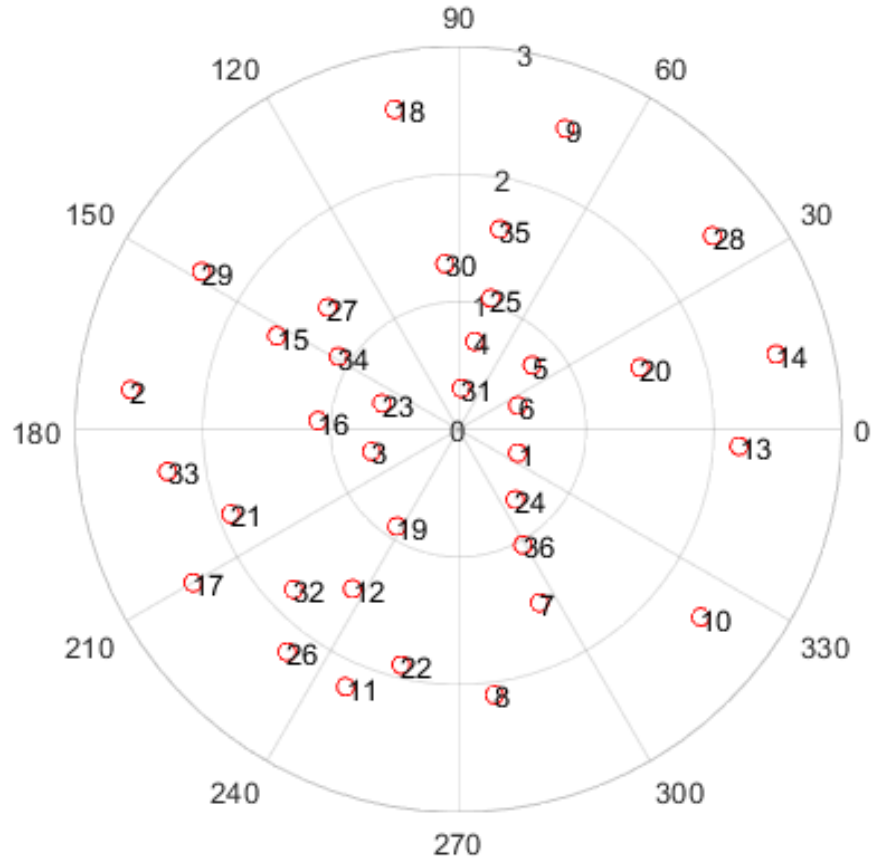


Figure 2.3: Polar plot of the pore's configuration, and the number associated to each pore.

#	ρ (mm)	θ (rad)	#	ρ (mm)	θ (rad)
1	0,500	5.902	19	0,900	4,147
2	2,584	3,021	20	1,500	0,328
3	0,700	3,393	21	1,900	3,499
4	0,700	1,388	22	1,900	4,474
5	0,765	0,717	23	0,632	2,813
6	0,500	0,379	24	0,708	5.931
7	1,500	5.149	25	1,057	1,329
8	2,100	4.848	26	2,200	4,057
9	2,500	1,229	27	1,400	2,392
10	2,400	5.624	28	2,500	0,652
11	2,200	4,299	29	2,361	2,590
12	1,500	4,127	30	1,300	1,652
13	2,200	6.223	31	0,321	1,502
14	2,554	0,232	32	1,800	3,914
15	1,600	2,666	33	2,300	3,286
16	1,100	3,079	34	1,100	2,597
17	2,400	3,666	35	1,600	1,368
18	2,554	1,768	36	1,037	5.220

Table 2.1: The configuration chosen to study the radial and angular factor ρ and θ , and the number associated to each pore

The last feature to be considered regarding the pores are the pores dimensions. The pores will have an average diameter of $320\mu\text{m}$, and an average height of $50\mu\text{m}$. We will have three disks, each having the same pores' configuration in terms of ρ and θ , the same diameter of $320\mu\text{m}$, and the same height of $50\mu\text{m}$. One last aluminum disk will be placed on top of the upper disk as a cover just to close the pores and make them internals instead of being open to the air as illustrated in figure 2.2. The reason why we will be studying three disks on top of each other is to take into consideration the vertical position of the disk, and see if the vertical position could have any influence on the readings of the XCT instrument.

2. The Case Design

The main issue that we could have with the pile design is the unwanted relative motion between the disks that could occur during the rotation of the pile during the tomography, this is of course due to the disk being in top of each without having something to keep them attached to each other. So, the need of a case comes up from the necessity of impeding the unwanted motion of the disks. It is necessary to fix the pile to the ground, making it possible to correctly conduct a precise tomographic measurement.

2.1 Giacomazzi's Case design

In the previous work [8], A simulation of the housing used to hold the cylindrical pile is illustrated in figure 2.4. The final design is simply a 3D printed cylindrical shaped case made of plastic that will house the disks on top of each other as shown in the following figure 2.4.

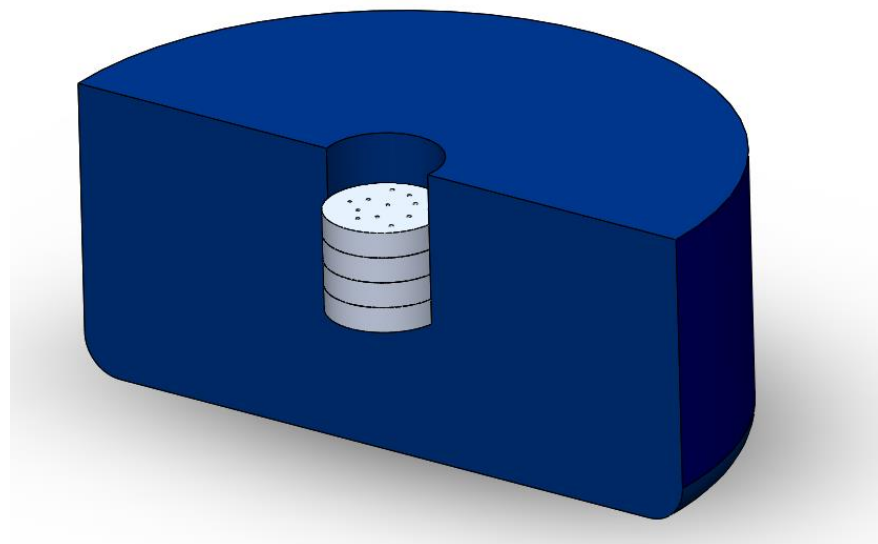


Figure 2.4:Section view of a simulation of Giacomazzi's Design of the lower case that will be housing the disks

As it can be seen from the previous figure 2.4, the design of the plastic case has a very large diameter compared to the disks that will be placed in its center creating a very thick wall case. The reason to this is to eliminate the problems that he had previously with a thin wall case design which are:

- The inclination problem.
- The multi-material problem.

The inclination problem is the one given by the 3D printing process where, due to the low wall thickness, the produced case can present an inclination of the lateral side so, when the pile is being scanned, there is the high risk of misalignment of the disks, with the formation of air gaps between them; in this way, the validity of our measurement would be nullified by the incorrect 3D reconstruction given by the failed stacking of the aluminum disks. But with having a larger wall thickness, the 3D printer is much more stable and precise during the printing of lateral walls of the case.

The second problem is the multi-material problem that exists due to the fact that now we will have three different materials to be scanned: Air, Plastic and Aluminum which will add another peak to the histogram during the thresholding process, making the thresholding process more complicated. So by having a thicker plastic wall, the entire scanned region, which were previously detected as air, will now be filled with the plastic material; In this way only two peaks will be on the radiation intensity histogram. In reality, there will always be the air-peak due to the presence of the holes.

One last improvement to impede the movement of the disks during the rotation of the table is to apply pressure on the pile by means of a counter-pile made of 3D printed spacers placed on top of the disks, then an upper case is placed on top of the lower case as a cover, and then the entire thing is wrapped in a masking tape which keeps everything tight together. The final design is shown in Figure 2.5.

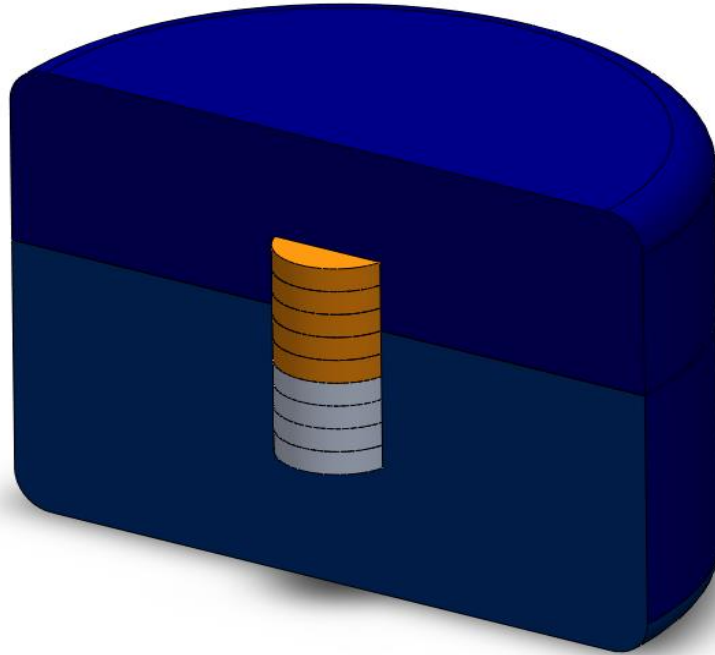


Figure 2.5: Final design of the case containing the aluminum pile, the spacers (in orange), and the upper case positioned on top

2.2 Drawbacks of Giacomazzi's Case design

Even though a case was built to prevent the unwanted motions of the disks, yet another issue has arisen due to the spacers that has been used to keep the disks in stationary position, and the way that was used to lock the case in place. As it has already been mentioned, the spacers are placed on top of the disks and then the upper case is placed on top of the lower case, and then the entire thing is wrapped in a masking tape which keeps everything tight together and under pressure. The main issue with this design is that the pressure that keeps the disks tight together might vary depending on how the spacers are placed and how the masking tape is wrapped around the case, which is of course done manually causing the pressure to vary from one experiment to another. And even if the tape is well wrapped around the case, there is a possibility that the tape might start to loosen up during the scanning process

causing a variation in the pressure, specially that it takes around 60 to 90 minutes to perform one single scan. And even if the variation might be of a non significant values, but this variation might lead to a significant variation in the air gap between the disks which will obviously lead to a non-replicable experiment, which is one of Giacomazzi's final outcomes.

2.3 Proposed Solution

To solve this problem, a new case design was required to be thought of, and the common suggestion was based on keeping the previous design somehow the same with adding slight modifications. The modifications will be mainly based on finding a different way to lock the upper and lower case together and keep the disks in position without having the pressure variation due to the spacers and the masking tape that we had in the previous design.

The first modification was that instead of using multiple number of spacers to keep the disks down, a vertical part attached to the upper case is to be 3d printed as seen in figure 2.6. This part will keep the disks down and in place.

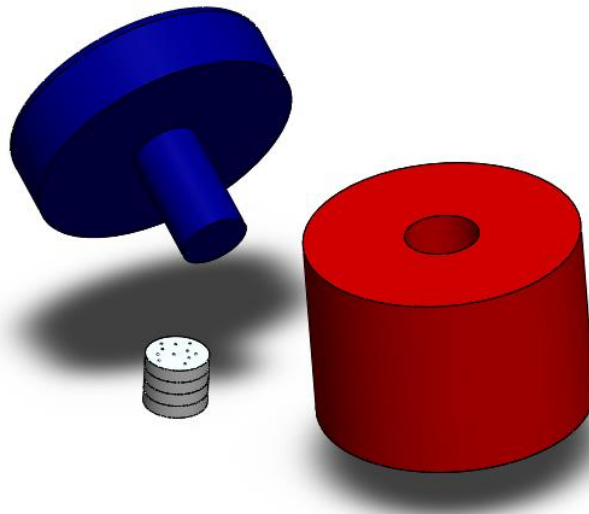


Figure 2.6: A 3D model of the case design with the first modification

As it can be seen from the last figure, the lower case is kept the same, the pile of disks and the upper case has an extra vertical part that will be pushing the disks downwards as they are placed inside the lower case. The second modification is related to how the upper and lower case are tightened together. The proposed method is to add threaded holes to the upper and lower cases, and using a screw to keep the two cases attached to each other. By using this method, simply a screw driver can be used to tighten up the screw and maintain the locking pressure constant during the scanning process. In this way the air gap between the disks will not vary or change during the scanning process, and a more stable and replicable experiment is obtained.

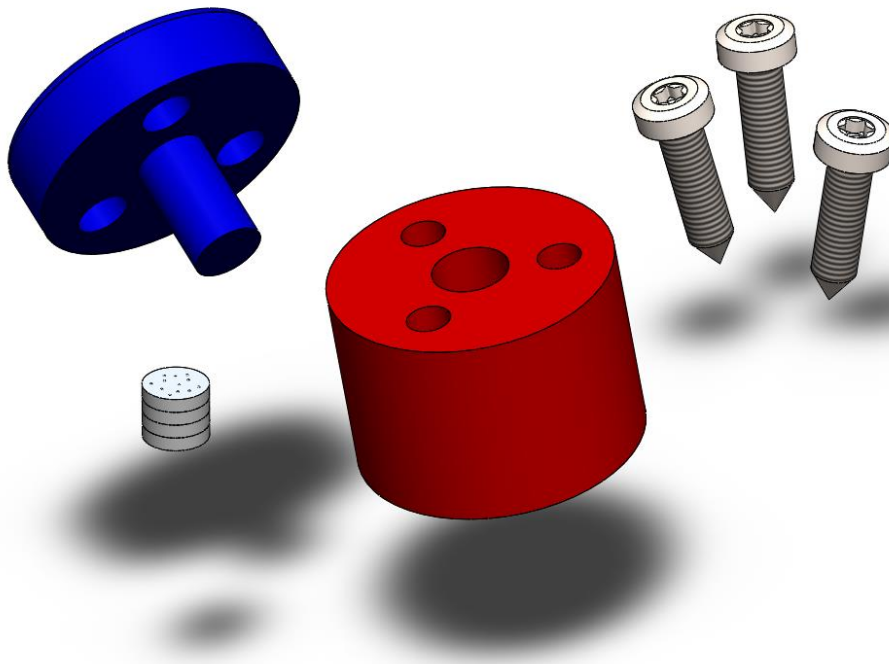


Figure 2.7: A 3D model of the case design with the second modification of the threaded holes and screws.

One note that has been taken into consideration during the 3D Model design was the multi-material issue due to the existence of the screws that are made of a material with a density close to the one of the Aluminum pile. This would cause the thresholding process to be more complicated and the possibility of having some troubles during the image reconstruction.

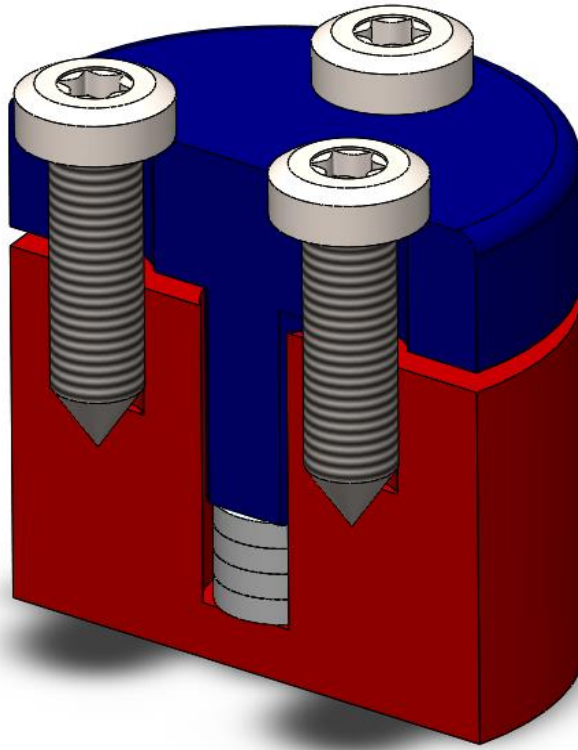


Figure 2.8: A section view of the complete model after placing the pile and the screws

In order to solve this problem, the design of the of the case was slightly modified in terms of dimensions in a way that the pile of disks are placed a little lower and the screws are slightly higher. As the model is placed horizontally during the scanning of the XCT instrument, we can control the XCT's field of vision in a way that the three screws are out of vision, and only the pile of disks is detected by the instrument.

As it can be seen from the following figure 2.9. We can control the limits of the XCT's field of vision in a way that the screws are above the upper limit, and so, the final image to be detected will only contain the pile of disks and the surrounding plastic case.

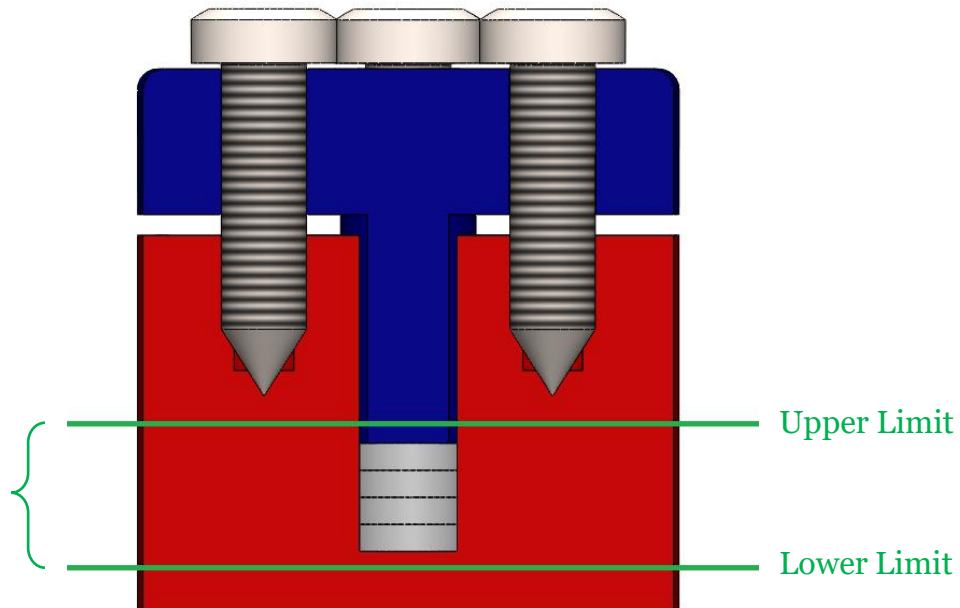


Figure 2.9: A section view of the model showing the upper and lower limits of the XCT's field of vision

2.4 Case Production

The final step of this campaign is related to the production of the designed case. Two decisions were to be made:

- 1) The screw type and size.
- 2) The dimensions of the upper and lower plastic case.

First we need to choose the screws that will be used to hold the upper and lower cases together. This is an important step as the size of the screws will have an influence on the dimensions of the plastic case.

Two different approaches are can be chosen from . The first approach is to choose a screw type and size that will fit the model and is at our disposal, then make sure that the screw is stored in the library of the CAD software, and finally design the threading

of the screw using the software, so the end model will have the threading printed by the 3D machine. The second approach is to once again choose a screw type and size, but instead of designing the threading using the software, we just create a cylindrical tube in the model with a slightly smaller diameter. Then after the case model is printed, the screw will be forcedly inserted through the cylindrical tube using a screwdriver, which will create the threading inside the cylindrical tube. After much consideration regarding the available alternatives and simpler options, we have decided to go with the second approach, as it's much easier and flexible option. The screw type that has been chosen is a pan head self-drilling screw, having an external threading diameter of 5mm shown in the following figure 2.10. The self-drilling feature of the screws will help to create the threading needed.



Figure 2.10: Example of pan head self-drilling screws as the ones used for the case model

The next step is to design the case using a CAD software, and the software chosen for this task is SolidWorks. Considering the size and the dimensions of the screw, the size of the upper and lower case had to be chosen carefully. The external diameter of the case has been chosen to be 26mm, which is slightly larger than Giacomazzi's case, in order to house the two screws. The main cylindrical tube where the disks were to be placed inside will have a diameter of 7mm, which is 1mm larger than the disk's diameter, in order for the disks not to get stuck inside of the tube. The upper case will have two cylindrical tube cuts of a 2.5mm in radius where the screw can go through. While the lower case will have a slightly smaller cylindrical tube radius of 2mm, which is 0.5mm

smaller than the external radius of the screws. This will prevent the screws from going through the lower case tube, but easily enough for the screw to be forcedly inserted into it using a screwdriver, and creating the threading needed.

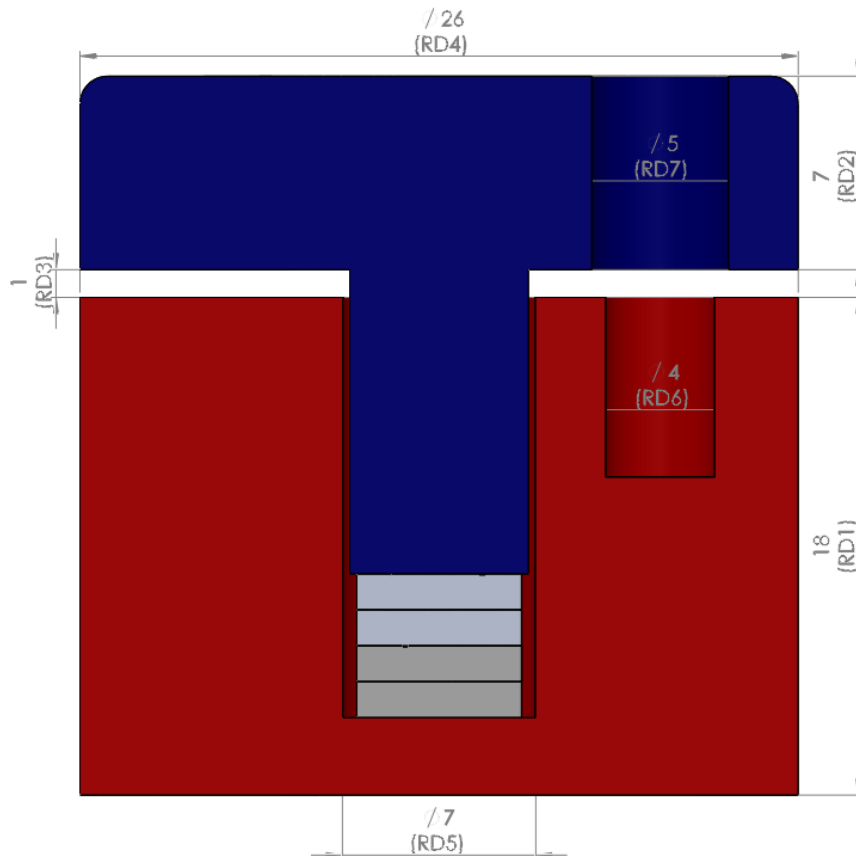


Figure 2.11: A section view of the case while its being designed using SolidWorks with dimensions assigned it.

One last modification in the dimensions was regarding the central extended part of the upper case which will be inserted in the central cylinder tube of the lower case. The extended part was designed to be 1 mm taller than the cylindrical tube after placing it on top of the disks as shown in figure 2.11. This way we will insure that that by placing the upper case on top of the lower case, the extended part will be pushing the disks down and keeping them under pressure preventing any kind of movements. And even though there will be a small gap between the upper and lower cases, they

will be kept in contact using the screws. Finally after the CAD design has been approved, the design has been saved as a .STL file which will be used later by the 3D machine to build the Model. The final model of the case is shown in figures 2.12.

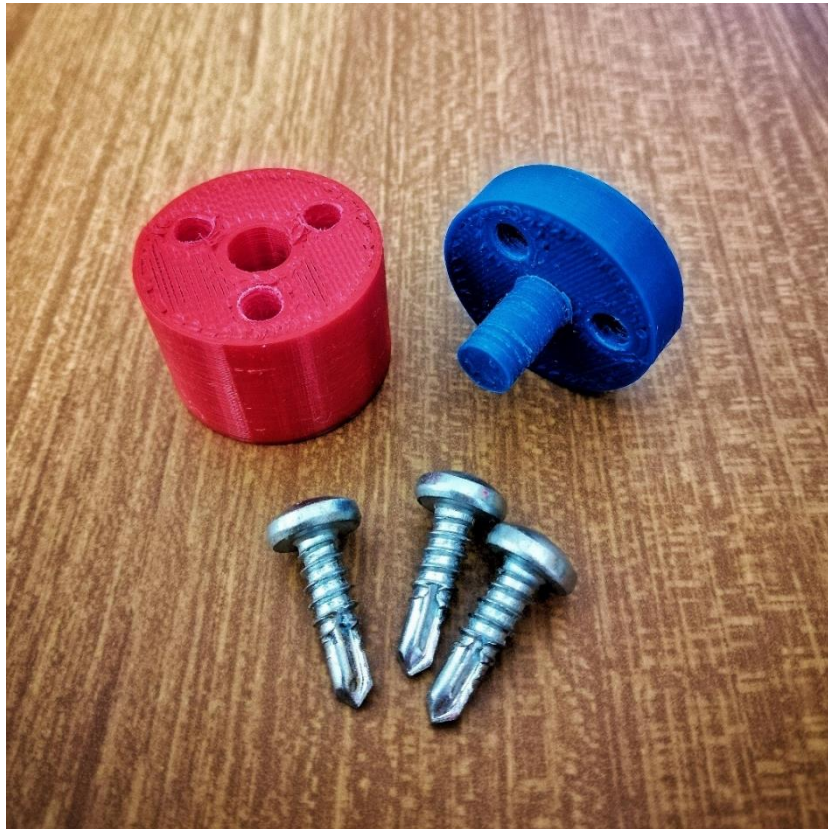


Figure 2.12: The Final model of the case after production including the three screws

After the production of the upper and lower parts of the case, one final testing is required to make sure that the all parts fit together. A screw driver has been used to push the screw through the slot drilled at the lower part case creating the threading. The four disks have been placed inside the lower part case easily, the upper part case is then placed on top of everything, and the three screws are screwed tightly to keep everything in place. The final result was a secure and robust case, maintaining the disks in contact, under pressure, and most importantly, free of movement.

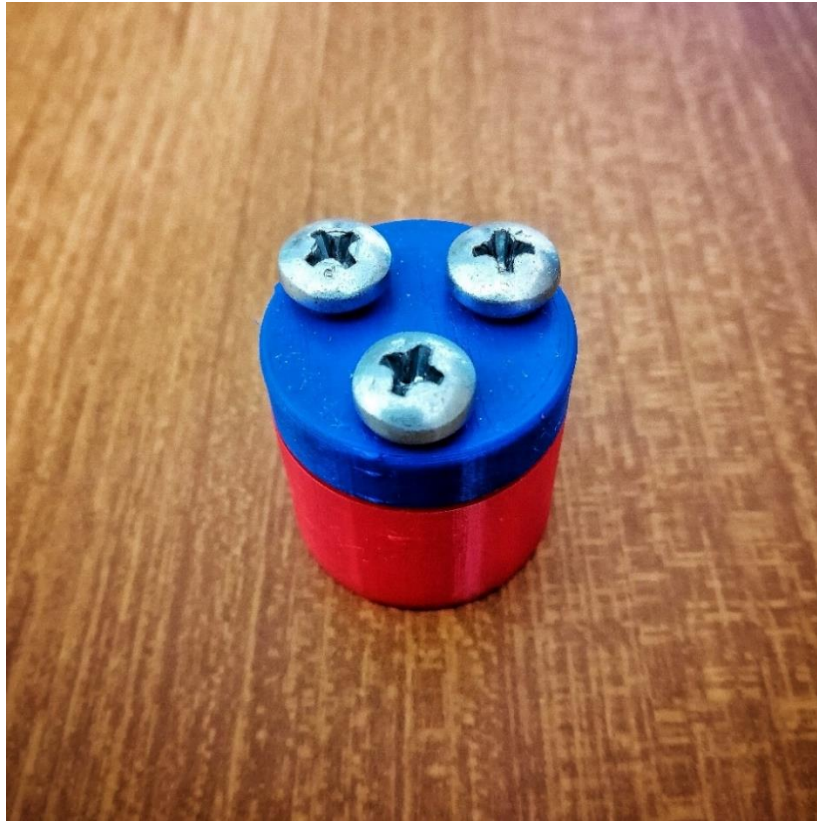


Figure 2.13: The Final model of the case after Assembly

3. The Powder

The last thing to be considered in this chapter is the powder that is used to simulate unprocessed powder. For this study we will be using $AlSi7Mg0.6$ (A357). A gas atomized powder produced by LPW Ltd. The powder has a particle size distribution that follows a log-normal distribution with a mean particle size equal to 40 μm .

Chapter 3

The Work Flow

As it has been mentioned earlier, the main objective here is to study the capability of an XCT instrument to detect unprocessed powder and the effect that it could have on the readings obtained by the instrument. The main approach to perform this test is to pour some powder on a disk that already has artificial pores in a way that the powder fill some of the cavities of the pores in a complete random manner. Using the XCT instrument we will measure the dimensions of the pores on the disk once without any powder and once again with the powder on it. Later we need to analyze the difference in the XCT readings between the two cases regarding the pores' geometrical dimensions to understand the influence of the unprocessed powder. A brief representation of this idea is illustrated in Figure 3.1. This figure shows two separated branches representing the two cases, the first one being the case without the powder and the second being the case with the powder, and their paths to reach the final data.

The two cases will follow exactly the same path with the only difference of powder added in the second case:

- Scanning of the disk using the XCT instrument.
- Extracting a set of grayscale images with .png extension as the output reading of the XCT instrument.
- Importing the set of images into Matlab and using the Matlab code and functions to measure the pores' properties.
- Finding the difference in the readings between the pore's dimensions in both cases and the reference values obtained by Alicona instrument. And using these differences in the readings (error) as the output response.
- Using Minitab to analyze the responses and evaluate the capability and accuracy of the XCT instrument.

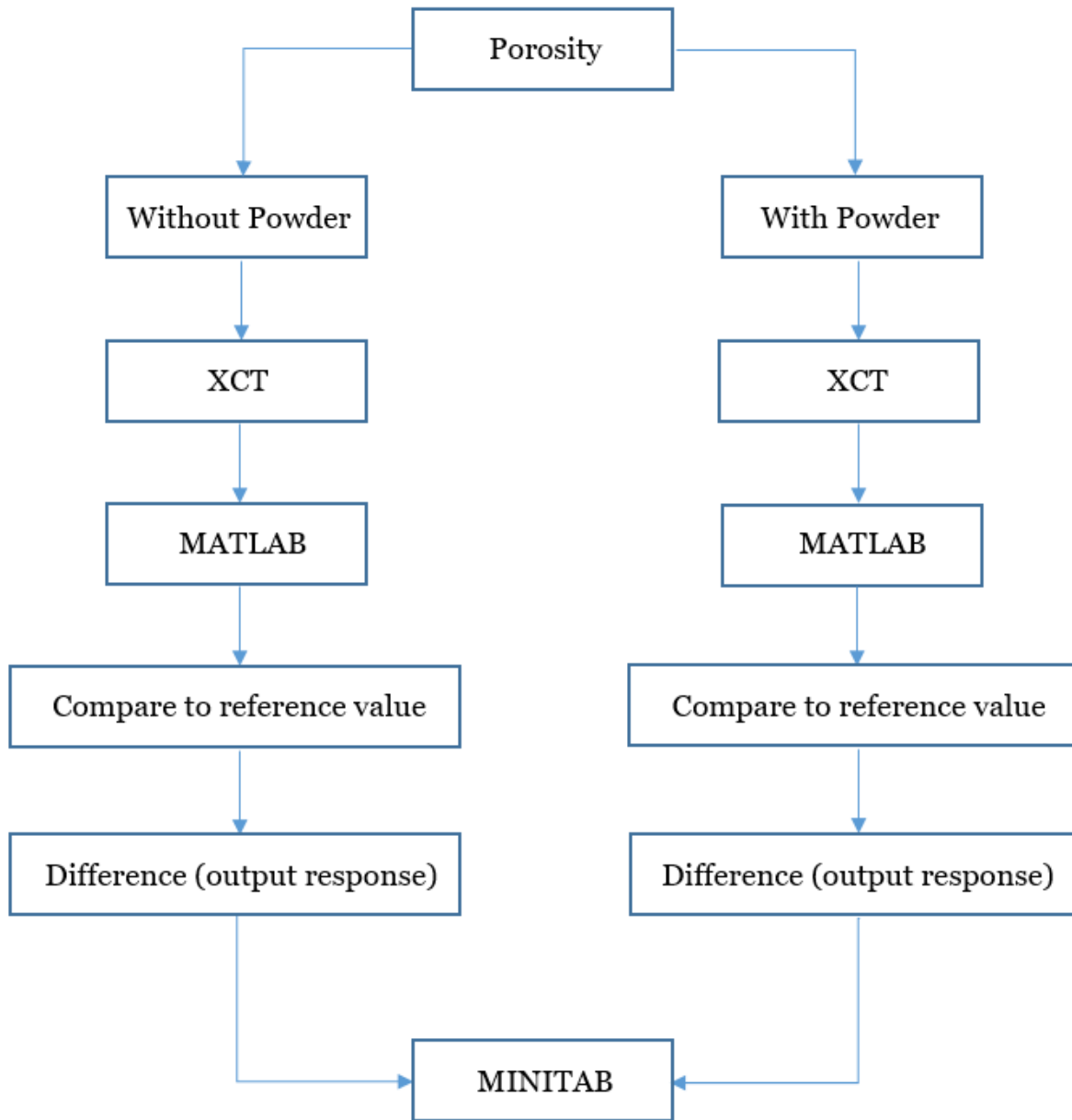


Figure 3.1: Schematic representation of the procedure activities and the work flow of the experiment campaign

1. Influencing Factors

The first fundamental element to define is a list of the influencing factors that we want to take into consideration. The first two factors whose influence is wanted to be studied are the angular and the radial position of a specific pore on the disk's surface $[\theta, \rho]$ as it's important to understand if and how the position of the porosity inside the scanned component can influence the XCT's measurement. Together with these two factors, the third factor to be studied is the vertical position. So, we define also the factor $[Z]$, which is the vertical position of the pore. Due to the fact that the pores are disposed on the planar surface of the disk, the factor $[Z]$ will be limited to a finite number of values, which is indeed the number of the disks forming the pile. So, it was decided to have 3 different levels of the factor $[Z]$, which are $-1, 0$ and $+1$, indicating respectively the lower, the in-between and the upper one, as in Figure 3.2.

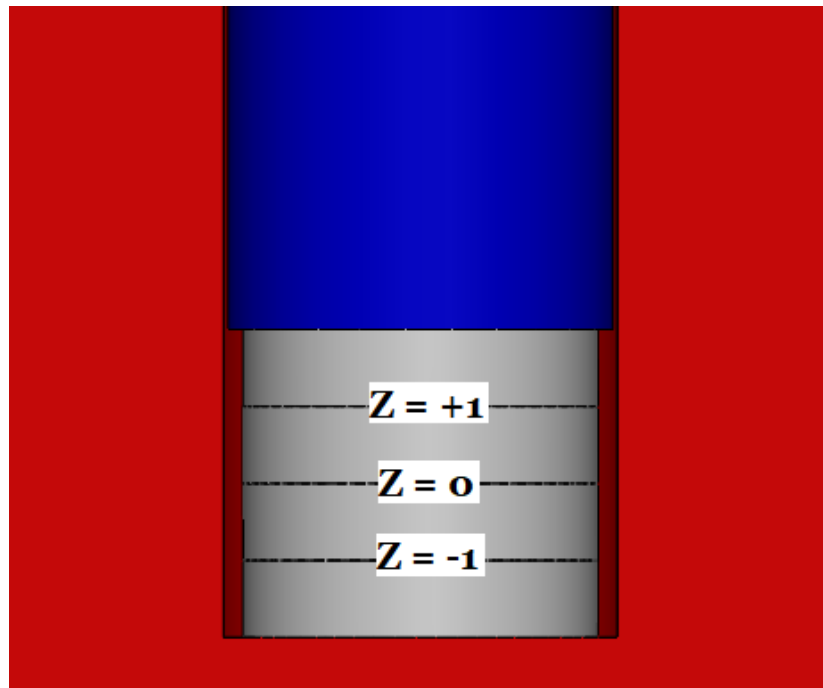


Figure 3.2: Schematic representation indicating where the cavities will be positioned regarding the vertical axis

As it has already been mentioned during the first chapter that one of Giacomazzi's conclusions about his experiment was that the accuracy of the XCT's measurement is independent of the angular position of the pores, or the orientation of the pile. This means that we already know in advance that the angular position [θ] is not of a significant factor. So, the angular position [θ] can be left out. Regarding the two other factors [ρ , Z], even though Giacomazzi's work shows that those factors have significant influence on the accuracy of the XCT, yet we can re-consider them in our experiment for couple of reasons. The first one is to double check that those factors are in fact significant and were not due to experimental errors. The second reason is to consider the different case scenario. Which in our case we are comparing between two cases which both will be conducted using the same XCT instrument, where one will be without powder and one with powder added.

Finally the last factor to be considered, which is probably the most important factor in this experiment. It's the one related directly to the powder. We will be calling this factor by the name of "Powder", and it will be given the letter [p]. Considering that the main objective of the experiment is to study the influence of the powder, there are two different ways of representing the levels of [p]. The first one is using \emptyset and 1, where \emptyset means no powder at all, and 1 means with powder regardless of the quantity. This way will help us to only study if the powder has an influence on the output response or not. The second way is to introduce different levels of [p], starting from \emptyset as no powder and increasing the digit number as the quantity of powder increases. But due to the fact that the powder is distributed randomly by hands; this makes it nearly impossible to control the amount of powder, making the best choice for this study is to use the two-level system of \emptyset , 1.

So our final influencing factors to be considered in our study are:

- Pore's radial position [ρ]
- Pore's vertical Position [Z]
- Powder [p]

2. Measured Dimensions

The idea of the experimental campaign is to perform two cases represented by the two branches in figure 3.1, and maintain the two branches as similar as possible to minimize any error from propagating through the branches. Then, in order to perform a comparison between these branches' outputs, the same porosity's dimensions have to be measured.

The idea is to extract and elaborate all the spatial dimensions of the cavities evaluated in both branches using XCT and to find the difference in measurements between them and the reference values obtained from the instrument ALICONA which will represent our output responses. The output responses of the two branches will be compared with each other to study if the powder has any significant influence on the readings obtained by the XCT. So in order to follow through the experiment, we have to first identify the measured geometrical dimensions chosen for this study that will be used to find our output responses.

- D_1 [μm]
- D_2 [μm]
- h [μm]
- A [μm^2]
- V [μm^3]

The variables D_1 and D_2 are the maximum spatial length along the directions x and y , while h is the depth of the cavity, A is the area of the external surface and V is the volume enclosed by the external surface.

Due to the fact that the porosities will be characterized by a circular section; instead of using D_1 and D_2 , the average value between these two values will be used instead, and will be referred to as the mean diameter [D_m]. Next, we take a look at the reference values.

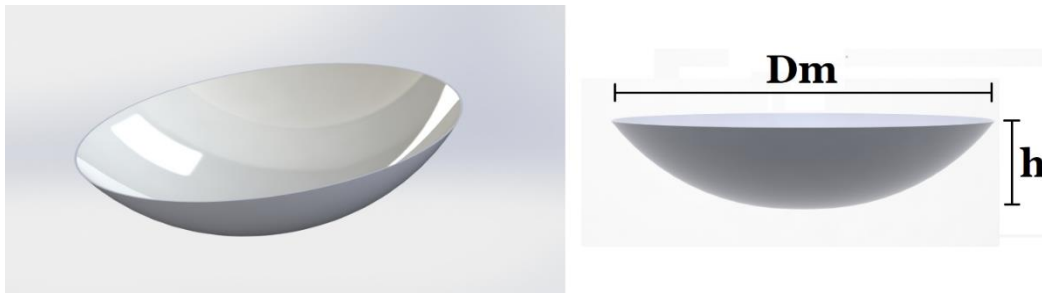


Figure 3.3: Representation of the variables chosen to study the porosities

3. Reference Values

The 3D micro coordinate measurement instrument *Alicona Infinite Focus*, illustrated in figure 1.3, is capable of performing measurements with very high resolution, high repeatability, and accuracy. This instrument will be used to measure the dimensions of the variables that have been mentioned earlier, and use these values as a reference where the dimensions measured by the XCT instrument will be compared to.

4. Response Variables

Considering that our influencing factors are:

- Pore's radial position [ρ]
- Pore's vertical Position [Z]
- Powder [P]

The response variable of the experiment can be described by the following equation:

$$\text{Difference } \Delta X = X_{\text{XCT}}(\rho, Z) - X_{\text{ALICONA}}(\rho, Z)$$

where X will correspond to the measured dimensions of the study [D_m, h, A, V].

5. Software and Matlab Code:

Once that all the tests have been designed, an acquisition procedure able to process all the data is needed. So, in order to extract all the information available from the scanned object, a software procedure is needed to construct a virtual 3D part and evaluate the dimensions of our interest. The X-ray Computed Tomography system comes with NSI raw data analysis software that is able to reconstruct a 3d model of the actual physical specimen that is being scanned. Using this software we are able to extract a set of gray scale images with .png extension representing the different layers of the specimen. These images will then be used as an input to our Matlab code.

5.1 Matlab

A Matlab code will be used to perform the required functions. It starts with the set of grayscale images being imported into Matlab, which then goes through each image, finds the threshold value according to Otsu's method and apply the thresholding to the gray scale image. It carries on with reconstructing a 3d model of the specimen that has been scanned with the artificial pores. The Matlab code is then able to detect the artificial pores which can be seen indicated in red in figure 3.4, and evaluate the dimensions of each pore individually using a set of functions.

The first thing to be performed is to calculate the 1D geometrical dimensions of the pores by means of the function *BoundingBox3d* [10]; this function extracts the 6 coordinates (2 for each direction) which defines the boundaries of the box entirely containing the 3D element studied (which is the pores in our case. By calculating the absolute value of the difference between the maximum and minimum coordinates in a certain direction, it is then possible to extract the dimensional lengths of the cavity (D_1 D_2 h).

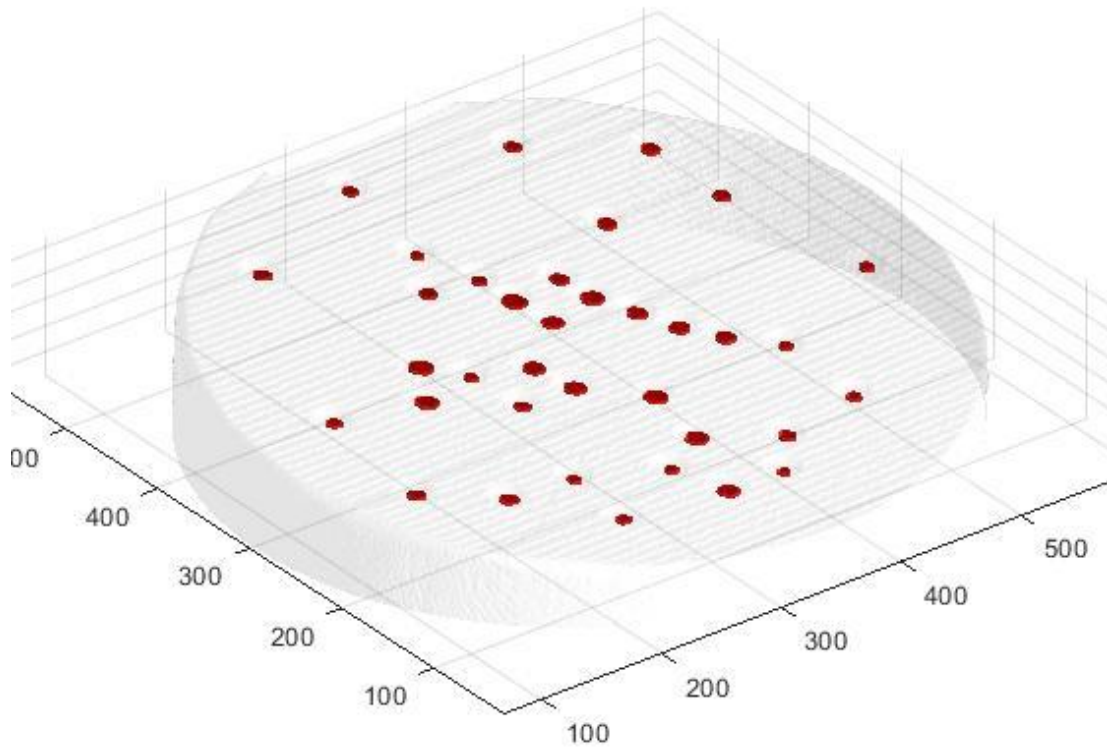


Figure 3.4: Reconstruction of the 3D model by the Matlab Code with the artificial pores indicated in red.

Having estimated the 1D geometrical dimensions of the cavity, it is now possible to extract the data about the external surface of the porosity and its volume occupied. These data are respectively evaluated by means of the function *MeshSurfaceArea* [10] and *MeshVolume* [10], which are able to evaluate the two needed responses by using the triangular elements and the vertices of the porosity.

MeshSurfaceArea computes the surface area of the mesh specified by a vertex array and a face array; it also iterates on faces, extracts vertices of the current face and then computes the sum of the faces' areas. Instead, the function *MeshVolume* computes the volume of the space enclosed by the polygonal mesh represented by the vertex array and the faces one; then, the total output volume is computed as the sum of the signed volumes of tetrahedra formed by triangular faces and the centroid of the mesh.

Now that all the data required have been calculated, it is then possible to extract all the dimensions from all the measurements performed in the two cases. Later, it is possible to study the differences between the results obtained by both cases, in order to be able to make a statement about the XCT's capability and accuracy.

5.2 CloudCompare

CloudCompare [9], is an open source 3D point cloud processing software that provides a set of basic tools for manually handling, editing and rendering 3D points clouds and triangular meshes. In this study, CloudCompare will be used to illustrate 3d model constructions of the pores, which will help us to study and have a closer look at the pores and perform comparisons as we will be seeing in the following chapters. The way the software is going to be used here is by taking advantage of the Matlab code. As the Matlab code is able to isolate the pores from the surrounding, these pores are read as 3D meshes that can later be saved as an .STL file, and be lunched by CloudCompare to perform the required tasks.

5.3 Minitab

After having extracted all the useful and needed information from the measurements performed in the two cases, the output response variables obtained are finally ready to be studied by means of the statistical software Minitab [10]. Using this software, it will be possible to perform some statistical tools to analyze and evaluate the XCT's measurements, understand which and how the influencing factors would have a significant influence on the response variables, and finally have a clear conclusion regarding this experimental work.

Chapter 4

Single Disk Experiment and Analysis

In this chapter we will be talking about the first experiment of the campaign; the scanning of a single Aluminum disk using the XCT instrument, the 3D construction of the scanned model, a close look at the measured dimensions, and finally analyzing the variable responses. Before building the plastic case to pile up the disks and perform the experiment, we decided first to try to scan a single aluminum disk with pores opened to the air, once without powder and once again with the powder. Then see if the XCT instrument is able to detect the presence of the powder, and if yes, will it cause any significant changes to the pores' geometrical dimensions or not⁵⁶. This will help us in terms of cost and time consumption to understand first if the XCT is able to detect the powder's presence and its effect without the need of having to build the plastic case, piling the disks on top of each other, and performing a more complicated experiment. So to sum things up, our campaign will go through two different experiments, the single disk experiment, using only one single aluminum disk with open pores simulating external pores, and the second experiment, piling up all the disks on top of each other which is to be held by the 3D-built plastic case simulating internal pores.

1. Single Disk Experiment

To start with the first experiment, we will only deal with one aluminum disk, so it's obvious that we won't have all the different influencing parameters such as the Pore's vertical position [Z]. Instead we will only consider the pore's radial position [ρ] and the powder [p]. The disk we will be using in this experiment will have artificial pores with characteristics of $320\mu\text{m}$ in diameter, and $50\mu\text{m}$ in height on average.

As for both experiments we will be performing two cases, the case without powder and the case with the powder. For both cases, The single disk is placed horizontally inside the XCT instrument, while trying to maintain the instrument's scanning configuration the same as possible in both cases.

1.1 Without Powder

The first case to be examined is the case without the powder. The experiment starts with placing a single disk into the XCT in a horizontal position. The XCT then performs the scanning phase and a 3d model of the disk is reconstructed using the NSI software that comes with the XCT instrument, but in order to be able to extract a useful output files that could be used as an input for our Matlab code, a set of grayscale images with .png extensions will be saved as our output. An example of these grayscale images can be seen in figure 4.1.

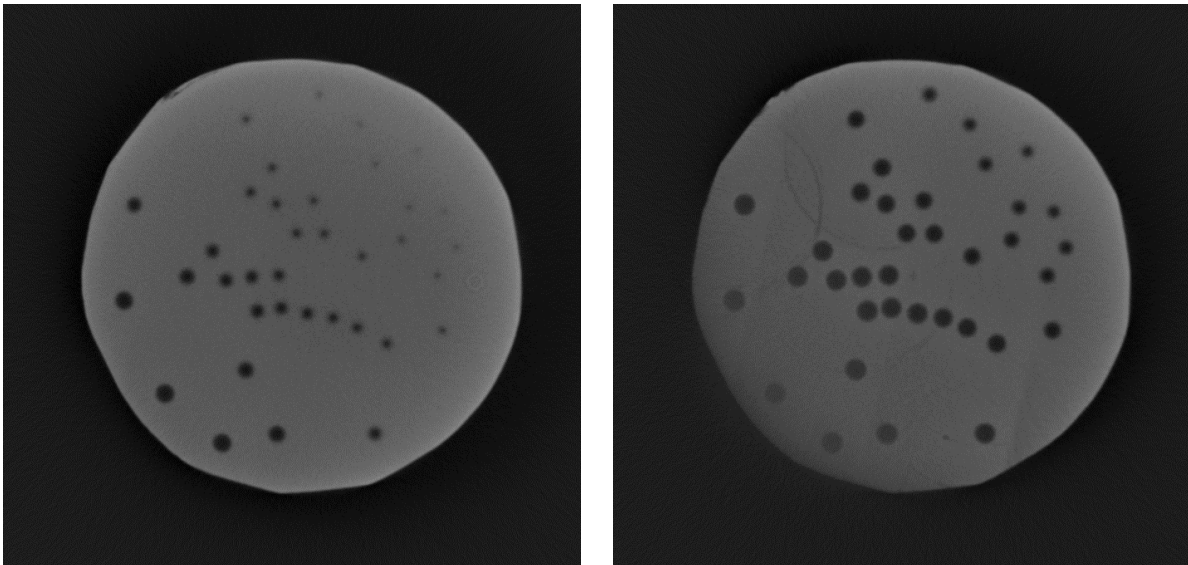


Figure 4.1: Examples of grayscale images that are obtained as an output of the XCT machine

Each image represents a very thin slice of layer of the scanned object. By placing all the layers on top of each other we are able to obtain a three dimension view of the object creating a 3D model. As it can be seen from figure 4.1, by looking at the grayscale image we are already able to detect the artificial pores, their placement and their shapes. Next, the images are used as an input to our Matlab code as it has been mentioned in the previous chapter. The images are singly thresholded using Otsu's method and a 3d model is reconstructed showing the disk with the pores indicated in red color. In the following figure 4.2, we can easily see the 36 artificial pores, where the Matlab functions that have been talked about in the previous chapter will evaluate the geometrical dimensions of the 36 pores.

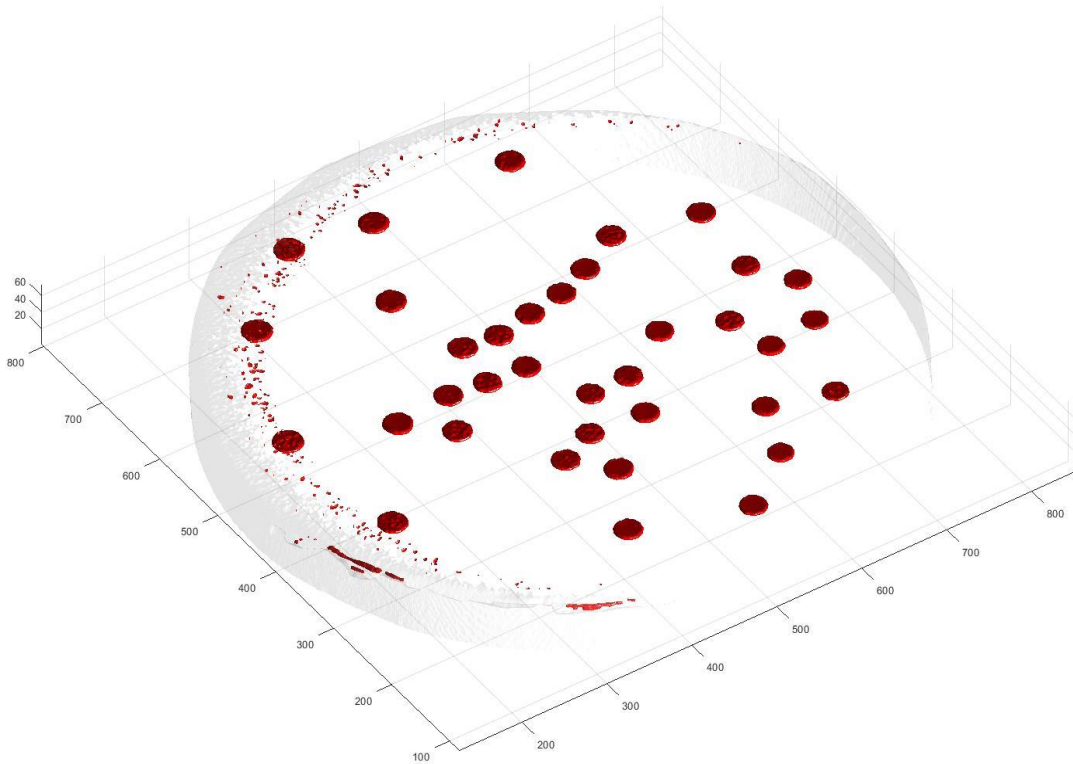


Figure 4.2: Reconstruction of the 3D model by the Matlab Code with the artificial pores indicated in red.

1.2 With Powder

The second case to be examined is the case with the powder. The experiment starts with placing some powder by hand on top of the disk randomly in a way that it represents unprocessed powder. The disk is then placed into the XCT instrument in a horizontal position. The XCT then performs the scanning phase and a 3D model of the disk is reconstructed, and a set of grayscale images with .png extensions will be saved as our output, exactly following the same procedure of the first case.

By looking at figure 4.3, we are already able to detect the artificial pores, their placement and their shapes. But in this case we are also able to see each individual powder particle, and how they are randomly spread all over the disk. By taking a close look at each of the pores, we realize that each individual pore has at least one single powder particle occupying its space, making the experiment valid to be conducted.

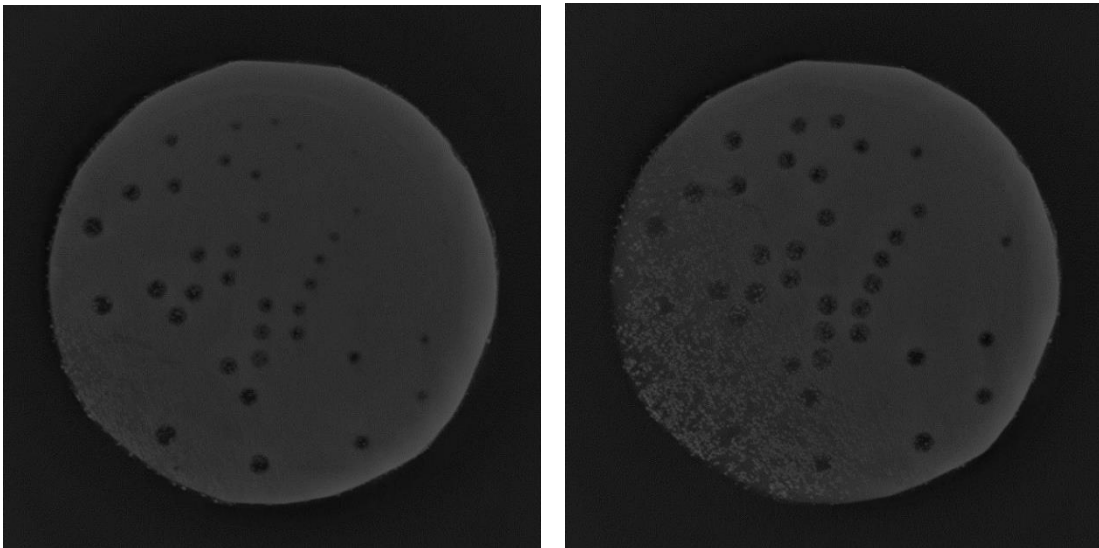


Figure 4.3: Examples of grayscale images with powder added

The images are used as an input to our Matlab code and the images are singly thresholded using Otsu's method and a 3D model is reconstructed showing the disk with the pores in a different color. In the following figure 4.4, we can once again see the 36 artificial pores, where the Matlab functions will evaluate the dimensions.

Looking at figure 4.4, we see that the powder particle has caused some major changes in the shape of most of the pores. Yet, in order to have a closer look at the pores and to compare the two cases together side by side, we can extract a .STL file from our Matlab code containing only the pores after it has been isolated from the rest of the disk. The .STL file can then be lunched using CloudCompare to see the isolated pores.

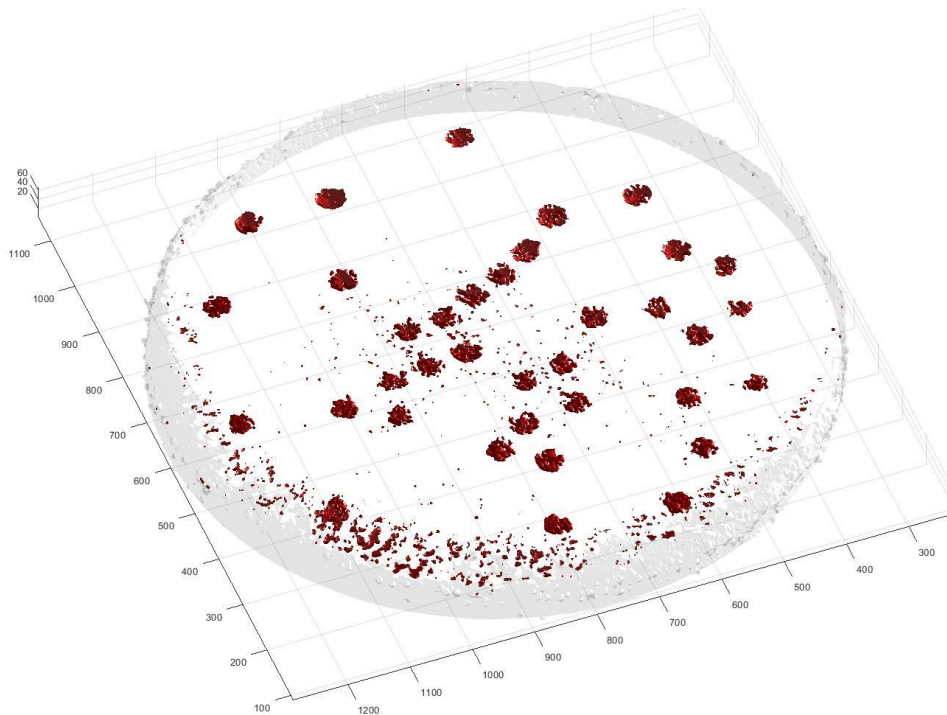


Figure 4.4: Reconstruction of the 3D model by the Matlab Code with the artificial pores indicated in red.

In order to have a clear comparison between the two cases, we will be eliminating the small extra pores that are being detected, and only keep the 36 artificial pores to be compared side by side. One main issue that we have with the scanned images is the orientation of the disk, as it can be seen from figure 4.1 and figure 4.3 that the disk in each case has a different orientation. So in order to solve this issue, a useful tool in CloudCompare called “Aligns two clouds by picking at least 4 equivalent point pairs” can be used to align the two images and place them next to each other so we can have a good view of the difference between the two cases as shown in figure 4.5.

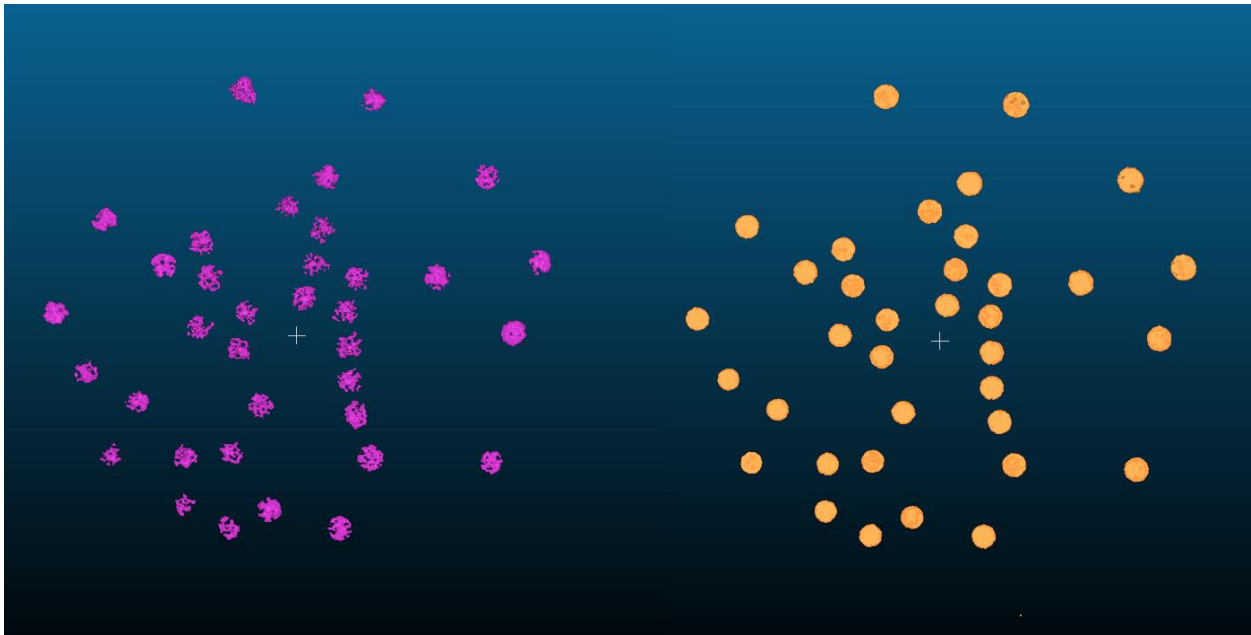


Figure 4.5: A side by side comparison of the two cases after alignment using CloudCompare

From figure 4.5 we can see how the two cases are compared side by side. The first thing we can realize is how some powder are trapped inside the pore creating what seem like holes in the pores themselves, and how other powder are located along the circumference of the pores causing the pores to not have a circular shape anymore. We can also notice that in general the pores seem to have reduced in size due to the powder. Yet, we will have to prove this statistically to see if the reduction in size is in overall significant or not.

As we mentioned before, the powder trapped within the pore's circumference will be taken as an influencing factor [p]. So as we are building the responses' table for this experiment, responses taken from the case without powder will have the factor [p] set to [0], while responses taken from the case with powder will have factor [p] set to [1].

The next step is to build our responses' table that will be used as our input to the software Minitab to analyze the data. Using the Matlab code we can find all the

geometrical dimensions, Diameter [D_m], Height [h], Area [A], Volume [V] associated with each pore for both cases. Then by calculating the differences between the corresponding measurement of each pore in the two cases and the measurement taken from the reference instrument ALICONA we can build our final table. As shown in table A.1 in the Appendix. The first Column represents the number associated to each pore according to the pores' configuration shown in figure 2.3. The next two columns represent the two influencing factors, the pore's radial position [ρ] and powder [p], and the last four columns show the variable responses ΔD_m (μm), Δh (μm), ΔA (mm^2), ΔV (mm^3) of each of the 36 pore.

After the responses' table has been constructed, its time to analyze the data and perform statistical analysis to understand if the any of the influencing factors have any effect on any of the response variables. The table will be used as an input to the statistical software Minitab which will be used as mentioned to be perform the analysis. The Analysis that will be performed on the data is basic ANOVA analysis, So starting from the next section we will be working with Minitab and the data shown in Table A.1.

2. ANOVA Analysis

The ANOVA analysis will be performed on each of the response variables independently of the others. So we will be performing the analysis following the order below:

1. Difference in mean diameter [ΔD_m]
2. Difference in height [Δh]
3. Difference in area [ΔA]
4. Difference in volume [ΔV]

2.1 Difference in Mean Diameter [ΔD_m]

We start by performing a scatterplot and a main effect plot on the response to see visually see how does the response change with the influencing factors.

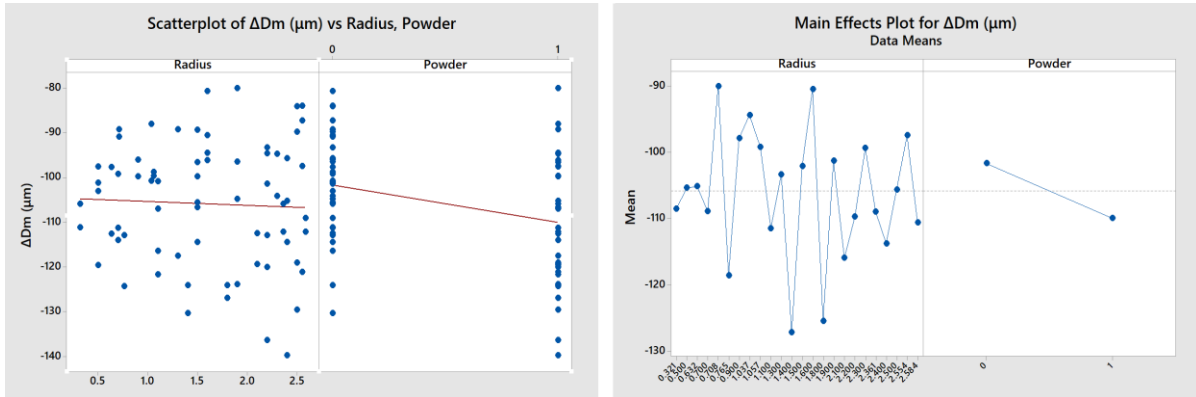


Figure 4.6: A scatter plot and main effect plot of ΔD_m

By looking at figure 4.6, the radius factor shows that the points are spread all over the place, and its almost impossible to detect a pattern. On the other hand regarding the powder factor, the main effect plot shows that there is a slight reduction in terms of diameter, but in order to check the significance of this reduction we will need to perform ANOVA analysis on the response [ΔD_m].

Analysis of Variance

Source	DF	Adj SS	Adj MS	F-Value	P-Value
Radius	23	5266	229.0	1.64	0.074
Powder	1	1235	1235.0	8.87	0.005
Error	47	6545	139.3		
Lack-of-Fit	23	2371	103.1	0.59	0.893
Pure Error	24	4174	173.9		
Total	71	13047			

Model Summary

S	R-sq	R-sq(adj)	R-sq(pred)
11.8008	49.83%	24.21%	0.00%

Table 4.1: ANOVA Table of the response [ΔD_m]

The ANOVA analysis is performed for all responses by eliminating the interaction factor, as it eliminates some of the problems we had when verifying the model. From the ANOVA table shown in table 4.1, the powder factor shows to have a significant influence on the response with a P-value of 0.005, while the radius has a P-value higher than 0.05, stating that it's not significant. The R-sq(adj) is quite low, and the lack of fit is not a significant factor with a P-value of 0.893. %. The hypothesis of the residuals are verified, and the model is accepted. So in the end we can conclude that regarding the first response [ΔD_m] that the radius is not a significant factor, but the powder is a significant one.

2.2 Difference in height [Δh]

Next we will be performing ANOVA analysis to study the influence of our factors on the height of the pores. Once again we start by performing the scatterplot and the main effects plot for the difference in height [Δh].

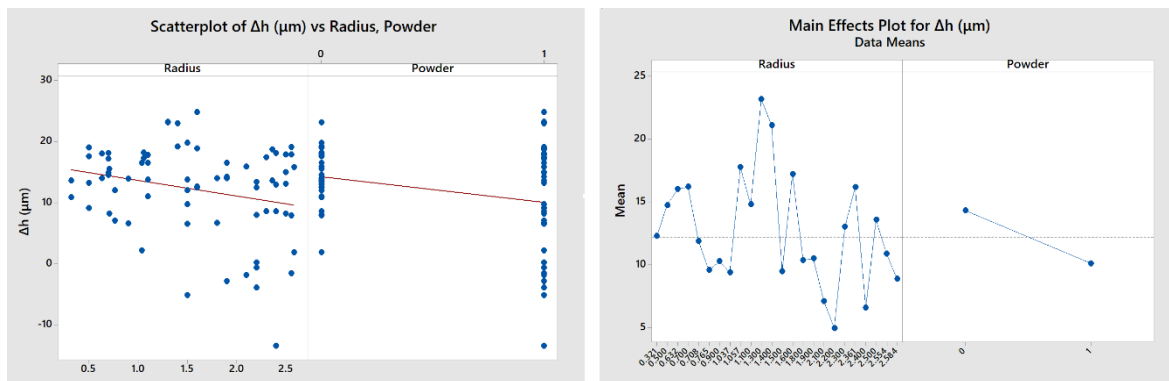


Figure 4.7: A scatter plot and main effect plot of Δh

It's important to mention that one of the observations that we got from the responses table is that the XCT instrument tends to overestimate the height of the pores, that's why, the response values will have a positive sign as the XCT values are compared to the reference ones, unlike the diameter measurement which tends to underestimate the diameter of the pores, so the response values will have a negative sign.

Looking at figure 4.7. We see that in the case of the scatterplot of the radius, the points are once again spread all over the place, and that we are not able to detect any kind of patterns. Also regarding the second factor [p], it seems that we have much larger variation due to powder, and the main effect plot shows once again a slight reduction in the height. Even though figure 4.7 is a qualitative approach to say that only the powder might be a significant factor, we still need to perform ANOVA analysis to confirm the results statistically.

Analysis of Variance

Source	DF	Adj SS	Adj MS	F-Value	P-Value
Radius	23	1373.2	59.71	1.30	0.222
Powder	1	319.2	319.20	6.93	0.011
Error	47	2166.2	46.09		
Lack-of-Fit	23	1244.7	54.12	1.41	0.205
Pure Error	24	921.5	38.39		
Total	71	3858.6			

Model Summary

S	R-sq	R-sq(adj)	R-sq(pred)
6.78885	43.86%	15.20%	0.00%

Table 4.2: ANOVA Table of the response [Δh]

The following table 4.2 shows the ANOVA test for the response [Δh]. The powder factor shows to have a significant influence on the response with a P-value of 0.011, while the radius has a P-value higher than 0.05, stating that it's not significant. The R-sq(adj) once again is quite low, and the lack of fit is not a significant factor with a P-value of 0.205. %. The hypothesis of the residuals are verified, and the model is accepted. So in the end we can conclude that regarding the second response [Δh] that the radius is not a significant factor, but the powder is a significant one.

2.3 Difference in Area [ΔA]

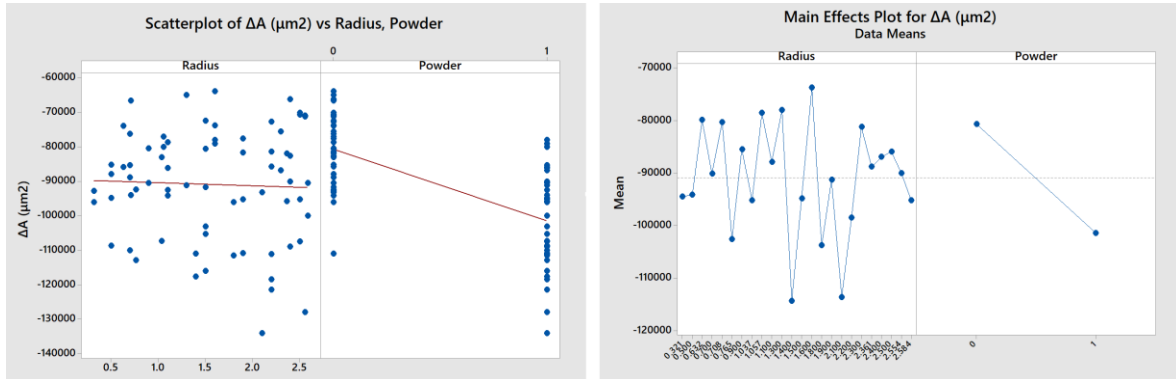


Figure 4.8: A scatter plot and main effect plot of Δh

Once again the scatterplot of the radius shows to have points spread all over the place, and the powder this time seems to have a more significant influence on the Area compared with the previous two responses. Next we need to perform the ANOVA test on the response [ΔA].

Analysis of Variance

Source	DF	Adj SS	Adj MS	F-Value	P-Value
Radius	23	6073890379	264082190	2.73	0.002
Powder	1	7656541191	7656541191	79.07	0.000
Error	46	4454457760	96836038		
Lack-of-Fit	23	2838389792	123408252	1.76	0.092
Pure Error	23	1616067968	70263825		
Total	70	18167461336			

Model Summary

S	R-sq	R-sq(adj)	R-sq(pred)
9840.53	75.48%	62.69%	42.07%

Table 4.3: ANOVA Table of the response [ΔA]

The ANOVA table in table 4.3 shows that both factors radius and powder are significant with P-values below 0.05. The lack of fit is not significant, and a R-sq(adj) is 62.69%. The hypothesis of the residuals are verified, and the model is accepted. Even though the ANOVA table shows that both factors have a P-value lower than 0.05; yet if we consider the F-value of both factors, where the radius has a F-value of 2.73, while the powder has a F-value of 79.07. This shows that the influence of the radius is too small compared with the influence of the powder to the point that it could be neglected. So in the end we can conclude that regarding the response [ΔA], only the powder is considered as a significant factor.

2.4 Difference in Volume [ΔV]

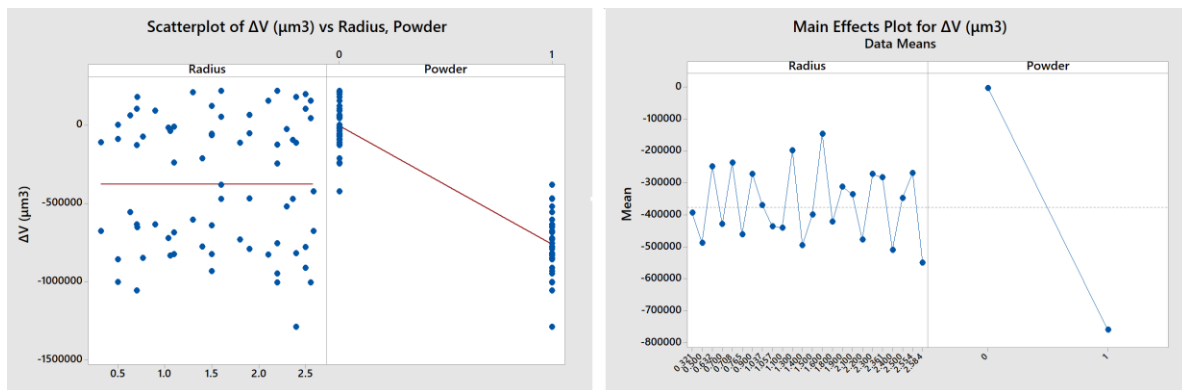


Figure 4.9: A scatterplot and main effect plot of ΔV

Once again the scatterplot of the radius shows to have points spread all over the place, and the main effect plot shows that the radius does not seem to be significant. On the other hand, both the scatterplot and the main effects plot are showing that the powder is having a significant influence on the volume. Unlike the previous responses. The volume seems to drop significantly in size due to powder. Next we perform the ANOVA test.

Analysis of Variance

Source	DF	Adj SS	Adj MS	F-Value	P-Value
Radius	23	7.58677E+11	32985959380	1.16	0.323
Powder	1	1.01637E+13	1.01637E+13	358.55	0.000
Error	46	1.30395E+12	28346678647		
Lack-of-Fit	23	6.75476E+11	29368504197	1.07	0.432
Pure Error	23	6.28472E+11	27324853096		
Total	70	1.22617E+13			

Model Summary

S	R-sq	R-sq(adj)	R-sq(pred)
168365	89.37%	83.82%	74.32%

Table 4.4: ANOVA Table of the response [ΔV]

The ANOVA table in table 4.4 shows that only the powder is significant with P-value equal to zero. The lack of fit is not significant with a P-value equal to 0.432, and a R-sq(adj) is 83.82%. The hypothesis of the residuals are verified, and the model is accepted. So in the end we can conclude that regarding the final response [ΔV], the radius is not a significant factor, but the powder is a significant one.

Conclusion

In conclusion we see that for all the responses, the pore's radial position [ρ], also mentioned as the (radius) during the analysis, shows not to have a significant influence on any of the response variables. While the second factor, the powder [p] turned out to be a significant factor for all the responses [ΔD_m], [Δh], [ΔA], and [ΔV]. It's worth mentioning that even though the powder turned out to have an influence on all of the pores' geometries; the ANOVA tests shows that the significance of the influence increases with the number of dimensions of the geometry. So the powder has just a slight influence on the 1-dimension geometries, the diameter and the height. A more significant influence on the 2-dimension geometry, the Area, and even a much more obvious one on the 3-dimensions geometry, the volume.

Chapter 5

Full Case Experiment and Analysis

In this chapter we will be talking about the second part of the experimental campaign. The main objective of this experiment is to have a case that is closer to a real life scenario; where the pores would be internal instead of being external and opened to the air, while at the same time having pores that are located at different vertical positions. This could help us to understand if the vertical position of the scanned object could have an influence on the measured values.

1. Full Case Experiment

For this experiment, three identical aluminum disks will be used and placed on top of each other with a fourth auxiliary aluminum disk that will be placed on the top to keep the pores of the first disk closed. Then the four disks are held tight together by the 3d plastic case that has been built and discussed previously in chapter 2.

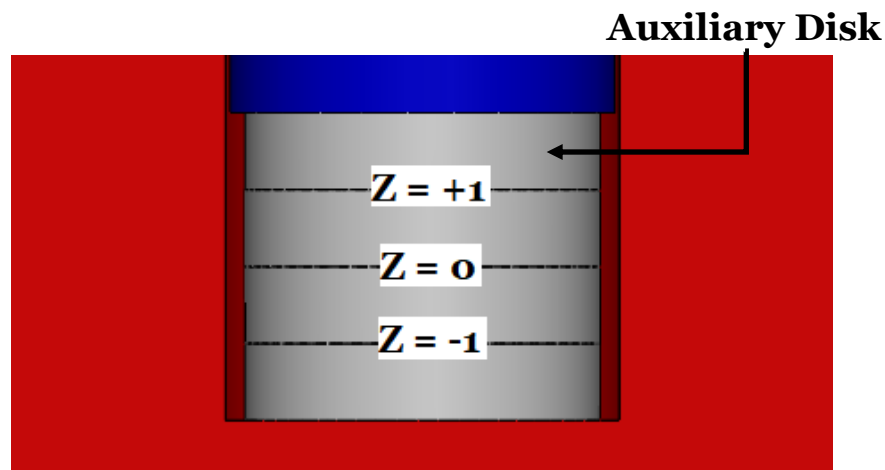


Figure 5.1: Schematic representation indicating where the cavities will be positioned regarding the vertical axis

So in this experiment the pore's vertical position [Z] will be added as an influencing factor along with the pore's radial position [ρ] and the powder [p]. And as we have seen in the first experiment, the same exact procedure is going to be followed by having two cases, the case without powder and the case with the powder. For both cases, The plastic case containing the disks is placed horizontally inside the XCT instrument, while trying to maintain the instrument's testing configuration the same as possible in both cases.

2. Preliminary Tests

Unlike the single disk experiment, the full case experiment is more complex due to the existence of multiple disks and the plastic case. The main issue with performing such an experiment is the size of the scanned object and its thickness. One can understand that the thicker the object is, the harder it is for the X-ray beam to penetrate through. This means that if we are dealing with a very thick object, most of the X-ray beam energy will be absorbed by the object material, giving a false measurement as it makes the object appear to be much denser than it really is. In this way the pores may not be detected or the pores will be underestimated in size.

The first design of the plastic case had a diameter size of 38mm. The plastic case turned out later to be very thick one making it hard for the X-ray beam to get through and construct a clear image of the pores. The next figure 5.2, shows a side to side comparison between a grayscale image taken during the single disk experiment, and the a grayscale image taken with the 38mm diameter plastic case. On the right side, the plastic case can be seen surrounding the disk with a small air gap between them. Yet the plastic case makes it really hard to create a good thresholding to separate the pores from the disk. It can be seen that the separation between the disk and the pores is not sharp or clear at all, making it really hard to detect the pores. And even though the main objective here is to study the influence of unprocessed powder, it's clear that adding powder will just make the image even harder to read.

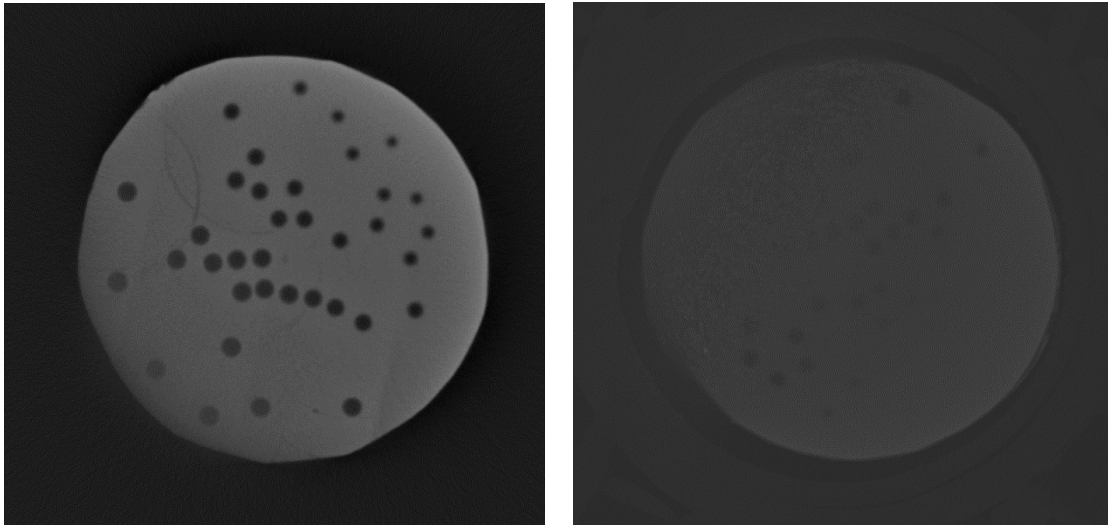


Figure 5.2: Comparison of the grayscale images obtained as single disk (Left) and with the 38mm diameter plastic case (Right)

So in order to solve this problem and just make the image clearer and easier to be read, we decided to reduce the size of the plastic case as much as we can without interrupting the position and the size of the screws. So we were able to reduce the diameter of the plastic case by 30%. Getting it down from 38mm to 26mm.

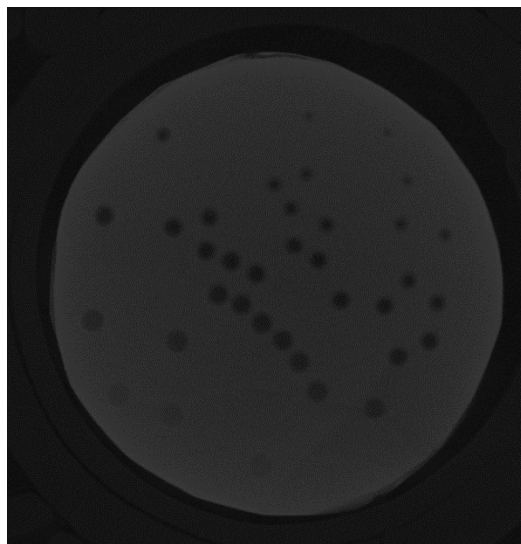


Figure 5.3: Grayscale image obtained with the 26mm diameter plastic case

One last note to keep in mind is the uneven distribution of powder across the faces of the disks as its done manually by hand. So each vertical position [Z] will have a different amount of powder distributed across it with a completely different pattern, making it possible to have a significant factor as the interaction between any of the main factors. We can now perform the experiment following the same steps of the single disk experiment where two cases will be performed, without powder [$p = 0$], and with powder [$p = 1$]. And the only difference here is that each of the two cases will have 3 different vertical position [Z]. The grayscale images will be read by the Matlab code, and the difference between the measured values and the reference values will be used to build our response table A.2 as show in the appendix.

3. ANOVA Analysis

As the previous experiment, we will be performing ANOVA analysis on each of the following response variables independently of the others :

1. Difference in mean diameter [ΔD_m]
2. Difference in height [Δh]
3. Difference in area [ΔA]
4. Difference in volume [ΔV]

3.1 Difference in Mean Diameter [ΔD_m]

Starting with the first response variable [ΔD_m], we perform the scatterplot and the main effect plot on the response to see visually how does the response change with the influencing factors. By looking at figure 5.4. Unlike the single disk experiment, the radius factor seems to follow a certain pattern as it shows reduction in the output response at higher radius values.

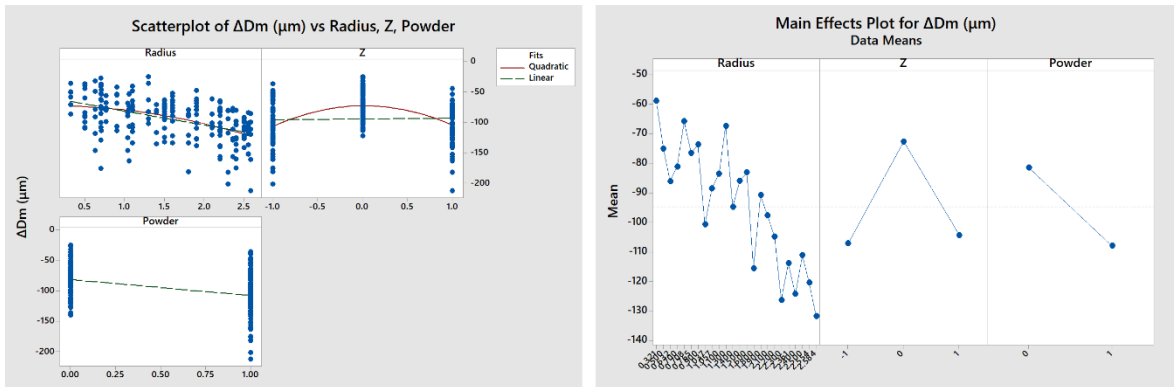


Figure 5.4: A scatter plot and main effect plot of ΔDm

The vertical position [Z] also seems to have an influence on the output response as we get higher values at $Z=0$, and slightly lower values at the two other levels. While once again, we see that the powder causes slight reduction in the diameter. So in order to verify the significance of this reduction we will perform ANOVA analysis on the response [ΔDm].

Analysis of Variance

Source	DF	Adj SS	Adj MS	F-Value	P-Value
Radius	23	76854	3341.5	8.02	0.000
Z	2	51607	25803.3	61.90	0.000
Powder	1	38021	38020.6	91.22	0.000
Radius*Z	46	23648	514.1	1.23	0.210
Radius*Powder	23	7161	311.4	0.75	0.781
Z*Powder	2	9826	4913.0	11.79	0.000
Radius*Z*Powder	46	11149	242.4	0.58	0.975
Error	72	30011	416.8		
Total	215	250402			

Model Summary

S	R-sq	R-sq(adj)	R-sq(pred)
20.4162	88.01%	64.21%	*

Table 5.1: ANOVA Table of the response [ΔDm]

From the ANOVA table shown in table 5.1,. The table also shows that all the main factors have a P-value equal to 0.000, concluding that all of them have a significant influence on the response. We can also see that the interaction between the vertical position and powder is also a significant factor with a p-value equal to zero. The reason behind this is the uneven distribution of powder at the different vertical positions [Z], as it has been mentioned before. We see that we have an accepted value of R-sq(adj) of around 64%. The hypothesis of the residuals are verified, and the model is accepted.

In the end we can conclude regarding the first response [ΔD_m] that all the three main factors [Radius, Vertical position, Powder] are significant, including the interaction factor between the vertical position and the powder, which can be eliminated in case we have a more even or completely randomized distribution of powder at the different levels. We will next move to the next response variable, the difference in height [Δh].

3.2 Difference in Height [Δh]

Next we will be performing ANOVA analysis to study the influence of our factors on the height of the pores exact steps as we did with the previous response [ΔD].

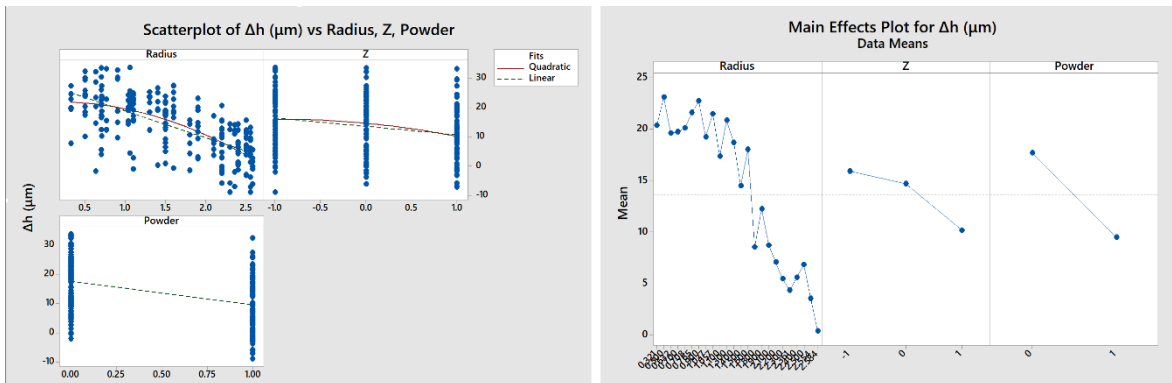


Figure 5.5: A scatter plot and main effect plot of Δh

Once again we start by performing the scatterplot and the main effects plot for the difference in height [Δh], then we continue with the same exact steps. Looking at figure 5.6, we see that in the case of the scatterplot of the radius, the points are once again following a specific pattern where we can see obvious reduction in the output response at higher radius values. Regarding the second factor [Z], it seems that we have less of the pattern we saw with the first response [ΔD_m], and instead we do not have much variation regarding the vertical position. Once again the powder seems to cause a slight reduction in the output response. Next we need to perform ANOVA analysis to confirm the results statistically.

Analysis of Variance

Source	DF	Adj SS	Adj MS	F-Value	P-Value
Radius	23	10193.4	443.19	18.01	0.000
Z	2	1075.6	537.81	21.86	0.000
Powder	1	3373.0	3372.98	137.10	0.000
Radius*Z	46	2015.3	43.81	1.78	0.007
Radius*Powder	23	605.3	26.32	1.07	0.389
Z*Powder	2	541.3	270.63	11.00	0.000
Error	118	2903.1	24.60		
Lack-of-Fit	46	1211.5	26.34	1.12	0.327
Pure Error	72	1691.6	23.49		
Total	215	21169.5			

Model Summary

S	R-sq	R-sq(adj)	R-sq(pred)
4.96007	86.29%	75.01%	53.49%

Table 5.2: ANOVA Table of the response [Δh]

The ANOVA table 5.2 shows a relatively high value of R-sq(adj) of 75.01%, with all the main factors being significant with a p-value equal to 0.00. We also realize that the interaction factors with the vertical positions [Radius x Z] and [Z x powder] are significant, once again due to the uneven distribution of powder at different Z levels. The hypothesis of the residuals are verified, and the model is accepted.

So in the end we can conclude that regarding the second response [Δh], that all of the three main factors [Radius, Vertical position , Powder] are significant, including the two interaction factors with the vertical positions which once again could be eliminated in case we have a more even distribution of powder at the different levels. Next we will move to the next response variable, the difference in area [ΔA].

3.3 Difference in Area [ΔA]

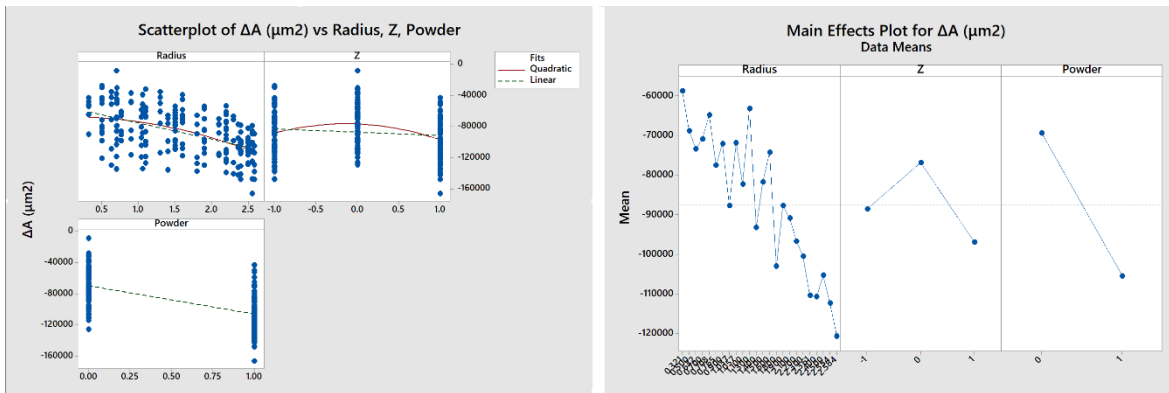


Figure 5.6: A scatter plot and main effect plot of ΔA

Once again the scatterplot and the main effect of the radius shows that the points are following a specific pattern where we can see obvious reduction in the output response at higher values of radius. Regarding the second factor [Z], it seems to follow the same pattern we saw with the first response [ΔD_m], where we get higher values at the $Z=0$, and slightly lower values at the two other levels. The powder this time seems to cause a more obvious reduction in the output response compared to the first two responses. Next we need to perform ANOVA analysis to confirm the results statistically.

The ANOVA analysis in table 5.3 shows once again that all main factors have a P-value equal to 0.000. Concluding that all three main factors are having a significant effect on the response. We can also see that the interaction between the radius and the vertical position is significant in this case with a p-value of 0.023. The table also shows a relatively high value of R-sq(adj) of around 77.37%, and no lack of fit issues with a high p-value of 0.926. The hypothesis of the residuals are verified, and the model is accepted.

Analysis of Variance

Source	DF	Adj SS	Adj MS	F-Value	P-Value
Radius	23	58323688719	2535812553	12.96	0.000
Z	2	14173917612	7086958806	36.21	0.000
Powder	1	61646882989	61646882989	315.00	0.000
Radius*Z	46	14407545835	313207518	1.60	0.023
Radius*Powder	23	4915014204	213696270	1.09	0.364
Z*Powder	2	631393421	315696710	1.61	0.204
Error	118	23093341761	195706286		
Lack-of-Fit	46	6927093712	150588994	0.67	0.926
Pure Error	72	16166248049	224531223		
Total	215	1.85919E+11			

Model Summary

S	R-sq	R-sq(adj)	R-sq(pred)
13989.5	87.58%	77.37%	59.29%

Table 5.3: ANOVA Table of the response [ΔA]

Once again we can conclude that regarding the third response [ΔA] that all the three main factors [Radius, Vertical position Z , Powder] are significant, including the interaction factor between the radius and the vertical position [Z]. Next we move to the fourth and final response variable, the difference in volume [ΔV].

3.4 Difference in Volume [ΔV]

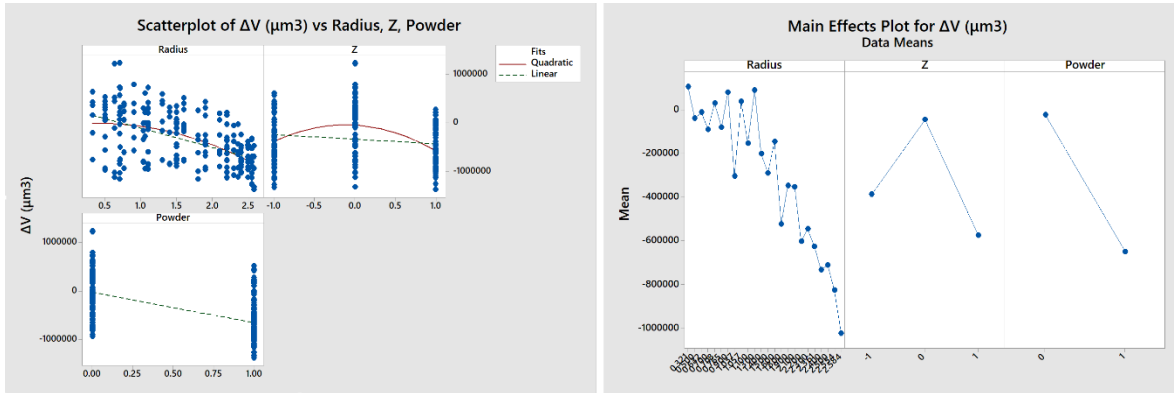


Figure 5.7: A scatter plot and main effect plot of ΔV

In figure 5.10, once again the scatterplot and the main effect plot of the radius shows that the points are following a specific pattern where we can see obvious reduction in the output response at higher radius values. Regarding the second factor [Z], it follows the same pattern we had for both responses [ΔD_m , ΔA], where we get higher values at the $Z=0$, and slightly lower values at the two other levels. The powder causes a very obvious reduction in the output response. Next we need to perform ANOVA analysis to confirm the results statistically.

Table 5.5 shows the ANOVA analysis for [ΔV] once again that all main factors have a P-value equal to 0.000. concluding that the three factors are having a significant effect on the response. But this time we see that all the double interactions are significant in this case with a p-value lower than 0.05, yet they have an extremely low F-value compared with the main factors, making their significance neglected compared to the significance of the main factors. The table also shows a high value of R-sq(adj) of around 84.43%. The hypothesis of the residuals are verified, and the model is accepted.

So regarding the forth and final response [ΔV], we conclude that all of the three main factors [Radius, Vertical position Z , Powder] are significant, including all the double interaction factors.

Analysis of Variance

Source	DF	Adj SS	Adj MS	F-Value	P-Value
Radius	23	2.02789E+13	8.81690E+11	18.64	0.000
Z	2	1.09262E+13	5.46310E+12	115.49	0.000
Powder	1	1.87807E+13	1.87807E+13	397.04	0.000
Radius*Z	46	5.56898E+12	1.21065E+11	2.56	0.000
Radius*Powder	23	1.94277E+12	84468088108	1.79	0.024
Z*Powder	2	3.56448E+11	1.78224E+11	3.77	0.026
Error	118	5.58163E+12	47301940717		
Lack-of-Fit	46	1.80085E+12	39148834081	0.75	0.856
Pure Error	72	3.78078E+12	52510869957		
Total	215	6.53295E+13			

Model Summary

S	R-sq	R-sq(adj)	R-sq(pred)
217490	91.46%	84.43%	71.62%

Table 5.4: ANOVA Table of the response [ΔV]

Conclusion

In conclusion of this experiment, we can say that unprocessed powder once again will cause reduction in the pore's dimensions regarding all the different geometrical dimensions [Diameter, Height, Area, Volume]. The vertical position [Z] appears to be a significant factor, as well as the radial position [ρ], unlike the single disk experiment where the radial position does not have an influence on the response. In the final chapter we will be giving more explanations and final thoughts about these results, as well as the double interaction factors that appeared also to have a role in this experiment.

Chapter 6

Powder's Influence on Pore's Reconstruction

In this chapter we will take a closer look at how the powder influences the pore's reconstruction. The main objective of this chapter is to have a further explanation of the results we got in both experiments of chapter 4 and 5. Both experiments show the same results regarding the powder. We saw that the powder caused a slight reduction in terms of pore's diameter and height; while it caused a larger reduction in terms of area and volume. In this chapter we aim to verify these results by understanding how the pore's reconstruction is influenced by the powder.

1. Pore's Reconstruction

The powder particle that remains inside a pore's cavity is practically just another piece of the artifact, and the XCT instrument will not be able to differentiate between the melted powder and un-melted powder as they are very close in density. So the only thing that could be physically seen is a change in the geometrical shape of the pores due to the powder's existence.

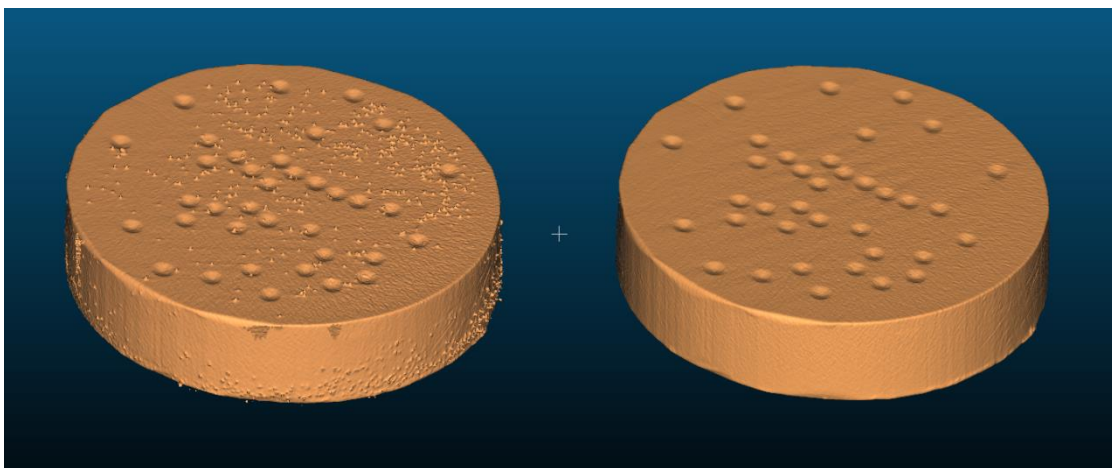


Figure 6.1: Reconstruction of a 3D model of the disk with and without powder using CloudCompare after being scanned by XCT

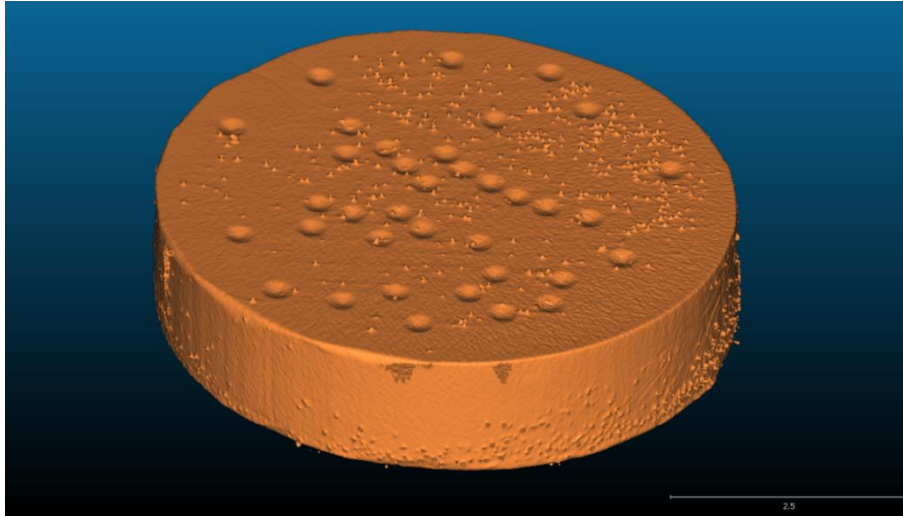


Figure 6.2: Reconstruction of a 3D model of the disk with powder using CloudCompare after being scanned by XCT

In the figures 6.2, Reconstructions of the 3D model of the disk has been performed using the open source software CloudCompare. Figure 6.2 shows clearly the powder particles as just another part of the disk. The next figure 6.3 is a close up shot of the disk. As it has been mentioned in the beginning that the powder is placed randomly, we can see how some pores do not have any powder particles in them, some will have powder on their edges, and some will have powder in their centers.

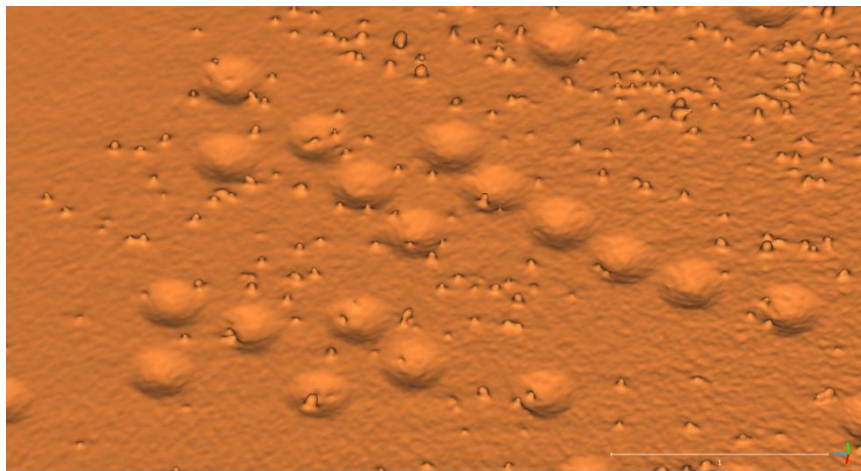


Figure 6.3: Close-up shot of the 3d Model constructed by CloudCompare

It's important to mention that during a real life scenario of additive manufacturing, the pores or cavities that are produced are internal closed pores, which means that powder particles that are left behind unmelted will be placed inside the pore cavity rather than on the edge of the cavity as in the case that could be seen with external open pores. So to keep this study coherent with real life cases, our focus will be mostly in the case where we have a powder particle left inside or in the center of the pore's cavity. We can start by having even a closer look at one of the pores that has a powder particle inside of it, and see how does the pore geometrically change in terms of diameter, height, surface area and volume. In order to do this, we need to have even a closer look at a single pore independently, which requires us to isolate a single pore from the rest of the disk.

1.1 Pore's Isolation – Manual Cutting Tool

The first method to do this is by using a cutting tool that is provided by the open source software CloudCompare. The main issue with this tool is that the cutting process is performed manually, which will lead to some margin of imperfection during the isolation of the pore. However, for the sake of this study, this tool is sufficient enough to generally realize the difference in geometry in terms of diameter and height. In the following figure 6.4, we have a comparison between a single pore that has been isolated. On the left we see the same pore but with a powder particle inside of its cavity.

Figure 6.4 shows a different side views of a single pore in both cases. The main thing that could be realized from the figure is that the diameter and the height of the pore is not affected by the powder existence inside the pore. This is due to the fact that the diameter of the pore is calculated as the average between the diameter in the X and Y direction, while the diameter in each direction is measured as the difference between the minimum and maximum coordinate in that direction. And as the powder particle is placed within these coordinates, then the diameter will still remain the same even though they might seem slightly different in the first image due to the manual cutting process.

So we can only expect a change in the diameter if the pore is placed on the edge of the pore which only will only happen in an open pore case. When it comes to the height, its partially the same. The height of the pore is calculated based on the difference between the minimum and maximum coordinate in the Z direction. So as long as the pore is placed inside the pore as shown in the figure, we won't expect a significant change in the height, unless the particle powder is laying at lowest part of the pore, then this will cause the minimum coordinate to slightly increase, which means a slight reduction in the height.

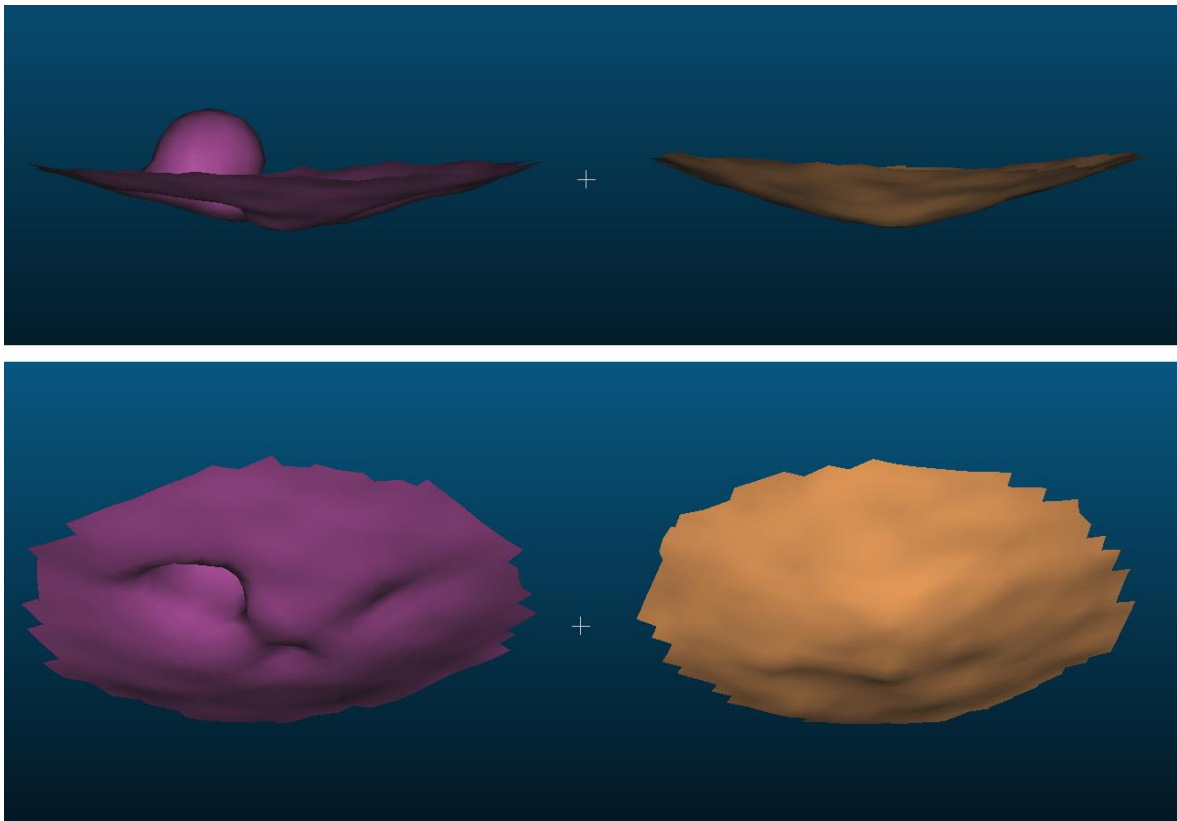


Figure 6.4: Different side views of a single pore isolated in CloudCompare – Pore without powder (Right) – Pore with powder (Left)

1.2 Pore's Isolation – Matlab Code

Even though by using CloudCompare software we were able to see how does a single pore particle placed inside the cavity can affect the pore's diameter and height, understanding the change in the surface area and volume requires much more accurate details which is hard to look at using CloudCompare due to the manual cutting process as it leads to some imperfections. So instead another method to study the pores will be covered next using our Matlab code.

As we have seen in the previous chapters how the Matlab code can be used to evaluate the geometrical properties of the artificial pores. The Matlab code starts with reconstructing the 3D model of the object that has been scanned, applying threshold value on the grayscale images, separating the pores from the rest of the disk and evaluate the geometrical properties of each individual pore.



Figure 6.5: Example of the pores after they have been isolated using Matlab and viewed by CloudCompare

The advantage of this code is that its able to isolate each single pore numerically eliminating any manual errors. So by taking advantage of this method, we can extract a .STL from our Matlab code containing only the pores after it has been isolated from the rest of the disk. The .STL file can be then lunched using CloudCompare to see the isolated pores as we can see in figures 6.5. This method can easily help us to have a side by side comparison of the shape of the pores without and with the powder as seen in figure 6.6.

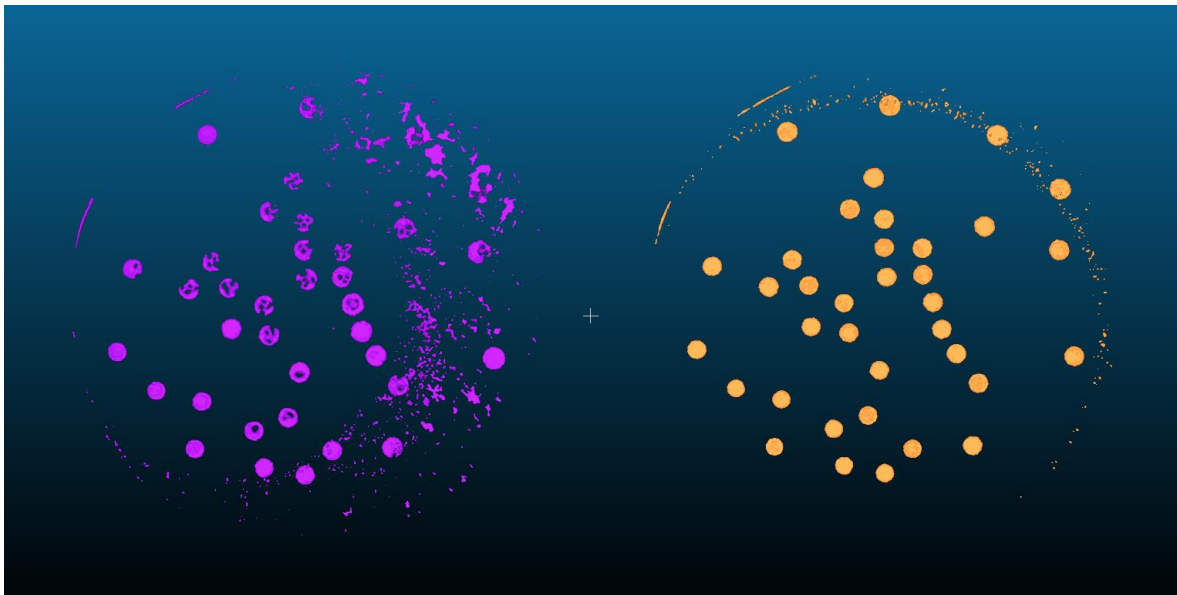


Figure 6.6: Comparison of the pores after they have been isolated using Matlab and viewed by CloudCompare

Each single pore has been isolated using the numerical approach based on the thresholding instead of manual cutting. The main difference here is that with this method compared with the previous method, the pores constructed are representing the air space or the cavity of the pore, which means that having a powder located inside the pore will occupy some space of this pore, which will be seen as a reduction in the pore size as shown in both figures 6.6 and 6.7.

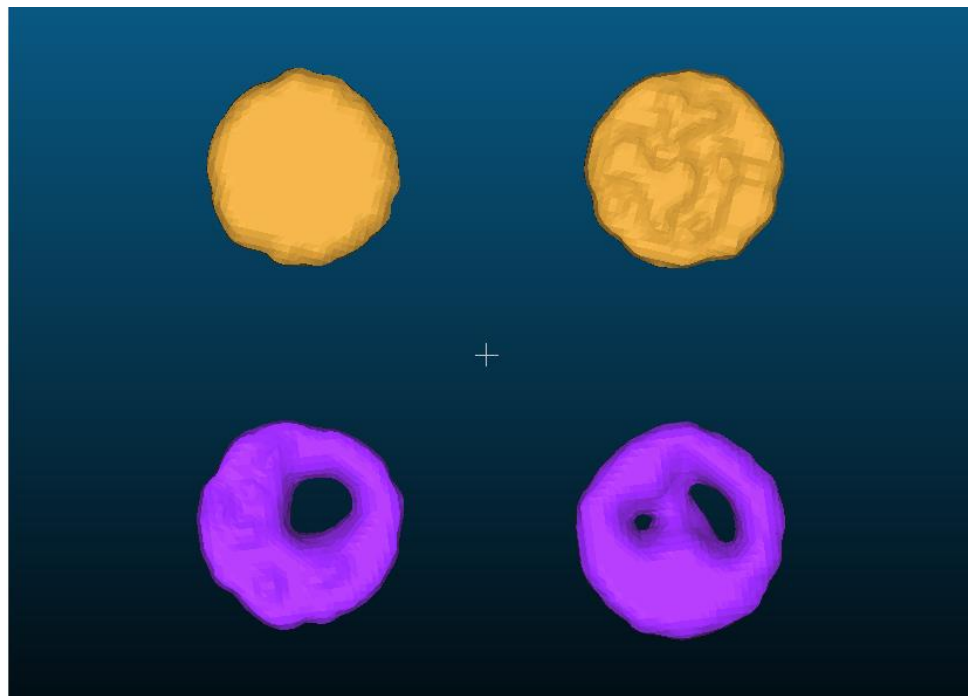


Figure 6.7: Plan view comparison of the corresponding pores without powder (up) and with powder (down)

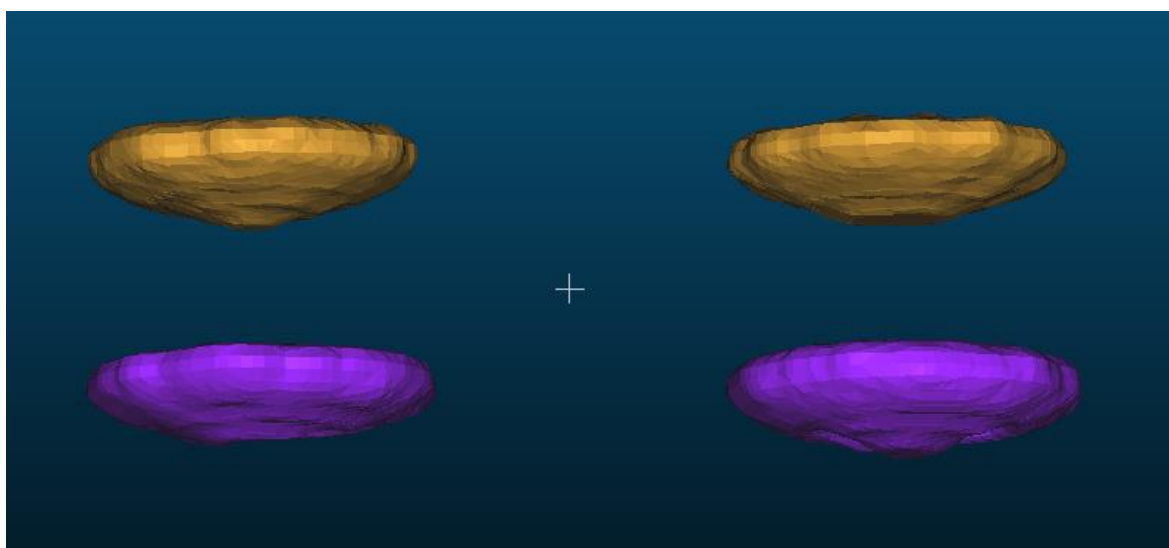


Figure 6.8: Side view comparison of the corresponding pores without powder (up) and with powder (down)

In both figures 6.7 and 6.8, we see once again that the existence of a powder particle in the center of the pore would not cause a significant change in the diameter, but obviously will cause a reduction in the area and the volume as the size of the air cavity is being reduced as it's being occupied by the powder particle as shown in figure 6.7. Regarding the height, we can consider looking at figure 6.8. In the right case, we have the powder particle locating away from the center of the pore, so we won't expect any change in the height. But looking at the left case, we have the particle placed slightly closer to the center, so we can see how the height is slightly reduced, even though the reduction might not be significant to our interest.

The last thing we will take a look at, is a case where the powder particle is placed close to the edge of the pore which can be seen in figure 6.9. The figure clearly shows how the mean diameter of the pore on the left side will be slightly reduced as well as the area and the volume. Regarding the height, it will follow the same idea we discussed earlier, where the height will slightly reduce in case a powder particle is occupying the center of the pore.

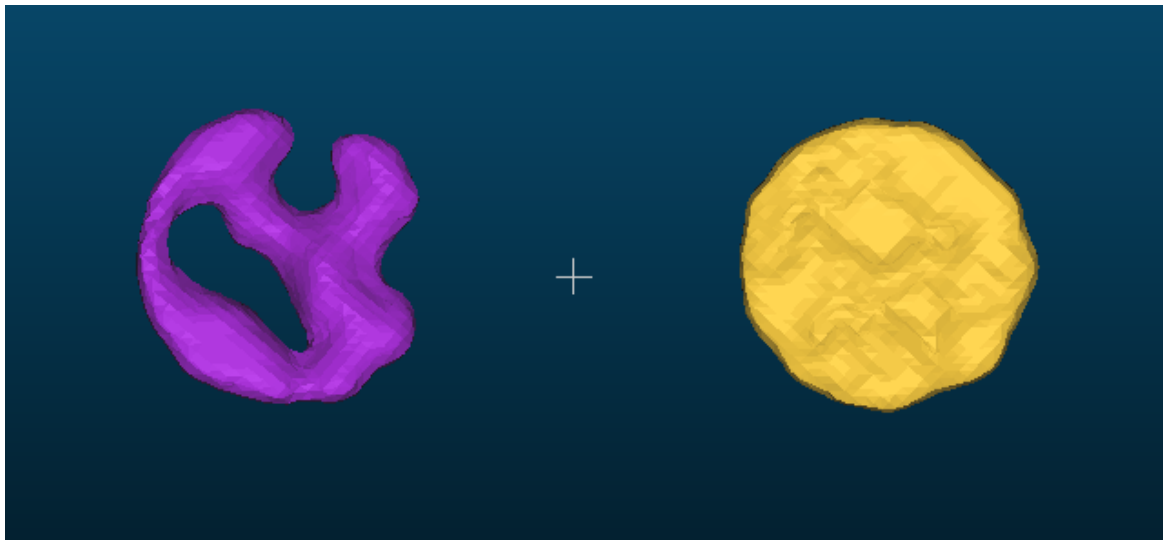


Figure 6.9: Plan view comparison of the corresponding pores without powder (left) and with powder (right)

The following tables 6.1, concludes the results we got in this chapter regarding the pore's geometrical dimensions.

	Observation
Diameter	Slight reduction (when the powder particle is near the edge)
Height	Slight Reduction (when the powder particle is near the center)
Area	Significant Reduction
Volume	Significant Reduction

Table 6.1: Geometrical dimensional changes due to unprocessed powder

This chapter shows that we were able to verify the results that we got from the previous two experiments. In case of diameter, the only reduction we get is when the powder is near the edge, otherwise the diameter stays the same. This shows that during the experiment, some pores will have a slight reduction in diameter, while others remain the same; so the overall reduction in diameter will be low. Same goes with the height, as the only reduction we get is when the powder is near the center, otherwise the height stays the same; so the overall reduction in height will also be low.

On the other hand, the area and volume does not depend that much on the location of the pore. So as long as we have powder that is occupying some space within the circumference or near the edge of the pore, we expect a significant reduction in the area and volume.

Chapter 7

Conclusions and Future Development

In this thesis work we demonstrated the influence that unprocessed powder have on the reconstruction of pores using XCT measurement. This study was carried out by performing two experiments, the single disk experiment and the full case experiment. In both experiments, an artifact containing a number of artificial pores are filled with powder. The evaluation of the capability and accuracy of the XCT instrument is based on the comparison between two cases:

- Case 1: Empty Pores (No powder added).
- Case 2: Filled Pores (powder added).

We also demonstrated the design and construction of a new and improved plastic case to house the artifact during the scanning phase as we have seen in chapter 2.

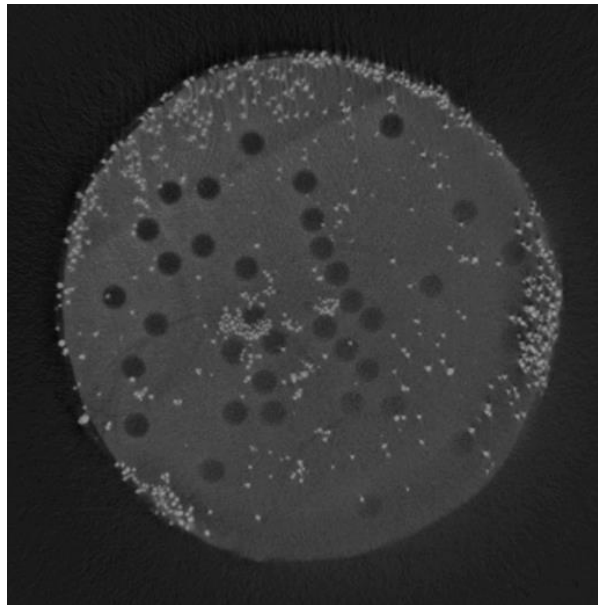


Figure 7.1: Examples of grayscale image with powder added

Conclusions

The first thing that this study has demonstrated is that the XCT machine is capable of detecting unprocessed powder and distinguish between a single powder particle and the continuous material. Figure 7.1 clearly shows that we are able to detect a single powder particle from the Aluminum disk and the pores.

As a consequence, it was interested to understand how this unprocessed powder can influence the XCT measurement of the pores, and by performing the two experiments of this study, the single disk experiment and the full case experiment; the results show that unprocessed powder will cause a significant reduction in the geometrical dimensions of the pore:

- Mean Diameter [D_m]
- Height [h]
- Area [A]
- Volume [V]

Meanwhile the two experiments show a completely different results when it comes to the radial position [ρ]. The single disk experiment shows that the dimensions are not influenced at all by the radial position, while the full case experiment shows that the pores are underestimated in size as we move away from the center.

The main reason to this difference is the size of the scanned object. In the case of a single disk, we are dealing with a much smaller object, so the X-ray beam is capable of scanning the entire object in a more uniform way without being subjected to the beam hardening artifact. On the other hand, the full case experiment, we are dealing with a much larger object due to the usage of a plastic case. The plastic case will make it much harder for the X-ray beam to get through, and will make it more subjected to the beam hardening artifact. The result of this artifact will appear as we are moving away from the center of the beam, where the beam energy gets weaker, making the outer zone of the object to appear much denser, which as a result underestimates the size of the pores.

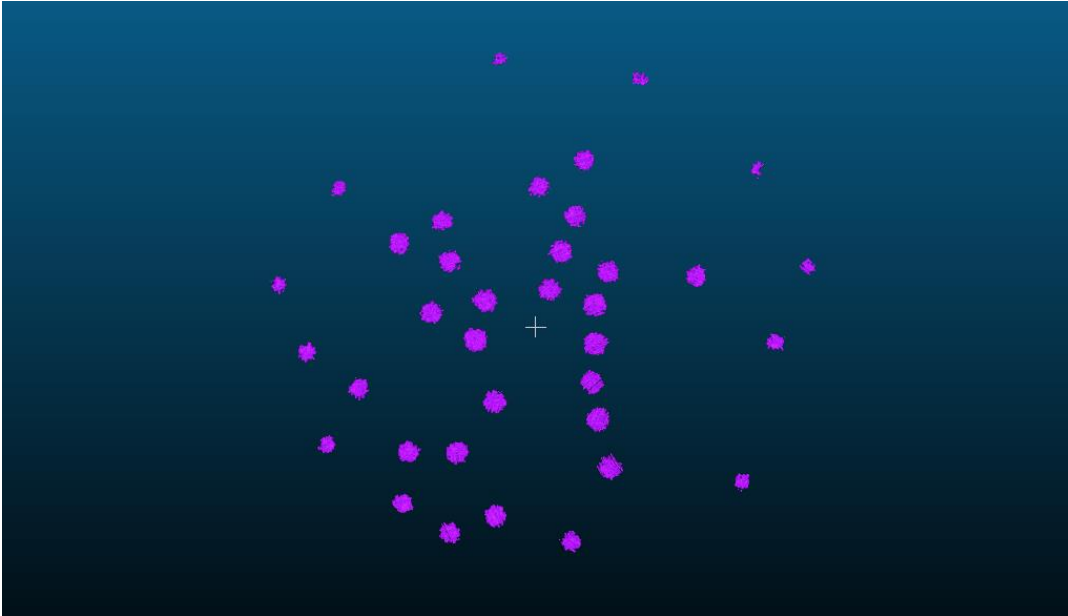


Figure 7.2: The beam hardening artifact influence on the construction of pores from the full case experiment

Figure 7.2 illustrates the beam hardening artifact influence on the reconstruction of pores from the full case experiment. One other result of the experiment was regarding the influence of the vertical position [Z], which is only examined during the full case experiment. The results show that the vertical position has an influence on the dimensions measured. In chapter 5 we see that in case of diameter, area and volume, the vertical position [$Z = 0$] will mostly have a larger measured dimensions, and at [$Z = -1$] and [$Z = +1$] we underestimate the values of these measurements.

The reason behind this is the Cone Beam Artifact [8], which is a problematic given by the proximity of the component to the source of the radiation. In particular, this artifact is expected in cone-beam XCT systems, like the one at our disposal. Due to this fact, we expect to have an influence of the vertical position because the pores in the middle position [$Z = 0$] will be less influenced by this artifact, while as we move away from the middle position, the pores will be more subjected by the artifact causing underestimation of the pore's dimensions and increase in the error.

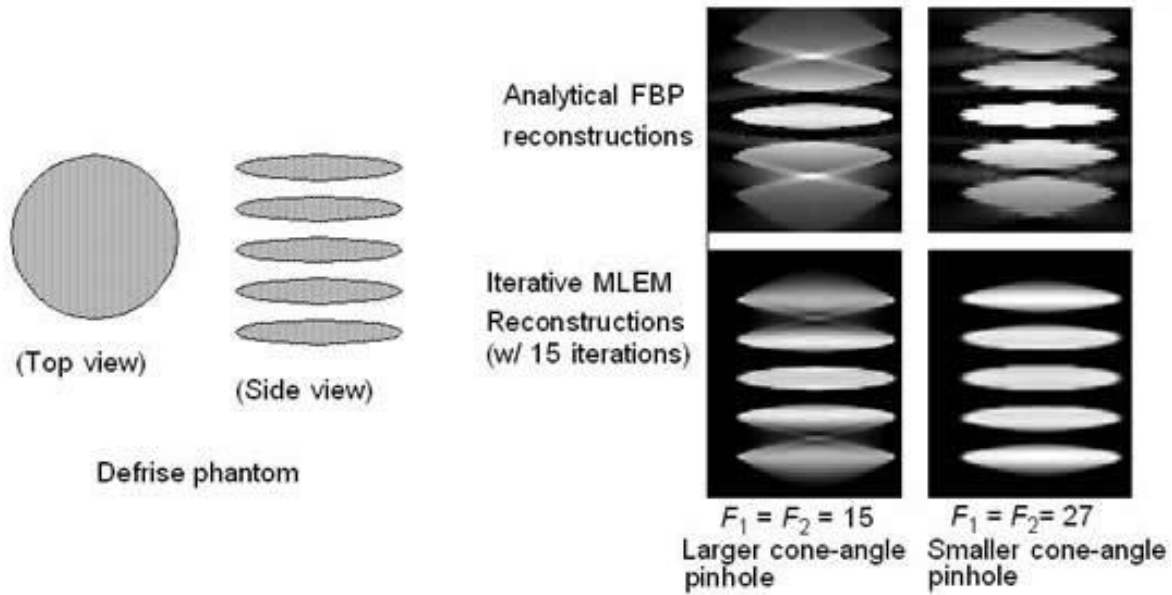


Figure 7.3: Cone Beam Artifact

Another result regarding the full case experiment is the significance of the double interaction factor between the vertical position [Z], radial position [ρ], and the powder [p]. Even though the significance of any double interaction is out of our interest, yet its important to mention that this significance is due to the uneven distribution of powder across the face of the aluminum disk and along the three disks. So taking an example with the full case experiment, it was realized that the central aluminum disk had less powder distributed across its face compared with the upper and the lower disk which had more powder across them, causing the interaction factor between the vertical position [Z] and the powder [p] to be significant.

The final result or observation regarding both experiments is the error while estimating the pore's dimensions when comparing it with the reference values. The XCT measurement tends to underestimate the diameter of the pores which is a horizontal measurement, while it tends to overestimate the height of the pores which is a vertical measurement considering that the aluminum disk is placed horizontally during the XCT scanning phase.

This study demonstrates that there are many different reasons that lead to the underestimation of the measured pores:

- The presence of unprocessed powder within the pores.
- The beam hardening artifact: Causing pores that are faraway from the center to be underestimated.
- The cone beam artifact: Causing pores that are located at high or low altitude, with respect to the beam level, to be underestimated.
- Measurement of pore's diameter when the artifact is placed horizontally in the XCT instrument.

As we saw in the introduction, the pore's size and shape are critical to determine the mechanical properties of the material such as the fatigue life. And according the Paris equation [4], the fatigue life is inversely proportional the pore or crack size. So in case the pores or cracks were underestimated in size, this will lead to overestimation of the fatigue life, which means that the mechanical part is being used beyond its safety limit.

Final thoughts regarding the process of the experiment will be concerning the Matlab code as it's mainly responsible of measuring the dimensions of the pores. The Matlab code starts with isolating the pores from the rest of the aluminum disk as it can be seen in figure 7.4, and then handles each pore as an individual pore with its own geometrical measurements.

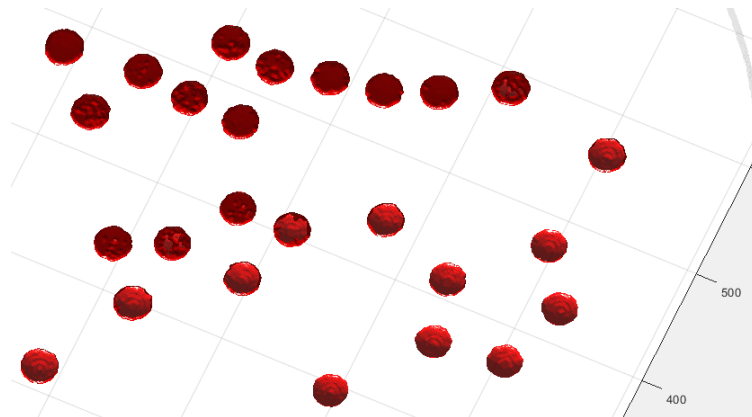


Figure 7.4: Example of the pores being isolated from the rest of the aluminum disk using the Matlab code

One of the main concerns regarding the Matlab code is measuring the pores when the powder is added. Several scenarios may occur:

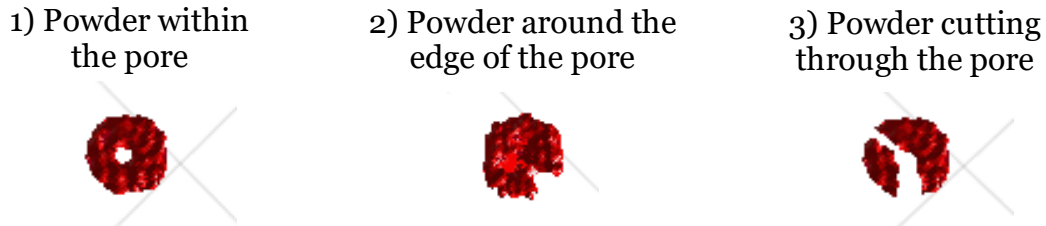


Figure 7.5: Different scenarios of adding powder into the pores, and constructed by the Matlab code

The scenario that we are most concern about is the third one. It's when we have a fair amount of powder spread across the pore in a way that it cuts through it and divides the single pore into two or more pieces as seen in figure 7.5 (3) . In this scenario the Matlab code reads each piece as a single individual pore instead of considering them a part of one single pore. So if we take the example shown in the figure. The Matlab code will consider the pore as two individual pores, and assign a specific geometrical dimension to each one of them. In this scenario, in order to have a more reasonable dimensions, we can approximate the diameter and height size, while adding up the area and volume of each of the pieces to find the overall area and volume of the pore.

Future Development

For future development purposes, some points can be taken into consideration from this study:

- The study shows that the XCT measurement tends to underestimate the diameter, while it overestimates the height. It's possible to compensate for this problem by placing the single disk at a certain angle instead of being placed horizontally or vertically, and finding the angle at which it minimizes the overall error of the diameter and height measurements.

- Regarding the cone beam artifact, one way to compensate for this problem is to use the Helical-Scan feature of the XCT instrument where the piece vertically moves up and down while rotating during the scanning phase. This particular scan will compensate for the Cone beam artifact in the expense of the process's time.
- In this study, applying the helical-scan feature is limited by the positioning of the screws, as moving the plastic case up and down will cause the screws to be scanned as well, which will cause a more complex reconstruction. It's possible to adjust the position of the screws to be slightly higher so it does not interfere with the helical-scan feature.
- One last concern to be mentioned is the type of powder that is used for this study. As the disk is made out of a standard aluminum bar while the powder used is a different aluminum grade *AlSi7Mg0.6 (A357)*. This explains why the XCT can easily distinguish between the disk and the powder, where the powder seems to have a lighter colour compared with the disk as it can be seen in figure 7.1. This contrast can also cause some minor issues when using the Matlab code, as the code will consider the contrast between the disk and the powder large enough during thresholding, and create some extremely small pores due to darker parts of the disk being surrounded by the powder. This can be seen clearly in chapter 4, figure 4.4. For future references, a study can be performed using a disk and powder made of exactly the same material.

APPENDIX

A. RESPONSES' TABLES

A.1 Responses' Table of the Single Disk Experiment

Pore	ρ	p	ΔD_m (μm)	Δh (μm)	ΔA (μm^2)	ΔV (μm^3)
1	0.500	0	-103.1	19.0	-87976	-421
2	2.584	0	-109.1	1.9	-90491	-423853
3	0.700	0	-99.2	14.5	-76218	102757
4	0.700	0	-111.3	18.1	-88854	-127983
5	0.765	0	-112.9	12.0	-92476	-73597
6	0.500	0	-101.2	17.6	-85270	-88414
7	1.500	0	-114.4	19.8	-91776	-65996
8	2.100	0	-112.5	15.9	-93247	154240
9	2.500	0	-84.1	17.9	-70669	103190
10	2.400	0	-95.7	18.1	-66169	178578
11	2.200	0	-101.4	13.4	-81445	-126814
12	1.500	0	-105.6	13.8	-80556	-55402
13	2.200	0	-93.3	12.5	-72776	216919
14	2.554	0	-84.0	17.9	-71032	152863
15	1.600	0	-90.6	12.6	-73816	51969
16	1.100	0	-100.9	13.8	-78720	-12110
17	2.400	0	-114.4	12.9	-82672	-113249

APPENDIX

18	2.554	0	-87.3	7.9	-71288	43003
19	0.900	0	-96.0	13.9	-80454	90291
20	1.500	0	-89.4	12.0	-72458	120221
21	1.900	0	-104.8	16.5	-81727	65408
22	1.900	0	-96.5	14.0	-77580	-54263
23	0.632	0	-97.7	14.0	-73905	60377
24	0.708	0	-90.9	15.5	-66676	177514
25	1.057	0	-98.8	18.2	-77106	-39888
26	2.200	0	-112.9	8.0	-85731	-245159
27	1.400	0	-130.3	19.2	-111027	-214760
28	2.500	0	-89.8	13.1	-70226	196976
29	2.361	0	-105.9	13.6	-81942	-95423
30	1.300	0	-89.2	23.1	-64988	208449
31	0.321	0	-111.2	10.9	-92828	-111594
32	1.800	0	-124.1	14.0	-96018	-113510
33	2.300	0	-104.1	8.6	-75580	-25242
34	1.100	0	-116.4	11.0	-94119	-240174
35	1.600	0	-80.7	12.5	-63976	218305
36	1.037	0	-100.8	16.5	-83114	-16346
1	0.500	1	-97.6	9.1	-94831	-859226
2	2.584	1	-112.1	15.8	-99997	-676071
3	0.700	1	-114.0	17.2	-85373	-636430
4	0.700	1	-111.3	14.9	-110065	-1057307

APPENDIX

5	0.765	1	-124.3	7.1	-112850	-849647
6	0.500	1	-119.6	13.2	-108674	-1004060
7	1.500	1	-96.6	-5.1	-116076	-932813
8	2.100	1	-119.4	-1.8	-134047	-826813
9	2.500	1	-129.6	15.0	-107483	-912024
10	2.400	1	-105.3	-13.4	-90163	-1287963
11	2.200	1	-120.0	-3.9	-111181	-1006267
12	1.500	1	-106.7	6.5	-103133	-825322
13	2.200	1	-94.6	0.2	-121441	-756534
14	2.554	1	-121.1	-1.5	-127978	-1004273
15	1.600	1	-96.2	18.9	-78095	-473005
16	1.100	1	-107.0	16.5	-92565	-826295
17	2.400	1	-139.8	8.6	-108931	-818293
18	2.554	1	-97.5	19.1	*	*
19	0.900	1	-99.8	6.6	-90528	-635137
20	1.500	1	-99.8	9.7	-105240	-641431
21	1.900	1	-123.9	14.2	-95225	-468687
22	1.900	1	-80.1	-2.8	-110819	-790327
23	0.632	1	-112.6	18.0	-85945	-558135
24	0.708	1	-89.2	8.2	-93996	-653087
25	1.057	1	-99.7	17.3	-80069	-832745
26	2.200	1	-136.4	-0.6	-118437	-947300
27	1.400	1	-124.1	23.0	-117688	-776552

APPENDIX

28	2.500	1	-119.1	8.2	-95308	-780777
29	2.361	1	-112.1	18.7	-95749	-471235
30	1.300	1	-117.5	23.2	-91145	-604342
31	0.321	1	-105.9	13.6	-96123	-676190
32	1.800	1	-126.9	6.7	-111606	-731528
33	2.300	1	-94.7	17.4	-86913	-520272
34	1.100	1	-121.7	17.8	-86212	-687767
35	1.600	1	-94.5	24.8	-79178	-382745
36	1.037	1	-88.0	2.2	-107312	-722989

Table A.1: Responses' Table of the single disk experiment

A.2 Responses' Table of the Full Case Experiment

Pore	p	Z	ρ	ΔD_m (μm)	Δh (μm)	ΔA (μm^2)	ΔV (μm^3)
1	0	-1	0.500	-36.7	30.2	-30016	371856
2	0	-1	2.584	-112.0	-0.1	-113926	-699057
3	0	-1	0.700	-62.8	30.4	-50031	573141
4	0	-1	0.700	-76.3	22.5	-44224	72007
5	0	-1	0.765	-56.7	33.3	-60838	399448
6	0	-1	0.500	-88.8	25.8	-27806	323176
7	0	-1	1.500	-78.1	14.3	-74766	83641
8	0	-1	2.100	-62.2	8.7	-70222	59464
9	0	-1	2.500	-122.0	3.8	-105647	-759968
10	0	-1	2.400	-136.7	5.0	-111115	-516464
11	0	-1	2.200	-64.8	15.3	-53581	215263
12	0	-1	1.500	-82.8	23.9	-69379	221577
13	0	-1	2.200	-76.8	-0.5	-73526	-364582
14	0	-1	2.554	-101.6	11.4	-86482	-341415
15	0	-1	1.600	-98.5	25.2	-75234	-49325
16	0	-1	1.100	-80.2	21.3	-66727	303079
17	0	-1	2.400	-127.7	12.3	-102750	-603470
18	0	-1	2.554	-118.4	5.0	-102818	-703799
19	0	-1	0.900	-68.9	32.8	-49191	404341
20	0	-1	1.500	-63.1	21.5	-62680	13177

APPENDIX

21	0	-1	1.900	-127.7	13.5	-96663	-453300
22	0	-1	1.900	-48.0	23.1	-54573	439596
23	0	-1	0.632	-78.8	28.7	-51812	446180
24	0	-1	0.708	-53.7	23.4	-46430	323003
25	0	-1	1.057	-53.3	33.7	-51511	613793
26	0	-1	2.200	-113.5	12.3	-84887	-486539
27	0	-1	1.400	-80.2	25.0	-69606	229193
28	0	-1	2.500	-99.8	6.2	-96915	-518182
29	0	-1	2.361	-127.5	-2.1	-107459	-651247
30	0	-1	1.300	-63.2	23.9	-50413	395357
31	0	-1	0.321	-50.9	24.6	-54413	367352
32	0	-1	1.800	-121.9	10.7	-89756	-352565
33	0	-1	2.300	-94.7	14.3	-71347	-261267
34	0	-1	1.100	-80.5	22.3	-68104	202639
35	0	-1	1.600	-80.7	27.5	-66728	-132441
36	0	-1	1.037	-89.6	24.3	-80800	-162417
1	0	0	0.500	-44.7	24.4	-46321	537534
2	0	0	2.584	-85.6	5.6	-89764	-477776
3	0	0	0.700	-27.7	33.5	-8388	1235830
4	0	0	0.700	-41.2	26.1	-38450	739197
5	0	0	0.765	-67.7	15.5	-62776	361725
6	0	0	0.500	-60.2	23.8	-50381	447320
7	0	0	1.500	-86.7	18.5	-75469	75052

APPENDIX

8	0	0	2.100	-87.1	17.1	-77831	195436
9	0	0	2.500	-93.6	9.9	-82217	-443687
10	0	0	2.400	-98.2	6.4	-98686	-814886
11	0	0	2.200	-67.5	15.6	-64966	-29716
12	0	0	1.500	-75.5	22.1	-54406	351426
13	0	0	2.200	-101.4	10.9	-81978	-347270
14	0	0	2.554	-113.9	3.9	-100587	-802131
15	0	0	1.600	-57.1	18.2	-45658	401825
16	0	0	1.100	-40.8	24.9	-32057	733762
17	0	0	2.400	-104.3	14.4	-78825	-237354
18	0	0	2.554	-84.2	1.3	-79119	-321551
19	0	0	0.900	-42.5	30.3	-37251	795655
20	0	0	1.500	-73.5	17.6	-70609	-96660
21	0	0	1.900	-61.7	20.1	-57834	313578
22	0	0	1.900	-68.8	19.1	-55047	150620
23	0	0	0.632	-32.0	32.2	-35722	1220986
24	0	0	0.708	-38.0	23.8	-30439	711808
25	0	0	1.057	-54.4	20.2	-39452	619093
26	0	0	2.200	-79.1	20.7	-61709	159794
27	0	0	1.400	-80.8	26.7	-76490	321681
28	0	0	2.500	-112.9	7.2	-94809	-693278
29	0	0	2.361	-77.4	12.2	-77774	-29198
30	0	0	1.300	-25.2	25.3	-35316	595018

APPENDIX

31	0	0	0.321	-36.1	27.4	-48148	639984
32	0	0	1.800	-80.0	15.6	-66016	254542
33	0	0	2.300	-80.2	12.4	-67107	-53116
34	0	0	1.100	-65.1	22.8	-56252	422616
35	0	0	1.600	-52.3	20.4	-39344	513493
36	0	0	1.037	-69.2	22.4	-58794	298820
1	0	+1	0.500	-45.0	29.4	-43161	274122
2	0	+1	2.584	-119.8	2.6	-104846	-933432
3	0	+1	0.700	-74.4	21.2	-69578	-221951
4	0	+1	0.700	-86.1	20.8	-67952	-26774
5	0	+1	0.765	-80.8	33.2	-66229	65611
6	0	+1	0.500	-84.5	24.4	-71834	54959
7	0	+1	1.500	-92.4	12.6	-77876	-216417
8	0	+1	2.100	-101.2	9.2	-88389	-582949
9	0	+1	2.500	-107.9	11.2	-100854	-706400
10	0	+1	2.400	-103.7	8.2	-87636	-469826
11	0	+1	2.200	-115.7	9.6	-96177	-635583
12	0	+1	1.500	-77.2	17.1	-65695	-117065
13	0	+1	2.200	-88.8	10.4	-75122	-305581
14	0	+1	2.554	-104.6	8.8	-89807	-525925
15	0	+1	1.600	-82.6	20.3	-71855	-148450
16	0	+1	1.100	-74.7	24.3	-60492	-45165
17	0	+1	2.400	-125.7	7.5	-99625	-737431

APPENDIX

18	0	+1	2.554	-137.2	6.1	-125387	-891714
19	0	+1	0.900	-54.2	29.8	-48391	224048
20	0	+1	1.500	-63.1	13.2	-59369	72042
21	0	+1	1.900	-79.6	13.6	-70084	-252044
22	0	+1	1.900	-101.5	11.7	-84128	-390696
23	0	+1	0.632	-91.5	20.3	-71231	-106982
24	0	+1	0.708	-64.1	27.4	-50189	211911
25	0	+1	1.057	-78.2	23.6	-65479	1050
26	0	+1	2.200	-140.6	4.6	-109936	-776801
27	0	+1	1.400	-83.9	19.4	-66165	-194385
28	0	+1	2.500	-91.8	9.5	-82370	-385895
29	0	+1	2.361	-111.4	11.0	-95067	-601676
30	0	+1	1.300	-83.0	18.4	-60780	23632
31	0	+1	0.321	-71.0	19.9	-52115	162122
32	0	+1	1.800	-89.8	14.4	-77444	-263937
33	0	+1	2.300	-117.7	14.4	-98652	-561465
34	0	+1	1.100	-79.2	19.2	-67704	-130728
35	0	+1	1.600	-72.7	18.8	-65855	-73558
36	0	+1	1.037	-84.2	20.1	-67914	-8250
1	1	-1	0.500	-108.3	20.4	-86685	-560208
2	1	-1	2.584	-161.1	1.4	-137992	-1331196
3	1	-1	0.700	-176.0	12.5	-134960	-1158499
4	1	-1	0.700	-108.6	26.1	-86139	-788710

APPENDIX

5	1	-1	0.765	-98.8	22.8	-86300	-608096
6	1	-1	0.500	-99.8	32.4	-82642	-287980
7	1	-1	1.500	-124.8	19.0	-104327	-667527
8	1	-1	2.100	-105.3	3.7	-76754	-246277
9	1	-1	2.500	-97.4	5.2	-106287	-755296
10	1	-1	2.400	-175.6	1.3	-131149	-1008321
11	1	-1	2.200	-112.3	12.4	-91196	-634813
12	1	-1	1.500	-132.8	14.7	-108600	-774913
13	1	-1	2.200	-156.9	2.7	-122436	-1023030
14	1	-1	2.554	-152.2	9.5	-125197	-1136679
15	1	-1	1.600	-134.1	27.4	-108396	-787139
16	1	-1	1.100	-108.7	17.2	-99441	-601932
17	1	-1	2.400	-146.7	4.3	-148018	-913835
18	1	-1	2.554	-152.9	-8.9	-147742	-1272321
19	1	-1	0.900	-107.2	18.8	-85180	-301347
20	1	-1	1.500	-109.9	18.5	-97438	-839371
21	1	-1	1.900	-127.1	13.7	-96556	-610359
22	1	-1	1.900	-110.0	14.8	-85136	-433866
23	1	-1	0.632	-146.5	14.7	-108768	-1026935
24	1	-1	0.708	-113.9	10.2	-96701	-503627
25	1	-1	1.057	-107.2	25.6	-88634	-280620
26	1	-1	2.200	-160.4	7.3	-125245	-1135144
27	1	-1	1.400	-136.1	21.9	-112365	-855893

APPENDIX

28	1	-1	2.500	-124.2	15.7	-116449	-911137
29	1	-1	2.361	-129.5	-2.1	-132515	-1114714
30	1	-1	1.300	-102.5	21.7	-76598	-163107
31	1	-1	0.321	-58.5	22.9	-43102	-203597
32	1	-1	1.800	-181.8	7.8	-137391	-1159593
33	1	-1	2.300	-201.6	-8.9	-126640	-939641
34	1	-1	1.100	-134.1	23.1	-103910	-869074
35	1	-1	1.600	-89.5	22.8	-70864	-181533
36	1	-1	1.037	-146.4	19.0	-119467	-798264
1	1	0	0.500	-40.3	20.4	-89085	170426
2	1	0	2.584	-99.8	-6.2	-129141	-1320099
3	1	0	0.700	-38.1	16.5	-79441	221472
4	1	0	0.700	-53.1	17.4	-49892	157049
5	1	0	0.765	-79.3	12.3	-90801	236498
6	1	0	0.500	-91.1	18.4	-79664	107090
7	1	0	1.500	-96.4	6.5	-85559	-493270
8	1	0	2.100	-109.5	5.7	-115156	-641831
9	1	0	2.500	-94.0	12.3	-127118	-472121
10	1	0	2.400	-80.6	0.7	-114775	-866468
11	1	0	2.200	-82.6	-1.6	-113485	-921175
12	1	0	1.500	-76.2	5.0	-100248	-755156
13	1	0	2.200	-108.4	-2.5	-126186	-1018731
14	1	0	2.554	-111.8	-3.9	-112773	-1038111

APPENDIX

15	1	0	1.600	-67.1	16.6	-68670	-28932
16	1	0	1.100	-48.8	15.8	-86963	1053
17	1	0	2.400	-104.0	0.2	-113027	-778708
18	1	0	2.554	-112.1	3.4	-110519	-909257
19	1	0	0.900	-55.9	14.9	-96015	-69645
20	1	0	1.500	-71.2	18.1	-70122	-14386
21	1	0	1.900	-65.1	9.3	-100075	-366469
22	1	0	1.900	-74.2	2.4	-108641	-676682
23	1	0	0.632	-49.6	23.5	-42879	522096
24	1	0	0.708	-47.2	18.7	-79353	184760
25	1	0	1.057	-74.5	21.4	-52292	214754
26	1	0	2.200	-81.5	-0.1	-114666	-770673
27	1	0	1.400	-71.3	19.0	-98993	123253
28	1	0	2.500	-122.7	7.0	-109803	-1121334
29	1	0	2.361	-80.9	14.0	-107148	-440115
30	1	0	1.300	-35.9	23.4	-42700	451045
31	1	0	0.321	-50.5	19.5	-64679	424377
32	1	0	1.800	-86.8	4.2	-119928	-616183
33	1	0	2.300	-81.6	6.4	-98451	-384479
34	1	0	1.100	-72.2	15.4	-99753	-63385
35	1	0	1.600	-64.1	20.4	-58969	278848
36	1	0	1.037	-90.2	14.3	-104541	-340120
1	1	+1	0.500	-91.0	17.4	-98238	-971908

APPENDIX

2	1	+1	2.584	-212.4	-1.1	-148262	-1378554
3	1	+1	0.700	-129.5	3.9	-118873	-851656
4	1	+1	0.700	-101.1	5.6	-103409	-1034632
5	1	+1	0.765	-76.4	12.4	-98487	-938187
6	1	+1	0.500	-110.3	10.1	-120981	-935446
7	1	+1	1.500	-69.4	9.2	-107756	-892333
8	1	+1	2.100	-121.2	7.8	-117256	-900671
9	1	+1	2.500	-126.8	-3.0	-112240	-961184
10	1	+1	2.400	-128.3	8.1	-101725	-801510
11	1	+1	2.200	-138.9	2.9	-122804	-1132881
12	1	+1	1.500	-109.7	0.9	-109548	-736094
13	1	+1	2.200	-77.5	12.9	-84043	-528777
14	1	+1	2.554	-103.2	13.1	-101169	-698014
15	1	+1	1.600	-122.8	-0.8	-102728	-761092
16	1	+1	1.100	-115.2	-1.1	-118883	-958188
17	1	+1	2.400	-160.6	-1.4	-141469	-1039401
18	1	+1	2.554	-153.0	-7.2	-166252	-1262213
19	1	+1	0.900	-113.6	9.7	-116719	-570924
20	1	+1	1.500	-65.1	7.9	-78884	-436164
21	1	+1	1.900	-139.1	2.5	-129989	-919061
22	1	+1	1.900	-87.8	3.0	-114215	-964263
23	1	+1	0.632	-118.5	-1.8	-129995	-1126854
24	1	+1	0.708	-78.4	17.0	-85986	-751524

APPENDIX

25	1	+1	1.057	-163.4	4.4	-134149	-943992
26	1	+1	2.200	-122.0	-5.9	-139222	-1128654
27	1	+1	1.400	-116.7	0.2	-135875	-836593
28	1	+1	2.500	-141.9	-3.3	-129010	-810034
29	1	+1	2.361	-156.9	-7.1	-142546	-925845
30	1	+1	1.300	-94.6	12.3	-113701	-770892
31	1	+1	0.321	-86.6	7.7	-90377	-755918
32	1	+1	1.800	-133.9	-1.5	-127857	-999977
33	1	+1	2.300	-182.3	-5.9	-140755	-1077293
34	1	+1	1.100	-104.4	2.8	-127333	-848855
35	1	+1	1.600	-77.0	-0.8	-117754	-770453
36	1	+1	1.037	-125.3	15.3	-94695	-808227

Table A.2: Responses' Table of the full case experiment

B. ANOVA Model Verification

After performing ANOVA analysis to a set of data, the model can not be accepted unless we are able to verify that the standard residuals (error) of the model are not violating the hypothesis, which are:

- Normally distributed.
- Constant variance between and within the factor levels.
- Standard residuals (models' error) vary between [-3 , 3].

In order to verify that the standard residuals are not violating any of the mentioned hypothesis, we need to perform three tests:

1. The Normality test:

Tested by the probability plot as it shows the normality distribution of the standard residuals. The normality is accepted if the P-value is above 0.05.

2. The test for equal variance:

To check that the variance are constant between and within the factor levels, the p-values needs to be above 0.05.

3. The scatterplot test:

The standard residuals has to be distributed in the scatterplot between [-3 , 3] for all factors.

B.1 Single Disk Experiment

1.1 Difference in mean diameter [ΔD_m]

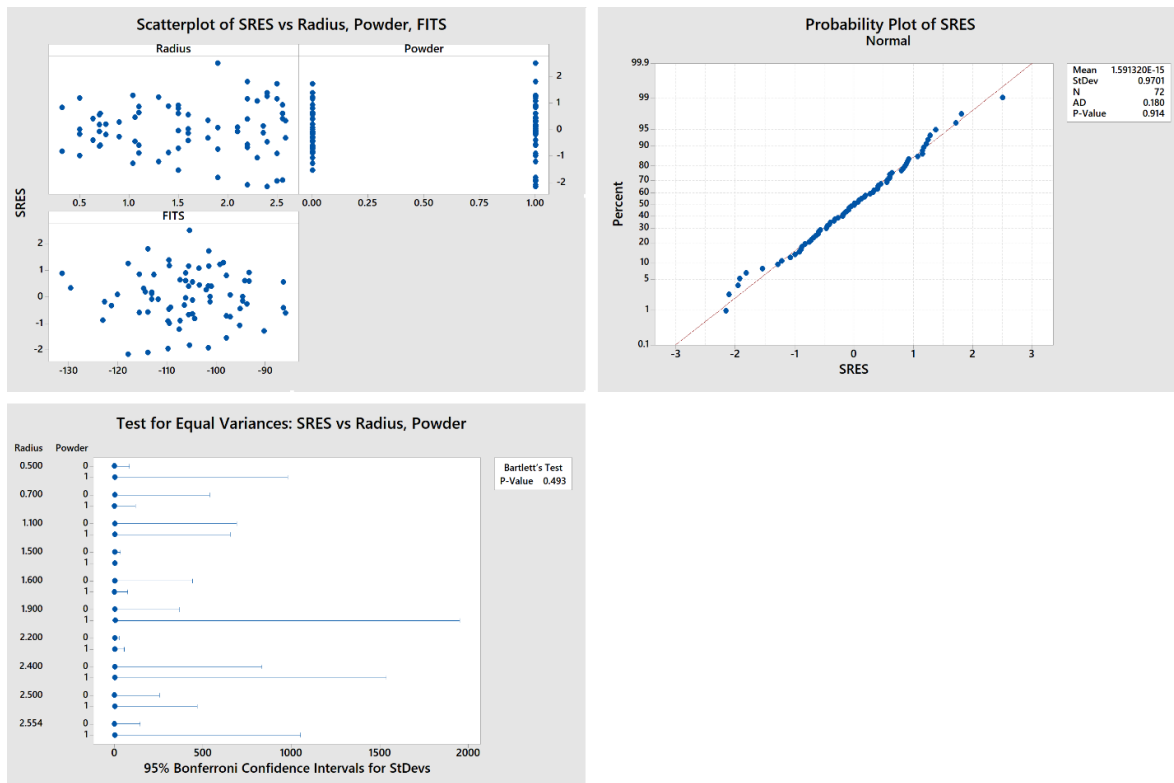


Figure B.1: Normality plot, Scatterplot and Test for equal variance of std. residuals of ΔD_m

Figure B.1 shows that the residuals have no problems in any of the three tests. The normality plot shows that the residuals are following a normal distribution with a P-value of 0.914, and the test for equal variances also shows no issues with a P-value of 0.493. Regarding the scatterplot, we see that we don't have any strong patterns that can cause any problems regarding the FITS, powder and the radius, and all the scatterplot belongs to $[-3, 3]$. The hypothesis of the residuals are verified, and the model is accepted.

1.2 Difference in mean height [Δh]

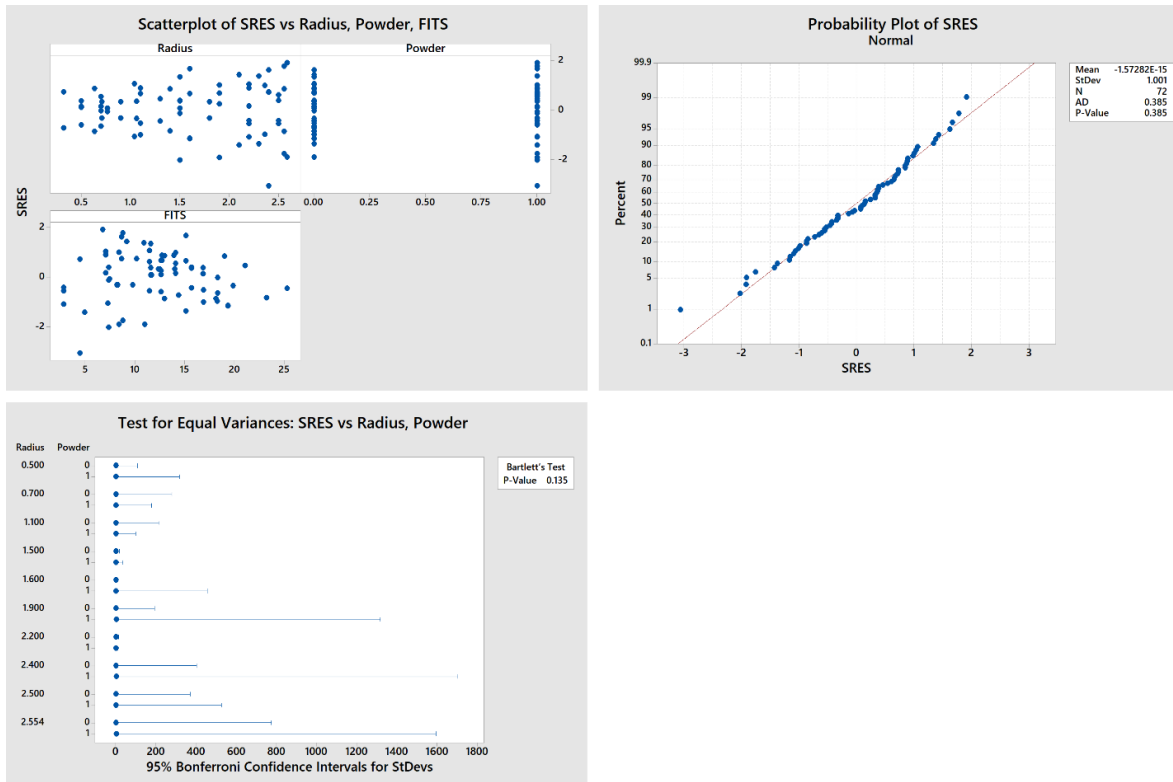


Figure B.2: Normality plot, Scatterplot and Test for equal variance of std. residuals of Δh

Figure B.2 shows that the residuals have no problems in any of the three tests. The normality plot shows that the residuals are following a normal distribution with a P-value of 0.385, and the test for equal variances also shows no issues with a P-value of 0.135. Regarding the scatterplot, we see that we don't have any strong patterns that can cause any problems regarding the FITS, powder and the radius, and all the scatterplot belongs to $[-3, 3]$. The hypothesis of the residuals are verified, and the model is accepted.

1.3 Difference in mean area [ΔA]

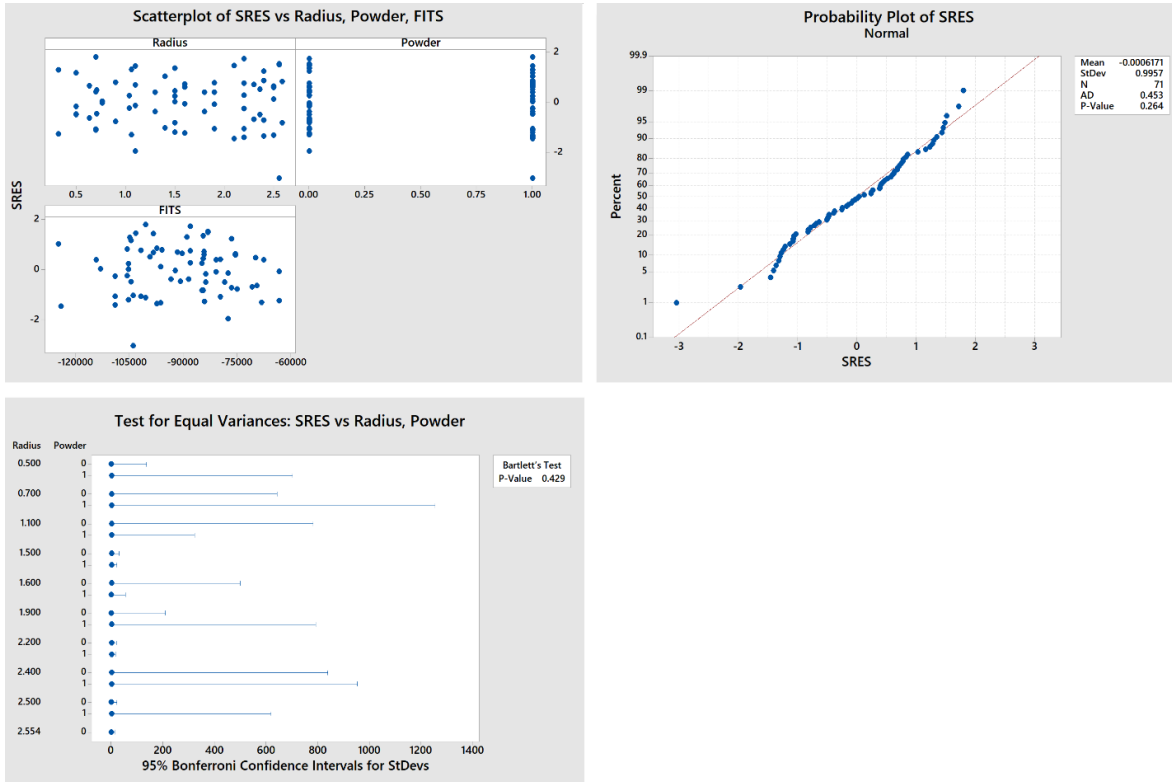


Figure B.3: Normality plot, Scatterplot and Test for equal variance of std. residuals of ΔA

Figure B.3 shows that the residuals have no problems in any of the three tests. The normality plot shows that the residuals are following a normal distribution with a P-value of 0.264, and the test for equal variances also shows no issues with a P-value of 0.429. Regarding the scatterplot, we see that we don't have any strong patterns that can cause any problems regarding the FITS, powder and the radius, and all the scatterplot belongs to $[-3, 3]$. The hypothesis of the residuals are verified, and the model is accepted.

1.4 Difference in mean volume [ΔV]

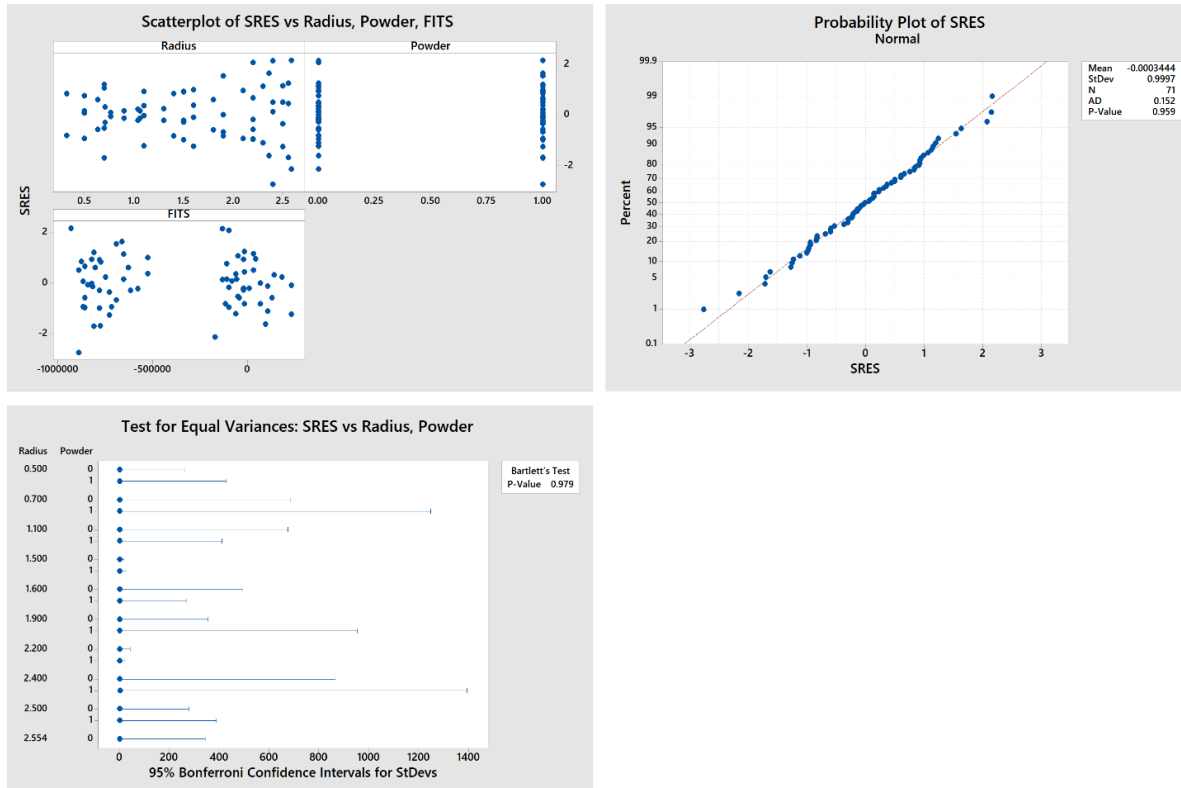


Figure B.4: Normality plot, Scatterplot and Test for equal variance of std. residuals of ΔV

Figure B.4 shows that the residuals have no problems in any of the three tests. The normality plot shows that the residuals are following a normal distribution with a P-value of 0.959, and the test for equal variances also shows no issues with a P-value of 0.979. Regarding the scatterplot, we see that we don't have any strong patterns that can cause any problems regarding the FITS, powder and the radius, and all the scatterplot belongs to $[-3, 3]$. The hypothesis of the residuals are verified, and the model is accepted.

B.2 Full Case Experiment

2.1 Difference in mean diameter [ΔD_m]

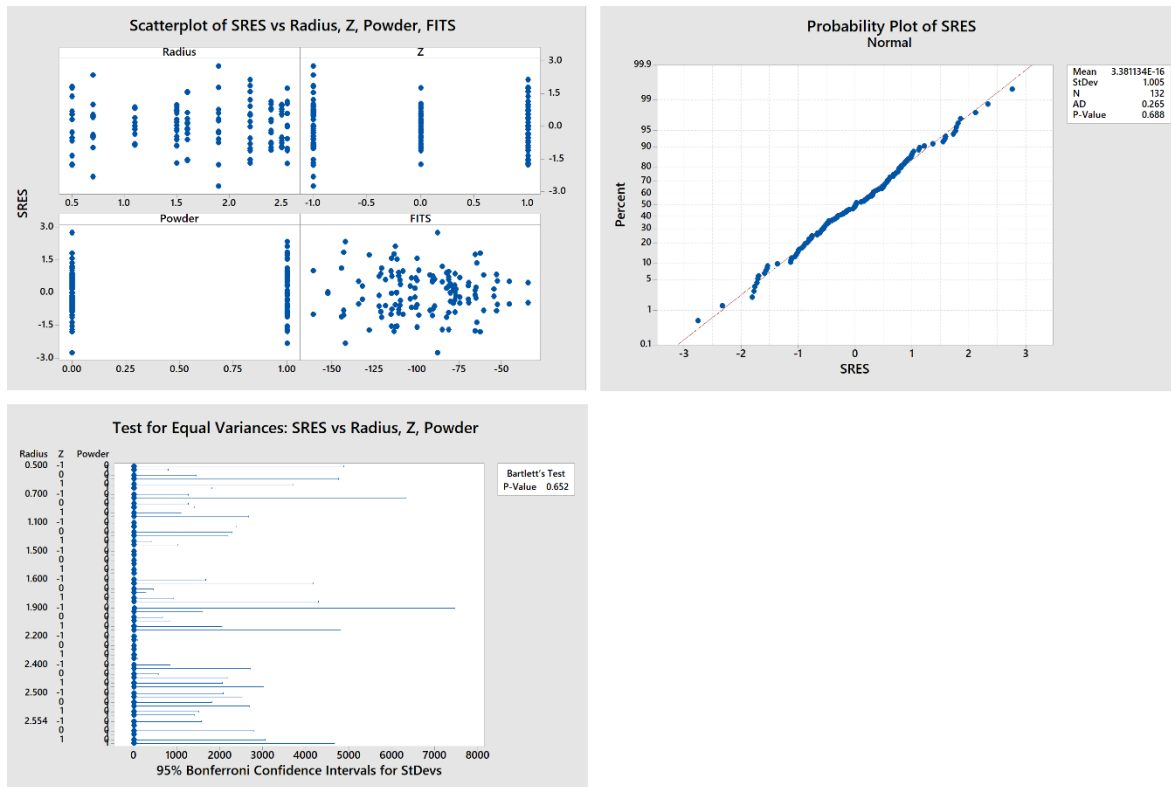


Figure B.5: Normality plot, Scatterplot and Test for equal variance of std. residuals of ΔD_m

Figure B.5 shows that the standard residuals have no problems in any of the three tests. The normality plot shows that the residuals are following a normal distribution with a P-value of 0.688, and the test for equal variances also shows no issues with a P-value of 0.652. Regarding the scatterplot, we see that we don't have any strong patterns that can cause any problems regarding the FITS, powder and the radius. The scatterplot shows that the residuals vary between $[-3, 3]$ while remaining in between. The hypothesis of the residuals are verified, and the model is accepted.

2.2 Difference in height [Δh]

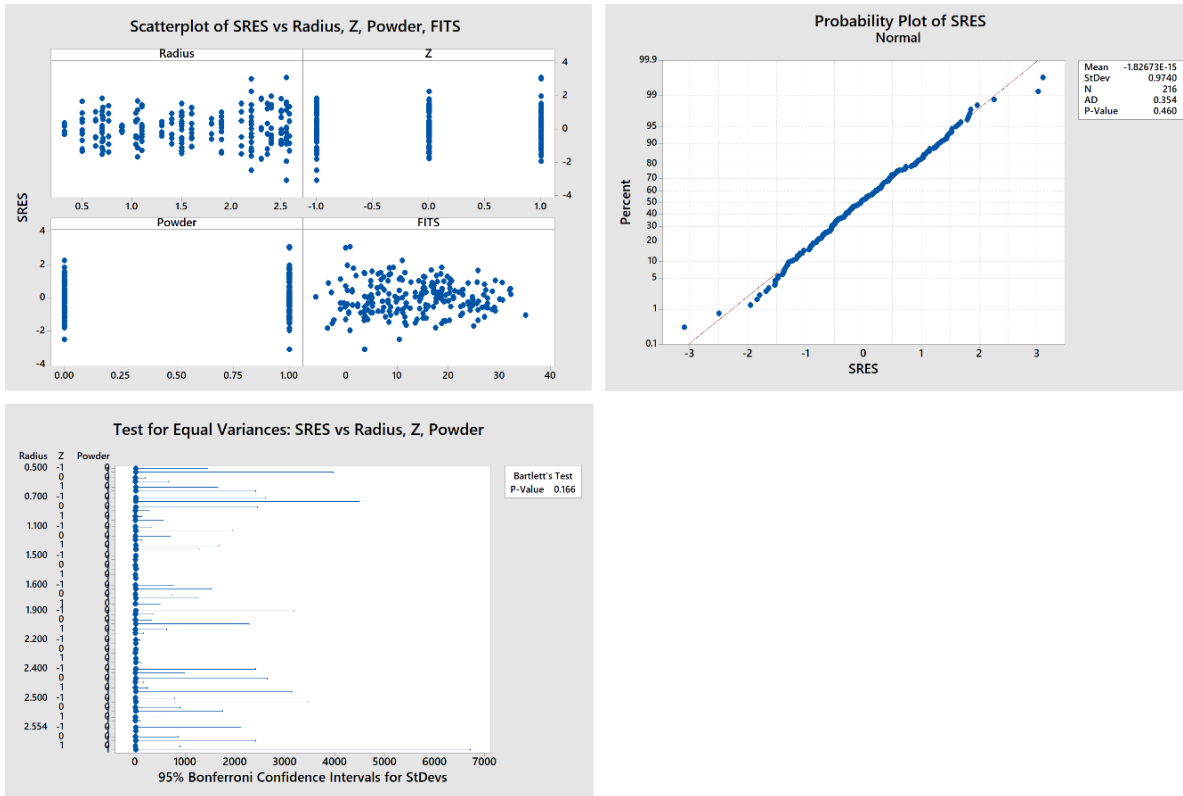


Figure B.6: Normality plot, Scatterplot and Test for equal variance of std. residuals of Δh

Figure B.6 shows that the residuals have no problems in any of the three tests. The normality plot shows that the residuals are following a normal distribution with a P-value of 0.460, and the test for equal variances also shows no issues with a P-value of 0.166. Regarding the scatterplot, we see that we don't have any strong patterns that can cause any problems regarding the FITS, powder and the radius. The scatterplot shows two points at -3.09, and 3.1, which are violating the $[-3, 3]$ hypothesis. By eliminating these two points and rechecking the analysis, the model stays almost the same. So we conclude that the two points are outliers, and the model is accepted.

2.3 Difference in area [ΔA]

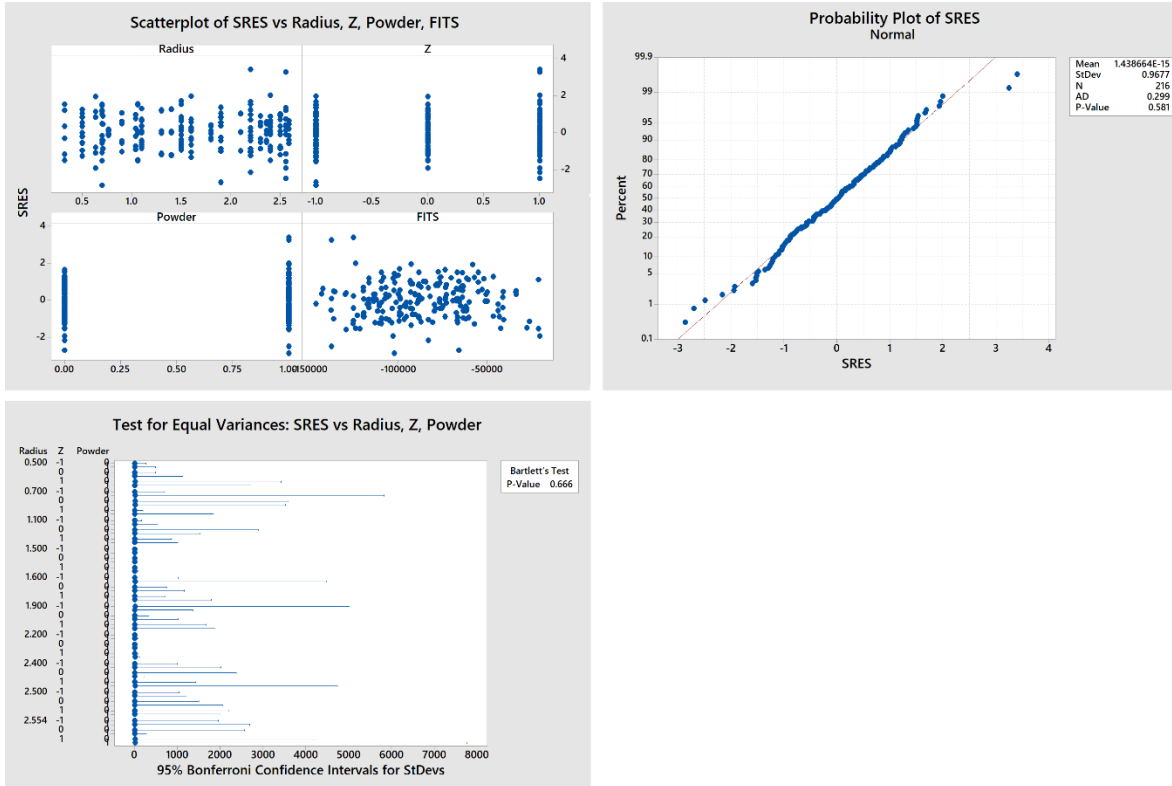


Figure B.7: Normality plot, Scatterplot and Test for equal variance of std. residuals of ΔA

Figure B.7 shows that the residuals have no problems in any of the three tests. The normality plot shows that the residuals are following a normal distribution with a P-value of 0.666, and the test for equal variances also shows no issues with a P-value of 0.652. Regarding the scatterplot, we see that we don't have any strong patterns that can cause any problems regarding the FITS, powder and the radius. The scatterplot shows two points at 3.4, and 3.25, which are violating the $[-3, 3]$ hypothesis. By eliminating these two points and rechecking the analysis, the model stays almost the same. So we conclude that the two points are outliers, and the model is accepted.

2.4 Difference in volume [ΔV]

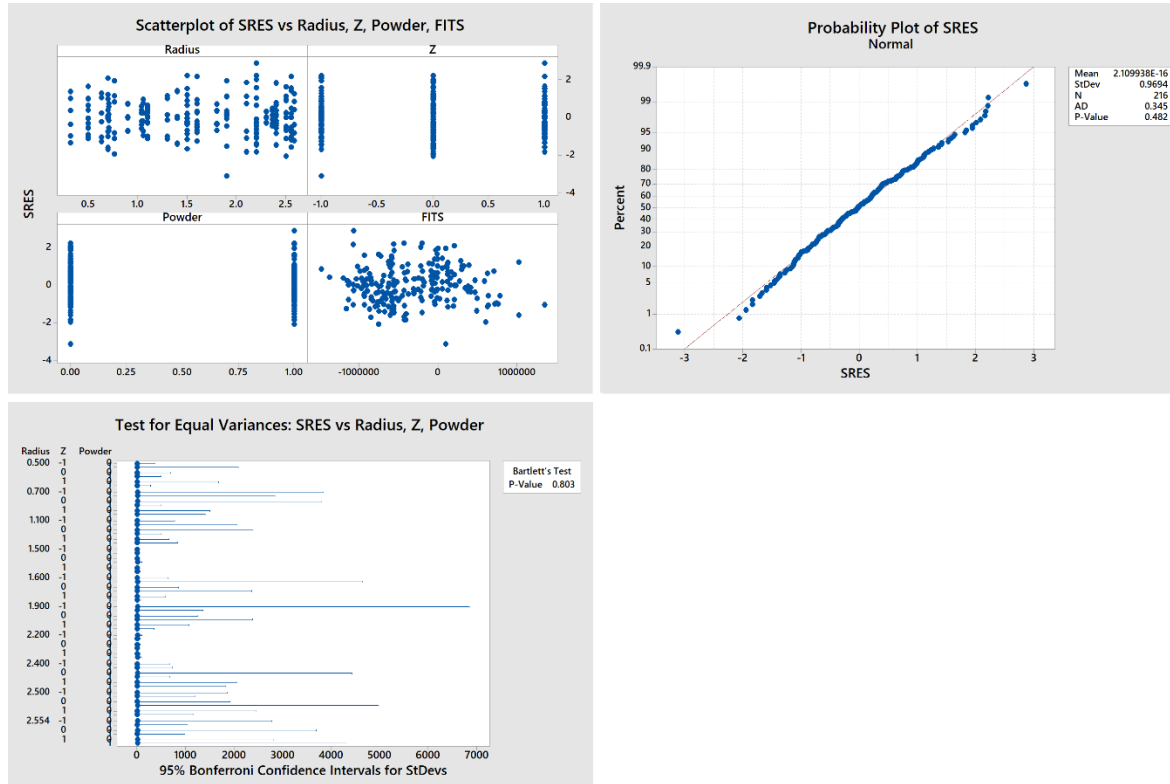


Figure B.8: Normality plot, Scatterplot and Test for equal variance of std. residuals of ΔV

Figure B.8 shows that the residuals have no problems in any of the three tests. The normality plot shows that the residuals are following a normal distribution with a P-value of 0.482, and the test for equal variances also shows no issues with a P-value of 0.803. Regarding the scatterplot, we see that we don't have any strong patterns that can cause any problems regarding the FITS, powder and the radius. The scatterplot shows one points at -3.1, which is violating the [-3 , 3] hypothesis. By eliminating this one point and rechecking the analysis, the model stays almost the same. So we conclude that the point is an outlier, and the model is accepted.

References

- [1] *Kim, Jaegon & O Jin, Seung & H Cho, Min & Y Lee, Soo, 2011, "Inter-plane artifact suppression in tomosynthesis using 3D CT image data", Biomedical engineering online.*
- [2] *H.C. Corcoran, S.B. Brown, S. Robson, R.D. Speller, M.B. McCarthy, 2016, "Observations on the performance of X-ray computed tomography for dimensional metrology".*
- [3] *https://www.researchgate.net/figure/Selected-regions-from-a-single-CT-slice-of-the-SLM-specimen-in-the-as-built-a-and-c_fig10_285607305*
- [4] *https://www.wikiwand.com/en/Paris%27_law*
- [5] *Nikishkov, Yuri & Airoidi, L. & Makeev, A., 2013, "Measurement of voids in composites by X-ray Computed Tomography", Composites Science and Technology".*
- [6] *Jansson, Anton & R Zekavat, Amir & Pejryd, L., 2015. "Measurement of Internal Features in Additive Manufactured Components by the use of Computed Tomography".*
- [7] *Hermanek, Petr & Carmignato, S., 2016, "Reference object for evaluating the accuracy of porosity measurements by X-ray computed tomography", Case Studies in Nondestructive Testing and Evaluation.*
- [8] *Simone Giacomazzi., 2018 "X-ray computed tomography: Design and application of a procedure for the estimation of the accuracy".*
- [9] *R. Laquai, B. R. Müller, G. Kasperovich, J. Haubrich, G. Requena & G. Bruno., 2018 "X-ray refraction distinguishes unprocessed powder from empty pores in selective laser melting Ti-6Al-4V".*

REFERENCES

- [10] <https://it.mathworks.com/matlabcentral/fileexchange/24484-geom3d>
- [11] <http://www.danielgm.net/cc/release/>
- [12] <http://www.minitab.com/en-us/>

